International Atomic Energy Agency

INDC(NDS)-281
Distr.: Sp L

INDC INTERNATIONAL NUCLEAR DATA COMMITTEE

NUCLEAR DATA FOR NEUTRON MULTIPLICATION IN FUSION-REACTOR FIRST-WALL AND BLANKET MATERIALS

Texts of Papers Presented at the Advisory Group Meeting

organized by the
International Atomic Energy Agency
in cooperation with
Southwest Institute of Nuclear Physics and
Chemistry (SWINPC)

and held in
Chengdu, China, 19-21 November 1990

Compiled by

A.B. Pashchenko and D.W. Muir
IAEA Nuclear Data Section

February 1993

IAEA NUCLEAR DATA SECTION, WAGRAMERSTRASSE 5, A-1400 VIENNA

INDC(NDS)-281
Distr.: Sp L

NUCLEAR DATA FOR NEUTRON MULTIPLICATION IN FUSION-REACTOR FIRST-WALL AND BLANKET MATERIALS

Texts of Papers Presented at the Advisory Group Meeting

organized by the
International Atomic Energy Agency
in cooperation with
Southwest Institute of Nuclear Physics and
Chemistry (SWINPC)

and held in
Chengdu, China, 19-21 November 1990

Compiled by

A.B. Pashchenko and D.W. Muir
IAEA Nuclear Data Section

February 1993

Reproduced by the IAEA in Austria
March 1993

93-00890

FOREWORD

This report contains the texts of the invited presentations delivered at the Advisory Group Meeting on Nuclear Data for Neutron Multiplication in Fusion-Reactor First-Wall and Blanket Materials. The meeting was organized by the International Atomic Energy Agency in cooperation with the Southwest Institute at Nuclear Physics and Chemistry (SWINPC) and held in Chengdu, China, 19-21 November 1990. The texts are reproduced here, directly from the Author's manuscripts with little or no editing, in the order in which the presentations were made at the meeting.

CONTENTS

Nuclear Data Needs and Issues for Fusion Power Reactors*

E.T. Cheng
TSI Research
Solana Beach, California
U.S.A.

* was presented at the meeting orally, and the main conclusions were included in the Summary Report of the meeting, published as report INDC(NDS)-264/G.

On a Status of ITER Neutronics Analysis

Compiled by D.V. Markovskij
I.V. Kurchatov Institute of Atomic Energy
Moscow
The Russian Federation

THE OVERALL OBJECTIVE OF THE ITER:

- TO DEMONSTRATE THE SCIENTIFIC AND TECHNOLOGY FEASIBILITY OF FUSION POWER

THE ITER WILL ACCOMPLISH THIS OBJECTIVE

- BY DEMONSTRATING CONTROLLED IGNITION AND EXTENDED BURN OF A DEUTERIUM AND TRITIUM PLASMA WITH STEADY STATE AS AN ULTIMATE GOAL
- BY DEMONSTRATING TECHNOLOGIES ESSENTIAL TO A REACTOR IN AN INTEGRATED SYSTEM
- BY PERFORMING INTEGRATED TESTING OF THE HIGH-HEAT-FLUX AND NUCLEAR COMPONENTS REQUIRED TO UTILIZE FUSION POWER FOR PRACTICAL PURPOSES

TO REACH THIS OBJECTIVE THE ITER WILL BE OPERATED IN TWO PHASES:

- A PHYSICS PHASE FOCUSED MAINLY ON ACHIEVING THE PLASMA OBJECTIVES
- A TECHNOLOGY PHASE DEVOTED MAINLY TO ENGINEERING OBJECTIVES AND TESTING PROGRAM

THE ITER REACTOR IS DESIGNED TO ACHIEVE:

- A FLUENCE GOAL OF ~ 3 $MW \cdot Y/M^2$
- 15 YEAR LIFE OF THE MACHINE OPERATION
- ~3.8 FULL POWER YEARS (FPY) OF OPERATION:
  0.05 FPY IN THE PHYSICS PHASE, 1100 MW OF FUSION POWER
  3.7 FPY IN THE TECHNOLOGY PHASE, 860 MW OF FUSION POWER

THE OVERALL DIMENSIONS OF THE REACTOR ARE FIXED IN BOTH PHASES

THE BLANKET DESIGN PHILOSOPHY:

- TO PRODUCE THE NECESSARY TRITIUM REQUIRED FOR THE ITER
- TO OPERATE AT POWER REACTOR CONDITIONS AS MACH AS POSSIBLE

THIS REQUIRES:

- ACCOMODATION CAPABILITY UP TO A FACTOR OF TWO CHANGE IN THE NEUTRON WALL LOADING WITHOUT VIOLATING THE DIFFERENT DESIGN GUIDELINES
- A CONTINUOUS TRITIUM RECOVERY FROM THE BLANKET
- USING OF BERYLLIUM FOR NEUTRON MULTIPLICATION AND SOLID BREEDER TEMPERATURE CONTROL
- USING OF WATER COOLANT AND THE SEPARATION OF THE TRITIUM PURGE GAS FROM THE COOLANT SYSTEM BY SEVERAL BARRIERS

US BLANKET CONCEPTS:

CONCEPT	BREEDER Li_2O (Li_2ZrO_3)	MULTIPLIER Be	STRUCTURE	COOLANT
1	SINTERED BLOCKS	SINTERED BLOCKS		
2(*)	PEBBLES	SINTERED BLOCKS	SS316	H_2O
3(**)	SINTERED BLOCKS	SINTERED BLOCKS		

(*) COMMON ITER BLANKET (**) RECOMMENDED BLANKET

LITHIUM-6 ENRICHMENT	95 %
BREEDER PURGE GAS	HE+0.2 % H_2
TRITIUM INVENTORY IN BREEDER	14 G
IN BERYLLIUM	~1.2 KG (END OF LIFE)
NET TRITIUM BREEDING RATIO	0.8-0.9 (2-3 BREEDER ZONES)
LOCAL TBR	0.75-0.9 (IB, DEPENDING ON PLACE)
	1.38-1.46 (OB)

US BLANKET CONCEPT

OUTBOARD RADIAL BLANKET CONFIGURATION AT THE MIDPLANE WITH TWO BREEDER ZONES AND TWO ZONES OF BERYLLIUM PEBBLES

ZONE	MATERIAL	THICKNESS, CM Z = 0	THICKNESS, CM Z = ±2.7 M
FIRST WALL LAYERS			
TILE(*)	C	2.0	2.0
FIRST WALL	STEEL	0.5	0.5
COOLANT	H_2O	0.4	0.4
BACK WALL	STEEL	0.5	0.5
BLANKET			
MULTIPLIER	BE PEBBLES (0.82)	0.7	0.9
CLAD	STEEL	0.1	0.1
BREEDER	Li_2O (0.80)	0.8	0.8
CLAD	STEEL	0.1	0.1
MULTIPLIER	BE BLOCKS (0.85)	5.3	6.5
COOLANT CHANNEL	STEEL	0.2	0.2
COOLANT	H_2O	0.2	0.2
COOLANT CHANNEL	STEEL	0.2	0.2
MULTIPLIER	BE BLOCKS (0.85)	8.3	11.0
CLAD	STEEL	0.1	0.1
BREEDER	Li_2O (0.80)	0.8	0.8
CLAD	STEEL	0.1	0.1
MULTIPLIER	BE BLOCKS (0.85)	5.3	6.3
MULTIPLIER	BE PEBBLES (0.82)	0.5	0.9
COOLANT CHANNEL	STEEL	0.2	0.2
COOLANT	H_2O	0.2	0.2
TOTAL FIRST WALL/BLANKET THICKNESS		24.5	30.0
TOTAL THICKNESS OF COMPACT BE		17.1	21.7
LOCAL TRITIUM BREEDING RATIO		1.387	1.336

(*) THE CARBON TILE IS USED ONLY IN THE PHYSICS PHASE ANALYSIS AND IS NOT INCLUDED IN THE FIRST WALL/BLANKET THICKNESS

JAPAN BLANKET CONCEPTS:

CONCEPT	BREEDER Li_2O	MULTIPLIER Be	STRUCTURE	COOLANT
1	PEBBLE MIXTURE			
2	PEBBLE LAYERED		SS316	H_2O
3(*)	PEBBLES	SINTERED BLOCKS		

(*) COMMON ITER BLANKET

LITHIUM-6 ENRICHMENT	NATURAL (PEBBLE MIXTURE) 50 % (PEBBLE LAYERED)
Li_2O/Be PEBBLES RATIO	1/3
PEBBLE PACKING FACTOR	60 %
NET TRITIUM BREEDING RATIO	0.75-0.8 (DEP. ON TILE)
LOCAL TBR	0.52-0.54 (IB, MID-PLANE) 1.25-1.49 (OB, DEP. ON PLACE)

ONE-DIMENSIONAL MODEL OF OUTBOARD PEBBLE MIXTURE TYPE BLANKET

MATERIAL	THICKNESS, CM
GRAPHITE	2.0
SS	0.3
SS : 0.333 H20 : 0.667	0.5
SS	0.7
BREEDER AND MULTIPLIER MIXTURE ZONE I Li_2O : 0.1121 SS : 0.05995 Be : 0.3364 H20 : 0.10665	14.85
BREEDER AND MULTIPLIER MIXTURE ZONE II Li_2O : 0.1247 SS : 0.04 Be : 0.3742 H20 : 0.0712	17.5
BREEDER AND MULTIPLIER MIXTURE ZONE III Li_2O : 0.1377 SS : 0.0194 Be : 0.4132 H20 : 0.03451	20.65
SS : 0.8 H20 : 0.2	100.0

MAIN FEATURES OF THE EC BLANKET CONCEPT:

- $LiAlO_2$ AS A BREEDER MATERIAL IN FORM OF SINTERED PELLETS CONTAINED IN STEEL CLADDING (FISSION REACTOR TECHNOLOGY). OTHER BREEDING MATERIALS ARE NOT EXCLUDED
- 316 SS AS A STRUCTURAL MATERIAL
- BERYLLIUM MULTIPLIER IN FORM OF ANNULAR, SINTERED PELLETS CONTAINED IN STEEL CLADDING (TO FACE POSSIBLE CRACKING) AND OPERATING AT LOW TEMPERATURE (< 150°C) TO REDUCE THE IRRADIATION SWELLING
- WATER COOLING IN POLOIDAL DIRECTION AT LOW PRESSURE AND TEMPERATURE (1 MPA, 60/100°)
- 'ON LINE' TRITIUM RECOVERY BY MEANS OF HE STREAM WITH SWAMPING ISOTOPE (Q_2 OR Q_2O, Q=D OR T SWAMPING ISOTOPE)
- HE GAP THERMAL BARRIER BETWEEN BREEDER AND COOLANT TO KEEP THE BREEDER AT A PROPER LEVEL FOR TRITIUM RECOVERY (> 400°), DESPITE THE LOW OPERATION TEMPERATURE OF THE COOLANT (60/100°)

BLANKET MODULES CONSIST OF POLOIDALLY RUNNING TUBES

INTERNALS OF THE BLANKET MODULE :

- CENTRAL BREEDER ROD (CONSISTING OF CYLINDRICAL PELLETS CONTAINED IN A DOUBLE STEEL CLADDING AND LOCATED INSIDE A POLOIDAL COOLING TUBE)
- HE GAP BETWEEN THE 1ST AND 2ND STEEL CLADDING PROVIDING THERMAL BARRIER BETWEEN BREEDER AND COOLANT AND ALLOWING PURGE THE FLOW FOR TRITIUM RECOVERY
- 1ST STEEL CLADDING PROVIDING BREEDER GEOMETRY CONTROL IN CASE OF CRACKING DURING THE OPERATION
- 2ST STEEL CLADDING PROVIDING CONTAINMENT OF THE PURGE HE AND COOLED BY WATER AT LOW TEMPERATURE (≤ 100 °C) TO REDUCE THE TRITIUM PERMEATION INTO WATER COOLANT
- BERYLLIUM ANNULAR PELLETS LOCATED OUTSIDE THE COOLING TUBE AND CONTAINED INSIDE THE OUTER STEEL CLADDING WHICH CAN ALSO PROVIDE A SECOND CONTAINMENT OF THE WATER COOLING

EC BLANKET DESIGN PARAMETERS:

$LiAlO_2$ DENSITY FACTOR	0.85
BE DENSITY FACTOR	0.85
LI-6 ENRICHMENT	50 %
NUMBER OF ROWS FOR BLANKET SECTIONS	
INBOARD	2
OUTBOARD	8

RADIAL BUILT OF BREEDER/MULTIPLIER UNITS IN THE EC BLANKET DESIGN

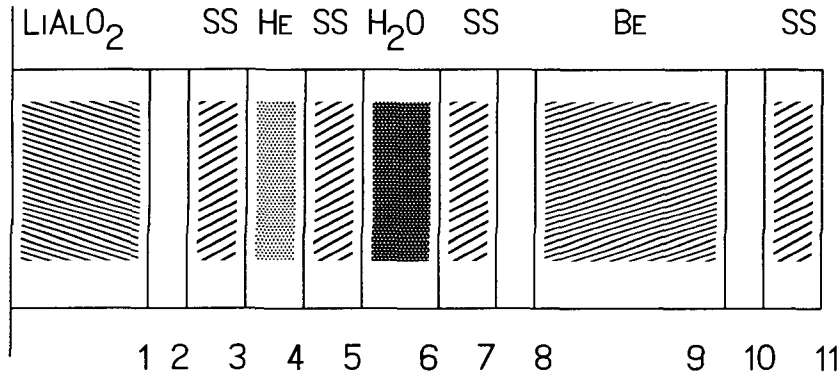

	ROW 1	... ROW 8
R 1	8.82	17.64
2	8.87	17.69
3	9.76	19.78
4	10.61	21.66
5	11.11	22.35
6	16.15	24.35
7	16.65	24.85
8	16.70	24.90
9	30.51	30.51
10	30.56	30.56
11	31.06	31.06

MATERIAL FRACTIONS

	SS	H_2O	Be	$LiAlO_2$-6	$LiAlO_2$-7
INBOARD					
1-ST ROW	0.0665	0.0656	0.3742	0.0411	0.0410
2-ND ROW	0.0507	0.0383	0.2365	0.0352	0.0352
OUTBOARD					
1-ST ROW	0.0456	0.0839	0.3387	0.0202	0.0202
8-TH ROW	0.0632	0.0360	0.1018	0.0509	0.0509

USSR DESIGN WITH LEAD-LITHIUM EUTECTIC $Li_{17}Pb_{83}$

IS DEVELOPED BY THE SOVIET SIDE ACCORDING TO THE UNDERSTANDING BETWEEN THE COUNTRIES-MEMBERS OF THE ITER PROJECT IN 1988

USE OF $Li_{17}Pb_{83}$ EUTECTIC AS A BREEDING MATERIAL HAS THE FOLLOWING PECULIARITIES

- AVAILABILITY OF LEAD AS NEUTRON BREEDER
- COMPARATIVELY SIMPLE TECHNOLOGY OF LEAD PRODUCTION AND ITS LOW COST
- LOW SENSITIVITY TO RADIATION DAMAGES
- LOW SENSITIVITY TO RADIATION POWER CHANGE
- RADIATION SHIELDING DESIGN IS SIMPLIFIED
- CIRCULATION BETWEEN BLANKET AND ITS EXTERNAL SYSTEMS TO RECOVER TRITIUM

THE OUTBOARD BLANKET SEGMENTS CONSIST OF

- SEGMENT CASE - A BOX STRUCTURE, THAT INCLUDES
  - THE FIRST WALL
  - SIDE WALLS WITH THE COOLING SYSTEMS
  - THE BOX TO LOCATE THE RADIATION SHIELDING AND COPPER PLATES OF THE LOOPS OF THE PASSIVE PLASMA STABILIZATION
- 3/11 (IB/OB) BREEDING CHANNELS FILLED WITH SOLID EUTECTIC ARRANGED IN THREE ROWS

THICKNESS OF THE BLANKET BREEDING ZONE	180/510 MM (IB/OB)
WATER CONTENT IN BREEDING CHANNELS, %	15.9/35.6 (1/2,3 ROWS)
^6Li ENRICHMENT	90 %
BLANKET STRUCTURAL MATERIAL	AUST. SS 04X16H11M3T (SIMILAR TO 316L)
CHANNEL DIAMETER	80/120 MM (IB/OB)
NET TBR	0.76-0.8
LOCAL TBR	0.69/1.04 (IB/OB)

SENSITIVITY OF LOCAL TBR TO THE BLANKET PARAMETERS VARIATIONS

US DESIGN

	Parameter variation	TBR variation, %
Breeder zone thickness, cm	0.8 - 1.6	+4.0
Breeder clad thickness, cm	0.1 - 0.2	-2.6
Li-6 enrichment, %	N - 95	+29.
Carbon tile thickness	~ - 7 %/cm	
Steel thickness of the first wall	~ - 14 %/cm	
First wall water zone thickness	~ - 21 %/cm	
Beryllium density factor (variation from designed values of 0.85 and 0.65)	±0.05	±2.3

USSR DESIGN

	TBR variation, % / %
Breeder zone	
Breeder zone thickness	+0.044
H_2O fraction	+0.003
Li-Pb fraction	+0.21
Steel fraction	-0.077
First wall	
Steel thickness of the first wall	~ - 0.13
First wall water zone thickness	~ - 0.07

GUIDELINE ACCURACIES FOR NEUTRONICS ANALYSIS

NEUTRON MULTIPLICATION IN BLANKET	3 %

RADIATION LOADS ON TOROIDAL FIELD COILS

NUCLEAR HEATINGS	
- LOCAL	20 - 30 %
- TOTAL	10 - 20 %
RADIATION DAMAGE (LOCAL)	
- INSULATOR (RAD)	20 %
- STABILIZER (DPA)	30 %
- SUPERCOND. (FLUENCE)	30 %
ACTIVATION	10 - 50 %

VACUUM VESSEL

NUCLEAR HEATING	IB	10 %
	OB	20 %
HE-GENERATION	IB	30 %
ACTIVATION		10 %
DECAY HEAT		10 %

BIOLOGICAL DOSE

PERSONNEL ACCESS AREAS	50 %
NO PERSONNEL ACCESS AREAS	1000 %

MATERIALS USED IN ITER NEUTRONICS ANALYSIS

First wall	Graphite	C
	SS, H_2O	Fe, Cr, Ni, Mn, Mo, ...
		H, O
Blanket	SS, H_2O	Fe, Cr, Ni, Mn, Mo, ...
	Li-Ceramics	Li, O, Al, Zr, Si
	Multiplier	Be, Pb
Vacuum vessel	SS, H_2O	Fe, Cr, Ni, Mn, Mo, ...
	Insulator (Al_2O_3)	Al, O
	B_4C, Pb, B-SS, W	B, Pb, W, Fe, Cr, Ni, Mn,..
Magnet	Superconductor	Nb, Sn
	Matrix	Cu
	Structure (SS)	Fe, Cr, Ni, Mn, Mo, ...
	Insulator	H,O,C,N,S,Si,Al,Ca,Mg
	He coolant	He
Biolog. shield	SS, H_2O, Pb	SS, H_2O, Pb, concrete
	Concrete	
Divertor		W, Mo, Cu, Nb

SOME PROPOSALS for a future

- Neutron codes unification
  - Transport
  - Sensitivity
  - Activation
- Neutron data unification
  - Evaluated data
  - Working (group) data
- Neutron data testing in benchmark experiments
- Recommended codes and data verification in analysis of experiments with the key physics models (Blanket and Shield)
- Safety factors formulation

REFERENCES

1. ITER Concept Definition, Vol. 1. ITER documentation series, No. 3., IAEA, Vienna, 1989.
2. ITER Concept Definition, Vol. 2. ITER documentation series, No. 3., IAEA, Vienna, 1989.
3. U.S. Technical Report for the ITER Blanket/Shield. B. Shield. ITER-TN-BL-5-0-6, July - November 1990.
4. Japanese contribution to blanket design for ITER. July 1990. ITER-IL-BL-5-0-10.
5. ITER Blanket Workshop 16-27 July 1990, Garching, FRG. EC contribution.
6. ITER Lead-Lithium Blanket (working material). ITER-IL-BL-6-0-7, July 1990.
7. Summary Report of ITER Expert Meeting on Shielding Experiments and Analysis. ITER-IL-BL-5-0-5, Feb. 1990.

Double Differential Neutron Emission Cross-Sections for Li-7, Be-9 and Pb*

H. Gruppelaar
Netherlands Energy Research
Foundation ECN, Petten
The Netherlands

* was presented at the meeting orally, and the main conclusions were included in the Summary Report of the meeting, published as report INDC(NDS)-264/G.

Status of BROND and Related Data Evaluation Activities*

D. Seeliger
Technische Universität
Dresden
Germany

* was presented at the meeting orally, and the main conclusions were included in the Summary Report of the meeting, published as report INDC(NDS)-264/G.

Status of ENDF/B-6 Evaluations for Li-7, Be and Pb*

E.T. Cheng
TSI Research
Solana Beach, California
U.S.A.

* was presented at the meeting orally, and the main conclusions were included in the Summary Report of the meeting, published as report INDC(NDS)-264/G.

Differential Neutron Emission Data of Neutron Multiplier and Structural Materials for Fusion Reactor

Mamoru Baba

Department of Nuclear Engineering, Tohoku University
Aoba,Aramaki, Sendai 980, Japan

Abstract:

A brief review is presented on the recent activity on differential neutron emission cross section measurements at Osaka and Tohoku universities in Japan for neutron multiplier, tritium breeder and structural materials in comparison with latest version of JENDL-3. Detailed discussion are made for (n,2n) cross sections and emission spectrum of Be, Pb and Li-6,7.

1. Introduction

Differential neutron emission cross sections of fusion reactor candidate materials are of prime importance for design of fusion reactors since they dominate the neutron spectrum, neutron multiplication and radiation effects, i.e, damage and nuclear heating. For accurate calculation of nuclear performance of fusion reactors, neutron emission data should be treated adequately both in energy and angular distribution to describe anisotropic neutron transport as shown by parametric studies of neutron spectrum in bulk media /1,2/ and tritium production rate /3/. Therefore, precise knowledge is required for energy-angular doubly-differential neutron emission cross section (DDX).

In recent years, the (n,2n) cross section and emission spectrum of neutron multipliers, Be and Pb, and structural materials are of special concern because the established cross section of the Li(n,n't) reaction is significantly lower than expected in the past /4/.

In Japan, experimental studies and evaluation of double-differential cross sections have been conducted fairly actively for completion of JENDL-3 through close collaboration between experiments and evaluation as well as integral tests.

This report presents a brief review of experimental data comparing with JENDL-3 to clarify the status of the evaluated data focusing mainly on activities in recent few years, since the status of previous version of JENDL-3, i.e., JENDL-3PR1, -PR2, is summarized by Maekawa at the IAEA Advisory Group Meeting for Fusion Reactor Technology, Gaussig 1986 /5/.

2. Recent activity in Japan

In April 1989, JENDL-3 was released /6/ after bench marking and revision of test version JENDL-3T. In these data testing, various data comparison have been made to find out the problems. Differential neutron emission data are one of the prime items in these test so as to confirm the applicability of JENDL-3 to fusion reactor neutronics. JENDL-3 adopts ENDF/B-V format as the standard.

Systematic experimental studies of DDXs have been made at Osaka university using intense 14 MeV neutron source OKTAVIAN /7,8/ and at Tohoku university using a 4.5MV Dynamitron accelerator as a variable energy neutron source /9,10/. In these experiments, neutron emission spectra have been measured over wide range of emission energy with good energy resolution to clarify various reaction component. Furthermore, in these studies, care is taken for proper data correction considering sample-dependent backgrounds caused by neutrons from parasitic reactions and target scattering, as well as multiple scattering in the samples. Technical development is also in progress to extend the meas-

urements to low energy part of emission spectrum where previous data were rather uncertain due to inferior S/N and uncertainty in detector efficiency.

In the data evaluation for JENDL-3, improvement of neutron emission data are one of highest priority. Then the evaluation of neutron emission cross sections employed updated nuclear model codes, the multi-step Hauser-Feshbach code GNASH and TNG, direct reaction code DWUCK or ECIS for consistent evaluation of neutron emission spectra and partial cross sections /6/. A versatile code system and the data base for the calculation was developed to systematize and simplify the calculation process /11/. In the evaluation, the experimental DDX data measured at Osaka and Tohoku Universities were utilized as references for emission spectrum and partial cross sections; this is especially the case for light elements for which theoretical prediction is rather difficult.

3. Data Status

In the following, recent experimental data are shown in comparison with JENDL-3 to clarify the present data status of fusion reactor materials.

3-1. Neutron multiplier; Be, Pb, Zr, Mo

Be and Pb are the most promising neutron multipliers, and special efforts were undertaken for (n,2n) cross section and emission spectrum.

Be: Experimental data at Osaka /8/ and Tohoku /9/ Universities for 14.1 MeV neutrons are in good agreement both in DDXs and (n,2n) cross section while their DDXs are systematically lower than those by Drake et al./12/ in low energy region. The results of (n,2n) cross section and DDX are shown in Table 1 and Fig.1, respectively. These (n,2n) cross sections are lower than that by Drake et al./12/ and JENDL-3T based on Drake's data by about 15 %, but agree with ENDL-86 evaluation for ENDF/B-VI/13/.

In the DDX, the experimental data are largely different from JENDL-3T both in shape and angular dependence. The JENDL-3T data were evaluated under the assumption that larger fraction of (n,2n) reaction proceeds through the sequential decay via the inelastic-scattering to *Be-9. The experimental data show much less pronounced peaks than JENDL-3T and suggest larger contribution of continuum neutrons through simultaneous breakup process. The analyses of emission spectra /8,9/ showed that the experimental data were reproduced consistently by considering 3- and/or 4-body simultaneous breakup process as shown in Fig.4 /9/.

In JENDL-3, the (n,2n) cross section was reduced (cf.Table 1) and the emission spectrum was modified by considering simultaneous breakup process to

Table 1; Be(n,2n) Cross Section at 14 MeV

Evaluation/ Experiment	cross section(b)	ratio to ENDF/B-VI
ENDF/B-VI(ENDL86)	0.485	1.00
ENDF/B-IV	0.536	1.11
ENDF/B-V	0.513	1.06
JENDL-3T	0.542	1.12
JENDL-3	0.482	1.00
Kneff et al (1986)*	0.506(±8%)	1.04
Measurements to 1978	0.491	1.01
LANL (1977)/12/	0.566(±14.8%)	1.17
Osaka Univ.(1984)	0.486(±6.2%)	1.10
Osaka Univ.(1987)/8/	0.478(±2.9%)	0.99
Tohoku Univ.(1988)/9/	0.492(±6.1%)	1.01

*Nucl.Sci.Eng., 92 491(1986)

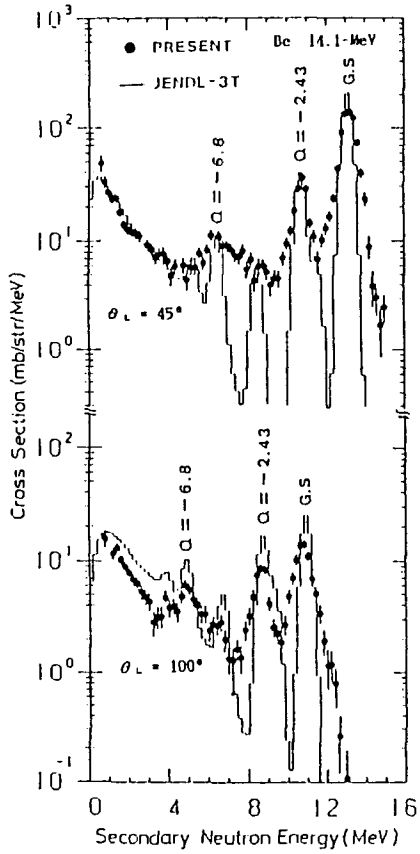

Fig.1 Be DDX at 14 MeV /9/

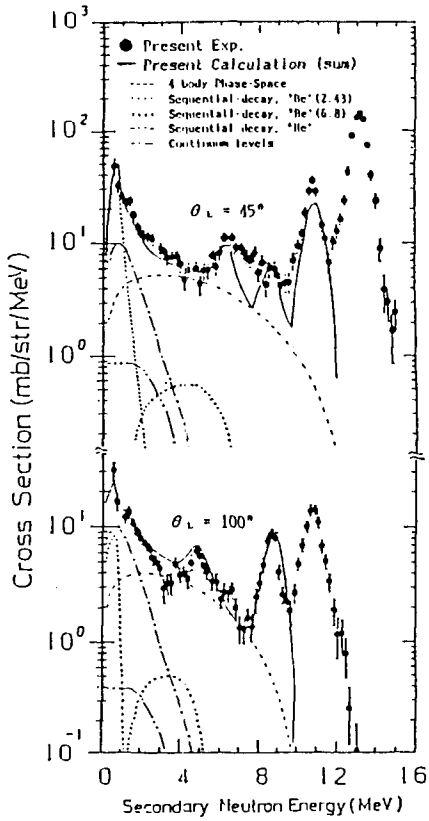

Fig.2 Analysis of Be DDX /9/

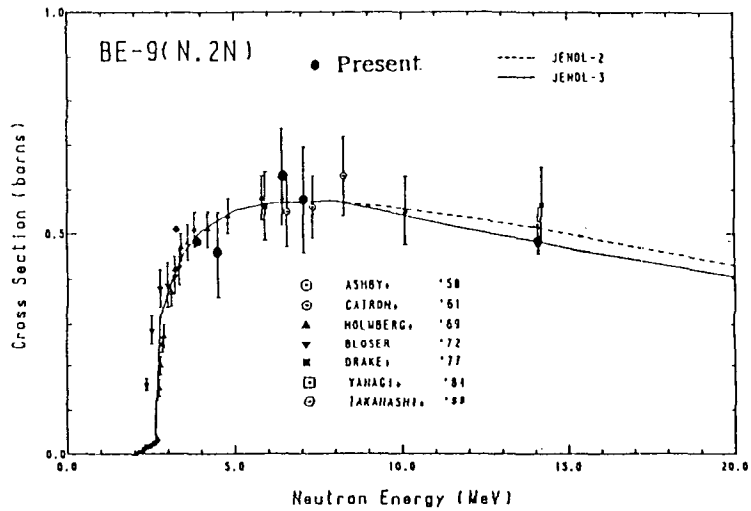

Fig.3 Be(n,2n) cross section /6/

be consistent with experimental observations. The JENDL-3 data are compared with the experiments in Figs.3 and 4; agreement is much improved and satisfactory. As shown in Fig.5, good agreement is confirmed also for the DDX at lower incident energies. Angular neutron flux measured for Be slab is also reproduced well by the analyses using JENDL-3 /14/. From these differential and integral data, the JENDL-3 data for Be seem adequate both in (n,2n) cross section and DDX.

Pb; The (n,2n) cross section and emission spectrum are shown in Table 2 and Fig.6, respectively. The experimental neutron spectrum in Fig.6 is that meas-

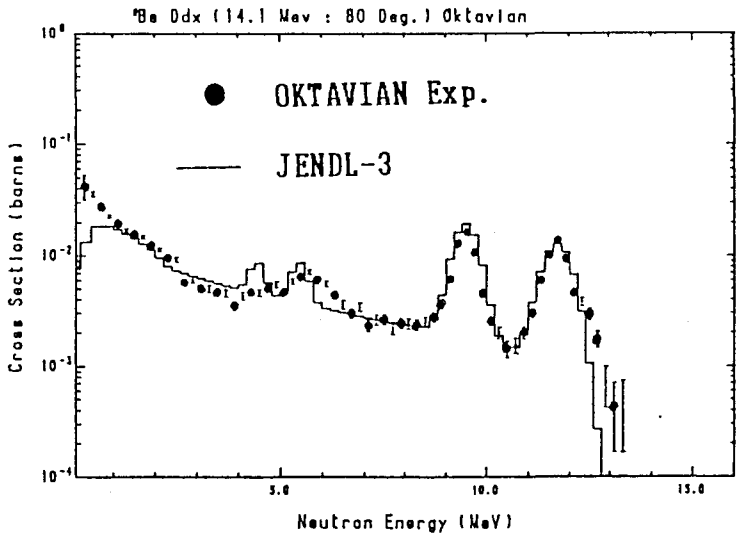

Fig.4 Be DDX at 14 MeV /8/

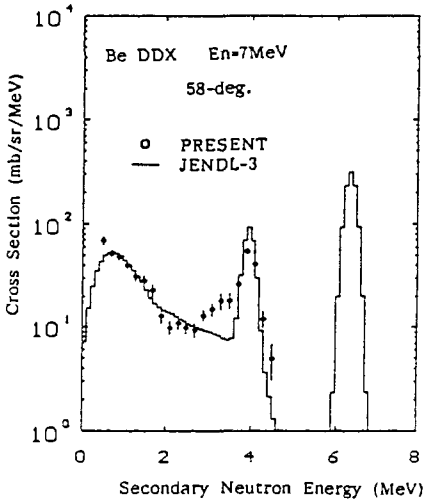

Fig.5 Be DDX at 7 MeV /9/

Table 2; Pb(n,2n) Cross Section at 14 MeV

Evaluation/ Experiment	cross section(b)	ratio to ENDF/B-VI
ENDF/B-VI	2.14	1.00
ENDF/B-IV	2.15	1.00
EFF-1	2.10	0.98
JENDL-3T	2.04	0.95
JENDL-3	2.18	1.02
Frehaut(1980)*	1.95(±7%)	0.91
Osaka Univ.(1984)	2.33(±5.2%)	1.09
Osaka Univ.(1987)/15/	2.43(±4.1%)	1.14
Tohoku Univ.(1988)/16/	2.21(±6.0%)	1.03

* to be revised about 10 % higher/2/

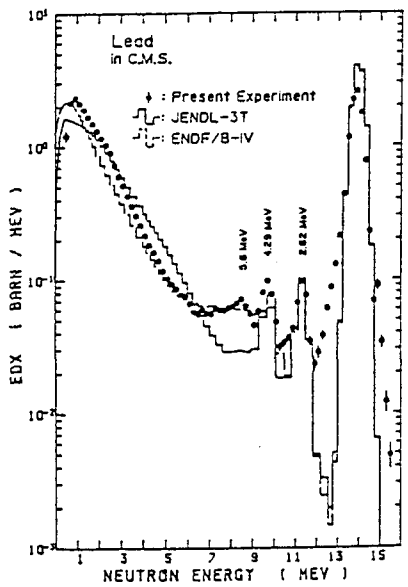

Fig.6 Angle-integrated neutron emission spectrum of Pb /15/

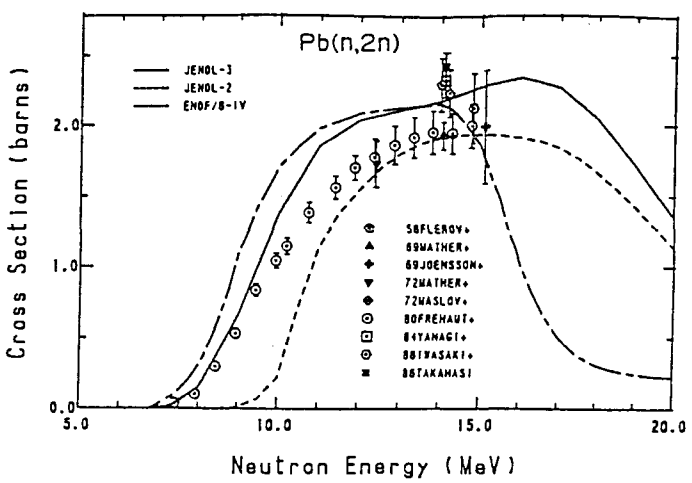

Fig.7 Pb(n,2n) cross section /6/

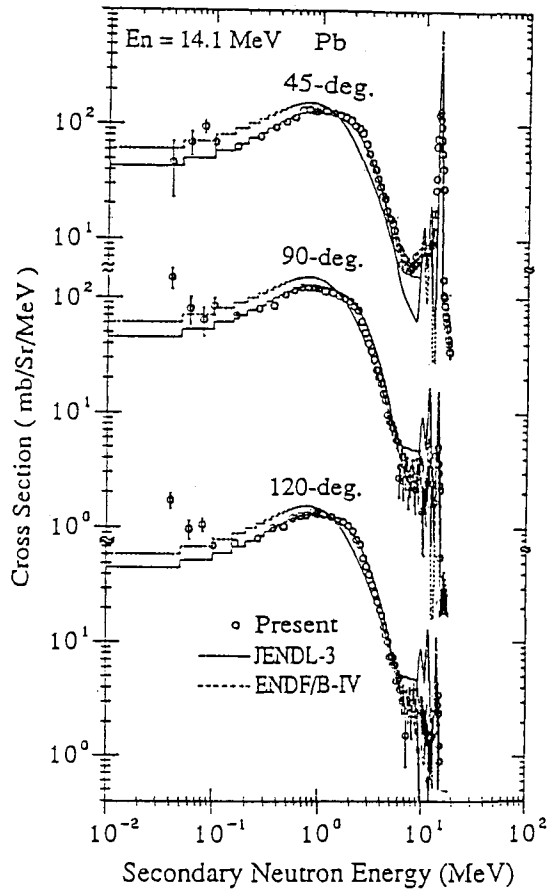

Fig.8 Pb DDX at 14 MeV /20/

ured at Osaka university /15/ and is in good agreement with that at Tohoku university /16/ and TU Dresden /17/ except for low energy region; these are softer markedly than JENDL-3T. The (n,2n) cross sections derived from these experiments are higher by several percent than JENDL-3T (cf.Table 2).

In JENDL-3, the (n,2n) cross section were raised by about 7%, as shown in Fig.7, to be consistent with averaged value of Frehaut /18/, Osaka /15/ and Tohoku /16/ Universities data. The emission spectrum was revised too by employing the level density formula by Ignatyuk et al /19/.

In Fig.8, the JENDL-3 data are compared with recent measurement at Tohoku university aiming at low energy part /20/. Agreement is very good down to about hundred keV except for high energy region where angular dependence is significant. Angular flux measurement for Pb slab reported similar observation /14/; therefore for further improvement of predictability, angular dependence of emission spectrum should be taken properly in file.

Zr,Mo; Experimental DDX for these nuclei are compared with JENDL-3 in Figs.9. For these nuclei, JENDL-3 systematically underpredicts the high energy neutrons probably because of improper fraction and/or energy distribution of neutron emission through pre-equilibrium process.

2-2 Li-6, Li-7

For these elements, JENDL-3T data were evaluated on the basis of DDX data at Tohoku /25/ and Osaka /26/ Universities, and the data were presented using pseudo-levels to take account of strong energy-angle correlation in emission spectra; therefore, JENDL-3T successfully interpreted DDXs and various integral data except that it underpredicted LLNL pulsed sphere experiments for Li-6 /23/. Then, for JENDL-3, revision was made only for the inelastic-scattering cross section of the second level of Li-7; this cross section

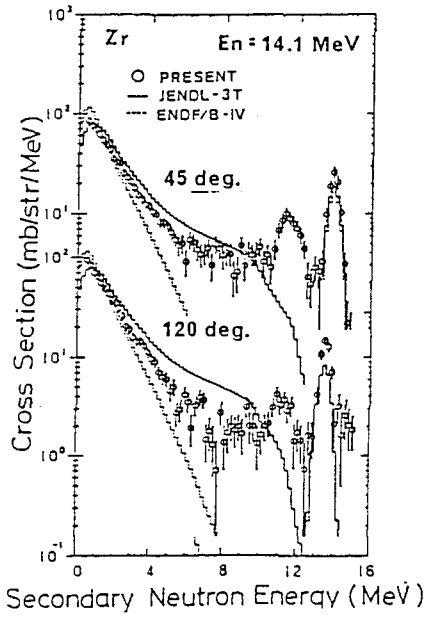

Fig.9 DDX of Zr and Mo at 14 MeV /9/

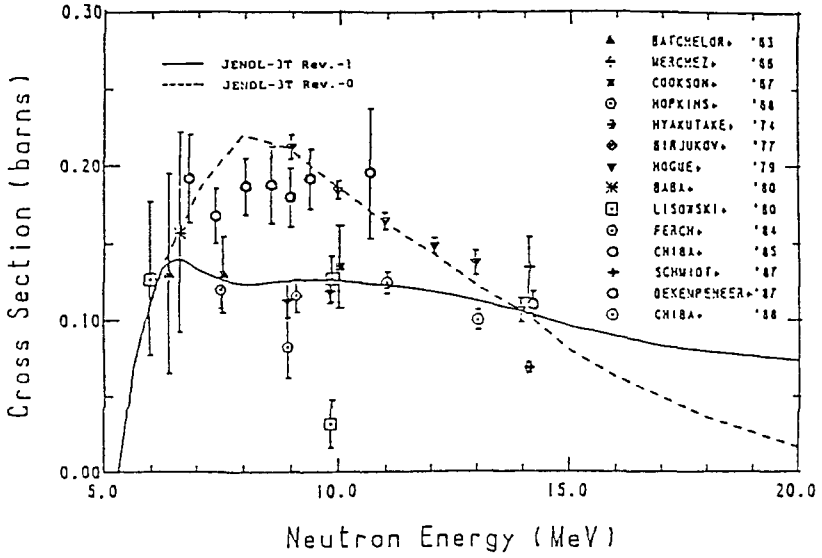

Fig.10 Li-7(n,n_2) cross section /6/

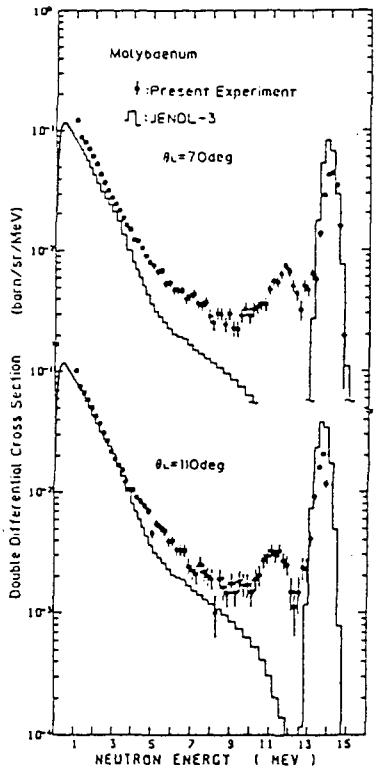

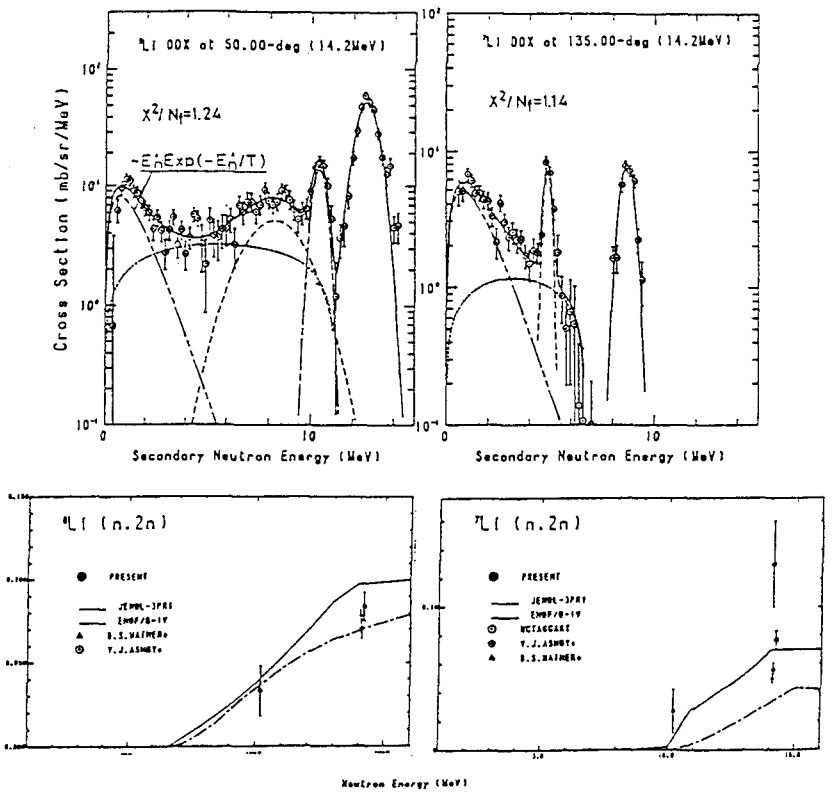

Fig.11 Neutron spectrum and cross section of Li-6,7(n,2n) reaction

was reduced significantly between 6 to 13 MeV, as shown in Fig.10, referring recent differential data at TU Dresden /24/ and JAERI /25/, keeping the tritium production cross section unchanged by compensating with the continuum neutron emission. The evaluated (n,2n) cross section of both elements are thought adequate too from the consistency between DDX and integral (n,2n) measurements as shown in Fig.11.

For Li-6, new experiments were made at Tohoku university /26/ to check the discrepancy between JENDL-3 and LLNL pulsed sphere data. DDX is shown in

Fig.12; this is in good agreement with previous data /21/ and shows higher values than JENDL-3 at higher energy region. The analyses of DDX, shown in Fig.13, suggest higher cross sections of discrete levels in Li-6. This might be of significant effect for the application to enriched lithium assemblies.

3-3. C, O

The JENDL-3T data were updated referring newest neutron DDX data and proved good enough for reproduction of integral data /23/. Therefore, only minor change was made for JENDL-3; that are the inelastic-scattering cross sections of second level in C, and cross section of discrete levels and energy distribution for O. Nonetheless, experimental DDX data of C show marked disagreement with JENDL-3 in the continuum region /26/, partly due to lack of energy-angle correlation in JENDL-3. These continuum spectrum are reproduced by considering simultaneous breakup mode similarly with the case of Be.

3-4 Structural Materials

The neutron emission spectrum data of JENDL-3T for structural materials were generally satisfactory as a result of adoption of modern nuclear model code and by referring experimental DDX data. Therefore neutron emission spectra and (n,2n) cross section were unchanged for most nuclei.

Figures 14 and 15 show respectively the examples of data comparison between JENDL-3 and experiments for Fe and Nb. For the case of Nb, also shown are the calculations using the Kalbach-Mann systematics /27/ to take account the angle dependence. Agreement is fairly good in spectral shapes for both nuclei. Recent measurements of low energy part for Fe are also in agreement down to around a few hundred keV /20/. Such agreement is seen for most of major structural materials, Al, Si, Cr, Ni, Cu.

For further refinement of the data, taking the angular dependence properly should be made using appropriate theoretical model or practical systematics. In Fig.15, Kalbach-Mann systematics reproduces fairly well the experimental DDX while it overemphasizes the forward rise as seen generally for other cases /28/. New systematics was proposed by Kalbach /29/ and Kumabe et al. /30/ to improve the predictability. Example of the comparison is shown in Fig.17 /31/. As shown in this figure, Kumabe's systematics gives better fit for medium-weight nuclei as well as Kalbach's one. Nonetheless, for lighter elements, Zr, Cu, Fe, these systematics still overpredict the forward rise as shown in Fig.18. Therefore, further studies will be needed including dependence on target mass and energy.

3-5 Th, U;

Th and U are known to very effective neutron multiplier through the neutron multiplication by fission. However, there have been reported very few data on neutron emission. Recently, measurement were performed at Tohoku university at several incident energies /11,32/. Figure 19 shows the results. In the case of Th, JENDL-3 reproduces fairly well the experiment except for middle energy region. For the case of U, JENDL-3 underpredicts high energy neutrons because of lack in pre-equilibrium components.

The angular distribution for both nuclei were found to be steeper than lighter elements and reproduced by Kalbach-Mann systematics if fission neutron spectrum is assumed to be angle-independent /11,32/.

4. Summary

Recent experimental data of neutron emission cross section are reviewed in comparison with JENDL-3. The experimental data at Osaka university and Tohoku university show general agreement and are providing a systematic data base which will be useful for refinement of evaluated neutron emission data.

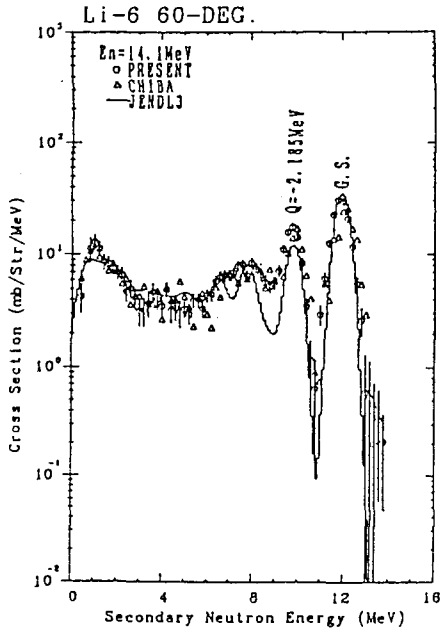

Fig.12 Li-6 DDX at 14 MeV /26/

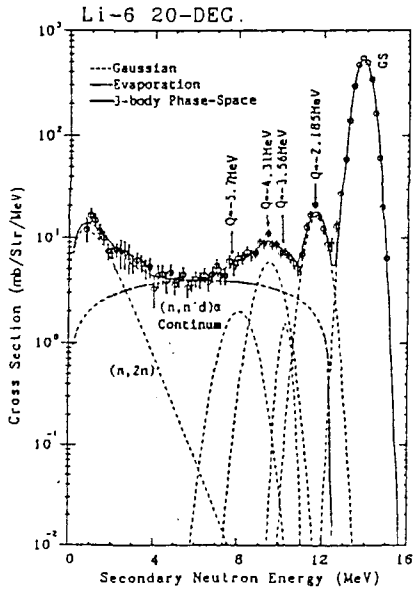

Fig.13 Analysis of Li-6 DDX

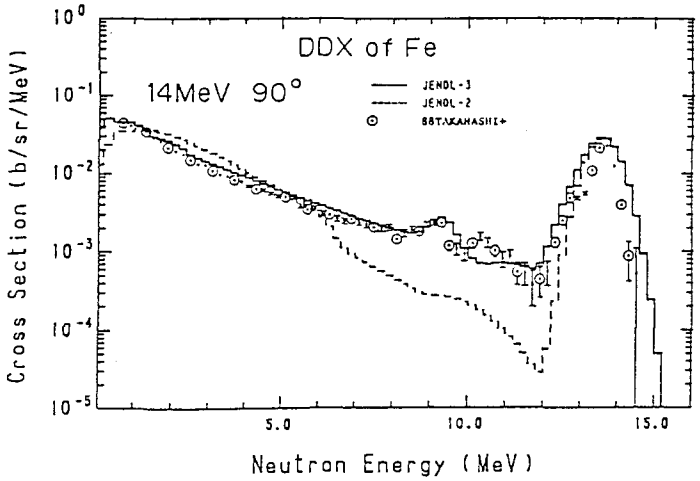

Fig.14 Fe DDX at 14 MeV /15/

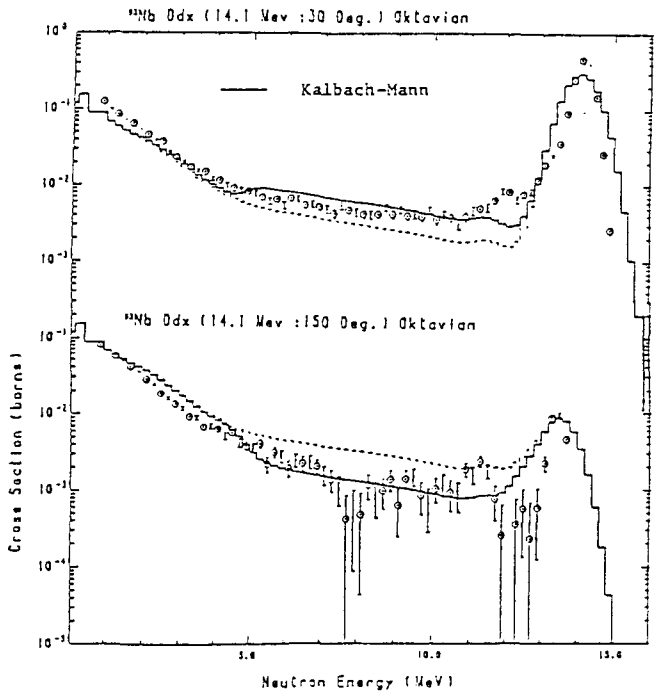

Fig.15 Nb DDX at 14 MeV;
Dot line shows JENDL-3

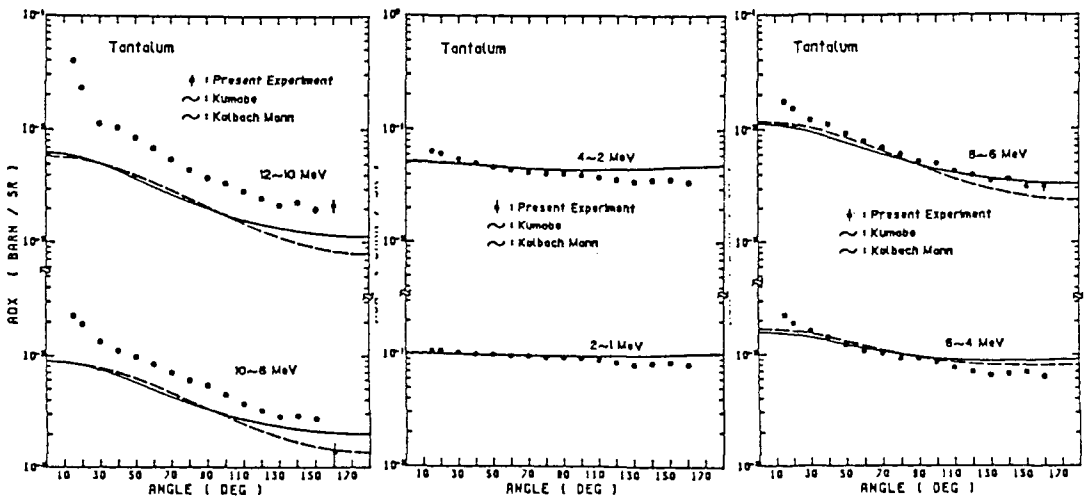

Fig.16 Angular distribution of continuum neutrons; Ta, 14MeV/31/

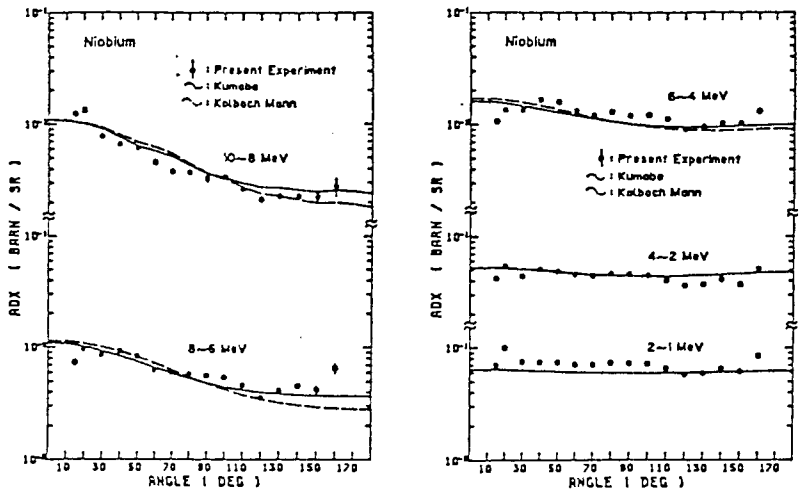

Fig.17 Angular distribution of continuum neutrons; Nb, 14MeV /31/

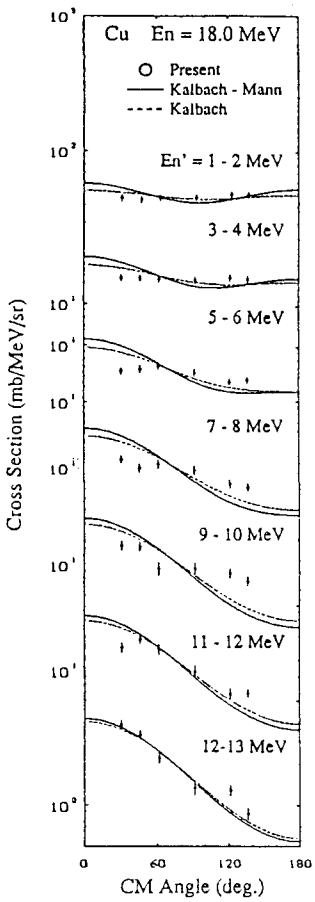

Fig.18 (right) Angular distribution of continuum neutrons; Cu,18MeV/9/

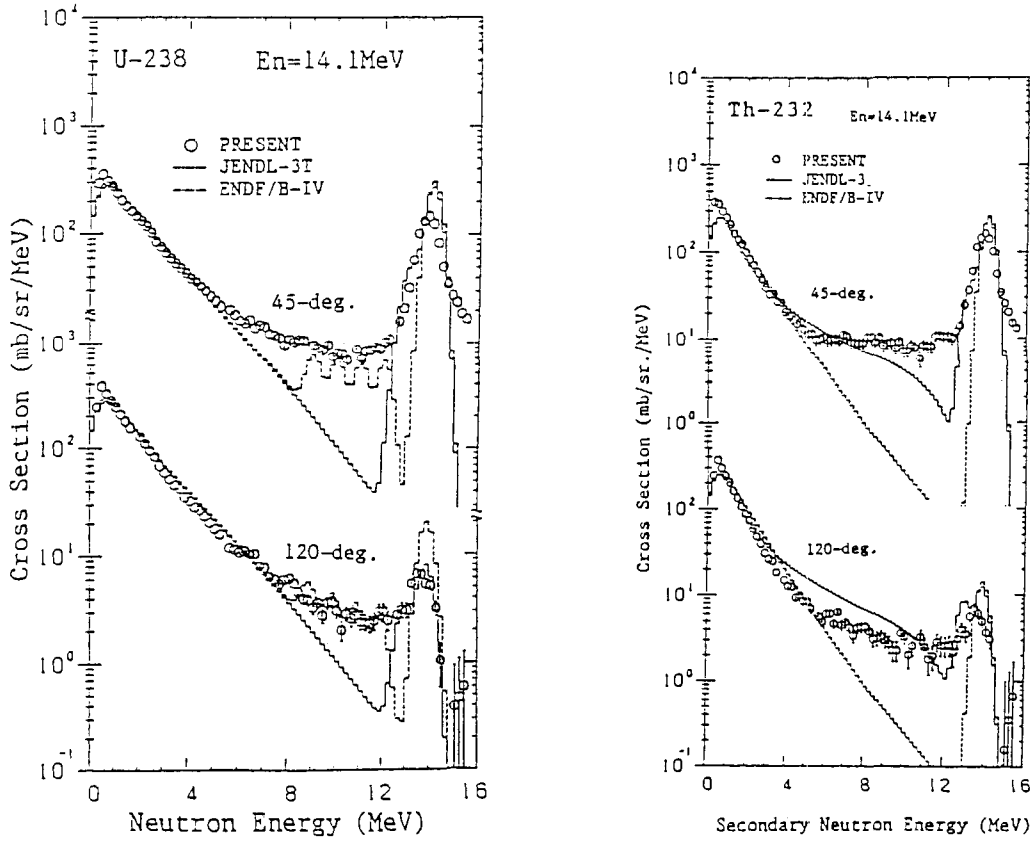

Fig.19 DDX of Th and U at 14 MeV /10/

From the data comparison, the JENDL-3 data proved to reproduce satisfactorily the differential neutron emission data both in spectral shapes and magnitude except for some cases, Zr, Mo, Th and U. In particular, (n,2n) cross section and emission spectrum of Be and Pb are much improved and seem adequate for fusion reactor neutronics calculation. However, to remove the existing discrepancy, inclusion of energy-angle correlation in emission neutron will be indispensable using File-6 in the present file or ENDF/B-VI format.

References:

1.C.Y.Fu & D.M.Hetrick: Trans.Am.Nucl.Soc.,53 409 (1986)
2.H.Gruppelaar:Proc.Int.Conf."Nucl.Data for Sci.& Technol.",Mito 1988,p.455
3.S.Pellori & E.T.Chen: Ref.2, p.267
4.P.G.Young: Ref.2, p.599
5.H.Maekawa: Proc.IAEA Advisory Group Meeting " Fusion Reactor Technol." 1986, Gaussig (IAEA 1986)
6.K.Shibata et al.: JAERI 1319 (JAERI 1990)
7.A.Takahashi et al.: J.Nucl.Sci.Technol.,25 215(1988)
8.A.Takahashi et al.:Ref.2, p.205
9.M.Baba et al.: Ref.2, p.209
10.M.Baba et al.: J.Nucl.Sci.Technol.,27(7) 601(1990)
11.N.Yamamuro: Ref.2, p.489
12.D.M.Drake et al.: Nucl.Sci.Eng.,63 401(1977)
13.S.T.Perkins et al.:Ibid.,90 83(1985)
14.H.Maekawa: JAERI-M 90-0125 (JAERI 1990) p.69
15.A.Takahashi: ibid, p.279
16.S.Iwasaki et al.:Ref.2, p.229
17.T.Elfurth et al.:INDC(GDR)-044/G1, INT(86)-12(1986)
18.J.Frehaut et al.:BNL-NCS-51245(1980) p.399
19.A.V.Ignatyuk et al.:Sov.J.Nucl.Phys., 21 256(1975)
20.K.Maeda et al.: Fall Meeting of Jap.At.En.Soc.,B-3
21.S.Chiba et al.: J.Nucl.Sci.Technol.,22 771(1985)
22.A.Takahashi et al.: ibid, 21 577(1984)
23.H.Maekawa: JAERI-M 88-065 (JAERI 1988)
24.D.Schmidt et a.: Nucl.Sci.Eng.,96 159(1987)
25.S.Chiba et al.: J.Nucl.Sci.Technol.,25 210(1988)
26.M.Baba et al.:Ref.14, p.383
27.C.Kalbach & F.M.Mann: Phys.Rev.,C23 112(1981)
28.P.E.Hodgson et al., Radiation effects 92-96 1033(1986)
29.C.Kalbach: Phys.Rev.,C37 2350(1988)
30.I.Kumabe et al.: Nucl.Sci.Eng.,104 280(1990)
31.A.Takahashi et al.: to be published from IAEA
32.M.Baba et al.: JAERI-M 89-143 (JAERI 1989, in Japanese)

THE BERYLLIUM SECONDARY NEUTRON SPECTRA INDUCED BY 14.7 MeV NEUTRONS

Zhang Kun, Wan Dairong, Dai Yunsheng and Cao Jianhua

Institute of Nuclear Science and Technology of Sichuan University, Chengdu 610064, Sichuan, P.R. China

Abstract: The beryllium energy-angular secondary neutron spectra induced by 14.7MeV neutrons have been measured with an associated partical time of flight spectrometer at the laboratory angles of 15, 25, 35, 45, 60, 75, 90, 105, 120 and 135 degrees. The flight path of secondary neutrons is 254cm. The threshold is 0.9MeV for the spectronmeter and the time resolution is about 1.5ns. The effective energy range is 1.0 MeV to 14.7 MeV for the secondary neutron energy spectra and the statistical error is 4-10%.

(Neutron emission, Double Differential Cross Sections, ^{9}Be, 14.7Mev, Secondary Neutron Spectra)

I. INTRODUCTION

The double differential neutron scattering cross sections and energy-angular neutron spectra of fusion reactor structural material are the basic and important nuclear data for neutronic design of fusion reactors. Since beryllium's unique characteristic of emitting two neutrons for each inelastic neutron interaction and often considered as the first structural material,the data for beryllium is especially important. The neutrons emitted from berylium can be used to produce tritium, one of the major components of the reactor. To calculat the tritium breeding rate in proposed reactor vessel walls requires detailed knowledge of the energies and angular distributions of the neutrons emitted from beryllium under the bombarding of energetic neutrons.

Some of the experiments of Beryllium were reported for incident neutrons of 5.9,10.1 and 14.2MeV<1>, and 14.1, 18.MeV <2,3>, and so on. In our work, We measured the angular distributions of the neutron emission spectra from beryllium at incident neutron energy of 14.7MeV. Now we are going to compare the data with the reported experiments and other evaluated data concerning the emission spectra and partical scattering cross sections derived from the energy-angular neutron spectra and double-differential neutron scattering cross sections. The reaction mechanism of Be(n,2n) will be studied in near furture. So, only the energy-angular secondary neutron spectra are given in this paper.

II. EXPERIMENTAL METHOD

To measure energy-angular continuum spectra of the beryllium (n,2n) reaction, the monoenergetic neutrons are essential. The primary monoenergetic neutron source in our experiment was obtained via the $T(d,n)^{4}He$ reaction with solid

trium-loaded titanium targets which were cooled by water. The emission angle is 39-degrees and the primary neutron energy is 14.7MeV. The measurements were carried out with an associated partical time of flight spectrometer at 10 laboratory angles.

The secondary neutron detector is consisted of a 100mm-diam x 50mm-thick NE213 liquid scintillator directly coupled to an XP-2401 photomultiplier. It was placed in a massive shield which was mede up of Li_2CO_3, paraffin, Fe and Pb,and set on a turning table.The neutron-gamma discrimination was completed by the CANBERRA, PSD-2610 NIM model based on the zero-crossover technique. The temperature affection for the stability of the PSD circuit is quite remarkable. When the temperature of the laboratory kept constant, the drift of the PSD bias was negligible.In this case,the neutron spectronmeter threshold is 0.9MeV, the time resolution is 1.5ns and the effective energy range is 1.0MeV to 14.7MeV for the secondary neutron energy spectra.

The scattering samples were machined into the shape of right circular cylinders, 40mm-diam x 20mm-thick for the beryllium sample , 33.8mm-diam x 24.5mm-thick for the polyethylene and 40mm-diam x 35mm-thick for the carbon, separetly. These samples were placed 10cm away from the target.

The time-of-flight information of the secondary neutrons was digitized into about 0.28ns per channel by CANBERRA TIME ANALYZER MODEl 2043 (TAC) and CANBERRA ADC 8075. The TAC was started by a pulse of neutron from the constant fraction discriminator and the stop pulse originated from Alpha detector. The data of time spectra were stored in Apple-IIe Computer.

The relative detector efficiency curve was determined by measuring the elastic scattering neutrons from the (n,p) reaction with polyethylene sample and (n,c) reaction with carbon in the neutron energy ranging from 0.98MeV to 14.5MeV. An efficiency plots are shown in Figure 1. The efficiency calibration error, considering statiatical error only,is about 1-2.5%,and the error is about 3% near the threshold point.

III. DATA ANALYSIS

To eliminate the counter of discrete levels of carbon in the polyethylene time spectra for the efficiency calibration, the spectra of carbon and polyethylene samples were measured simultaneously at each angle, and the peak counter of discrete levels were normalized in the standard of the elastic scattering peak for the time spectra of carbon. Figure 2 presents the time spectra of polythylene and carbon at 45 laboratory degrees.

For the time spectra acquired with an associated partical time of flight spectrometer, the channal caunterson the right in elastic peak were not correlative each other and

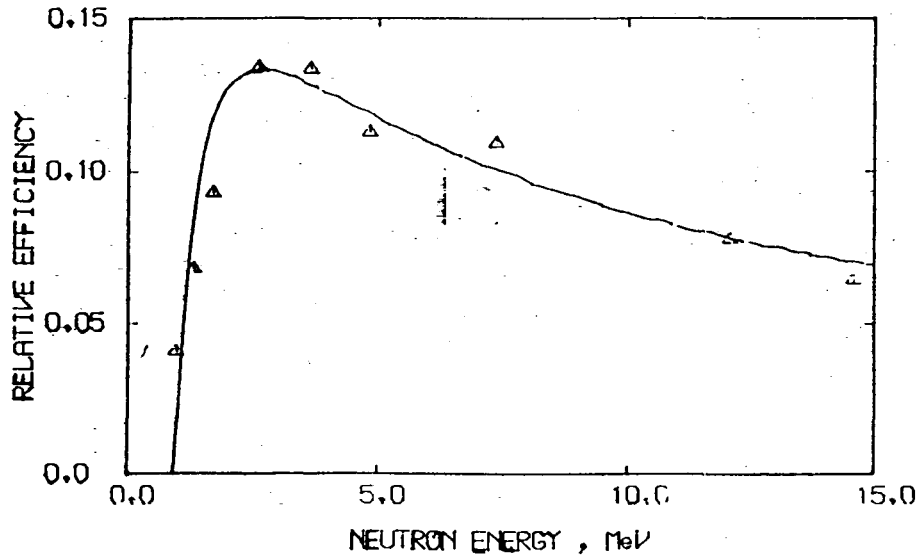

FIG.1 RELATIVE EFFICIENCY OF THE NEUTRON DETECTOR VERSUS ENERGY

were only accidental coincident. The everage counter of these channels is named average background for the time spectra. The effective time spectra were obtained via the counter of every channel minus the average background.

The time secondary neutron spectrum of beryllium and its background spectrum at 75 degrees are shown in Figure 3. For the background spectrum, there is no different betwent the high energy side and the low energy side. Their average values are equal.

In the nonrelativistic condition, the flight time of neutron is as following(4):

$$t(ns)=72.298L(1+0.798\times10^{-3}E)/\sqrt{E} \qquad (1)$$

here L is the flight path of the secondary neutron with energy E. Therefore, the channel address ni of the neutron with energy Ei can be determined by the following function for the time spectra:

$$ni=ne-72.298[(1+0.798\times10^{-3}Ei)/\sqrt{Ei} - (1+0.798\times10^{-3}Ee)/\sqrt{Ee}]L/W \qquad (2)$$

here Ee and ne are the scattering neutron energy and channel addess, respectively; W is the channel time width of the time spectrum.

Using this formula, secondary neutron energy spectra can be obtained from the time spectra. According to the energy resolution of the spectrometer, each of nine channels we added in calculation togather in energy range of less than 5MeV, and so did for each of five channels in 5-8MeV and three channels in 8-10MeV for time spectra. Near the elastic peak, energy spectra were calculated channel by channel.

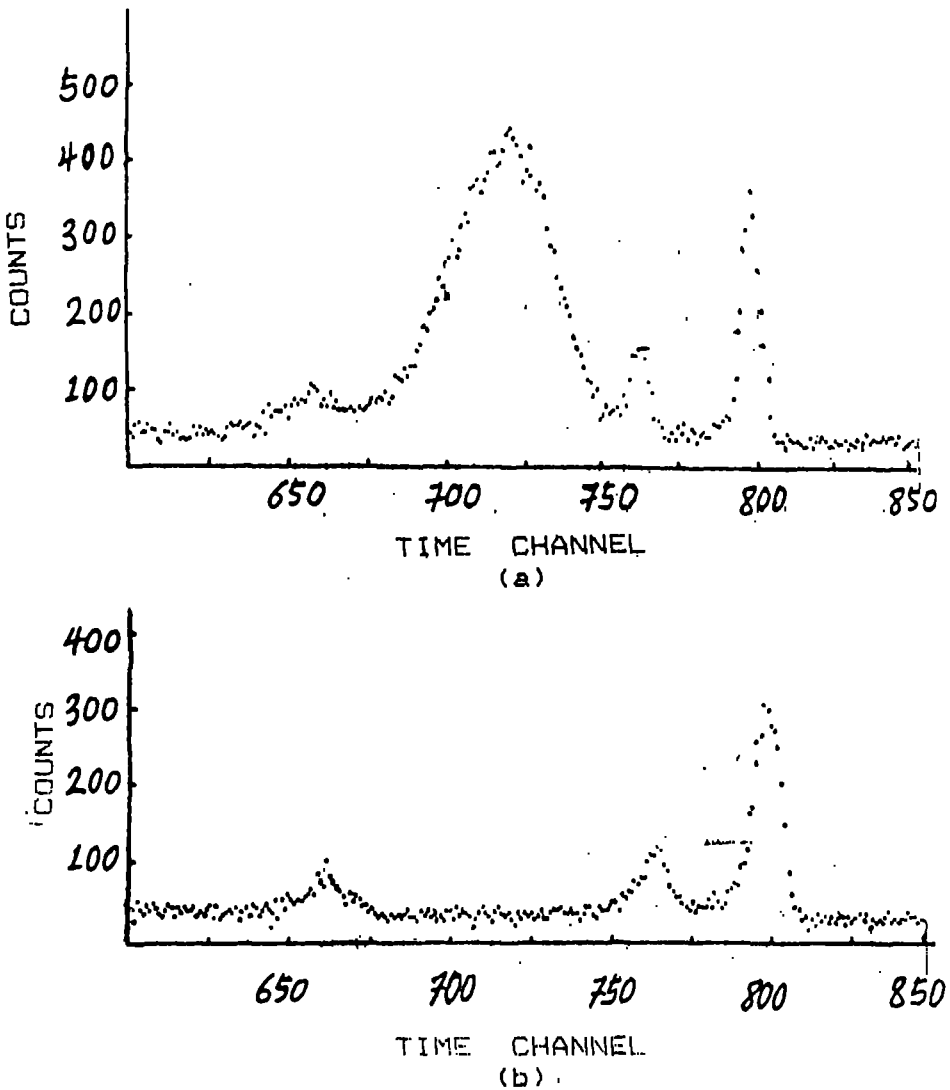

FIG.2. Emission neutron Time-of-Flight spectra from polyethlene (a) and carbon (b) at 45 degrees

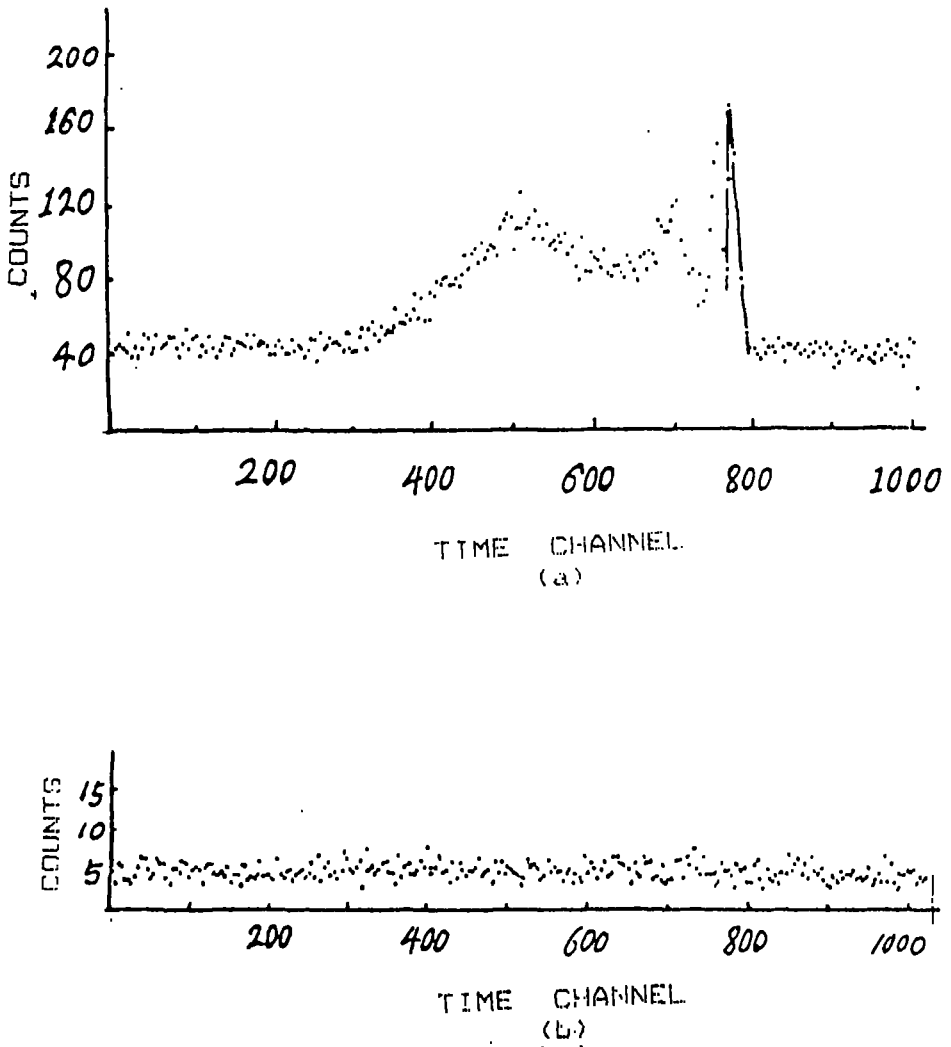

FIG.3. Emission neutron Time-of-Flight spectra from beryllium (a) and its background (b) at 75 degrees

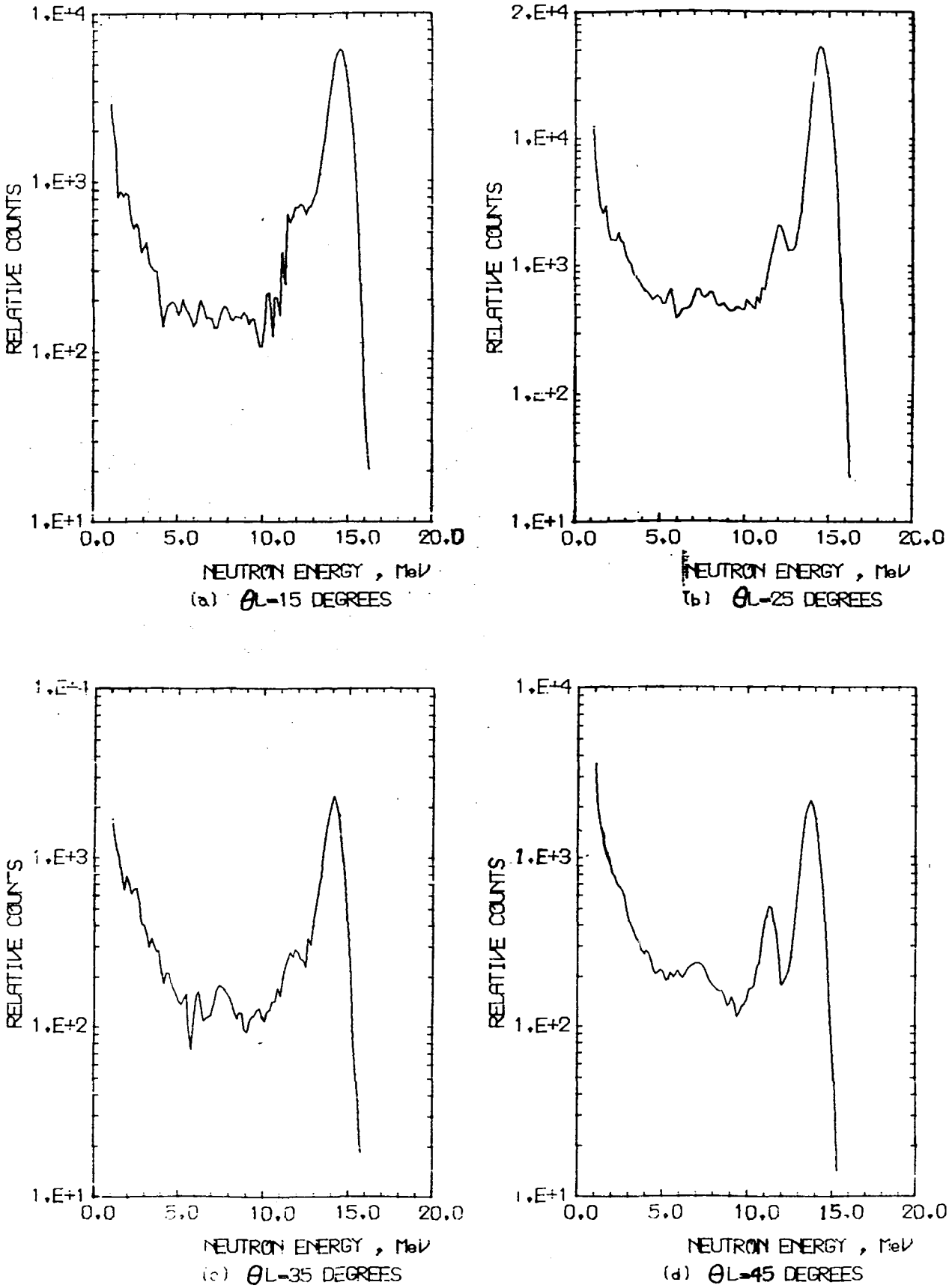

FIG.4 EMISSION NEUTRON SPECTRA OF BERYLLIUM AT THE LABORATORY ANGLES OF 15,25,35,45.60,75,90.105,120,135 DEGREES BY INDUCED 14.7MeV NEUTRONS

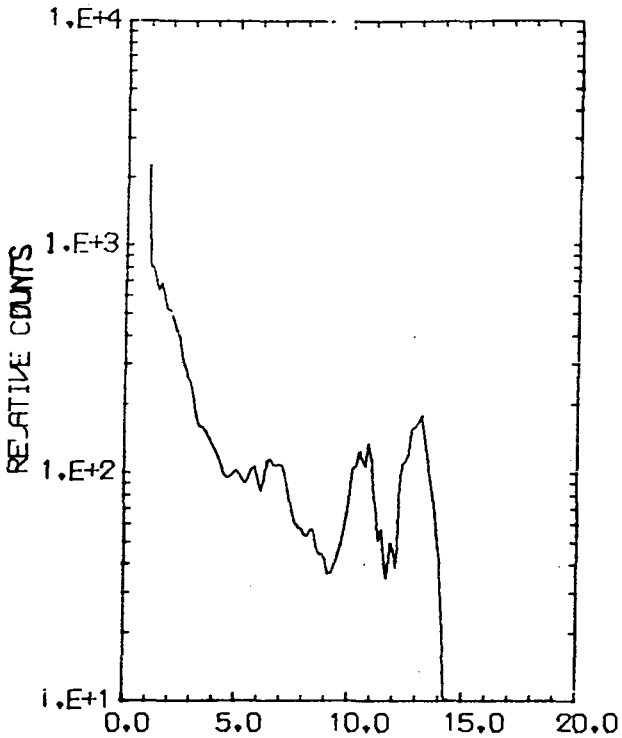

(e) θL=60 DEGREES

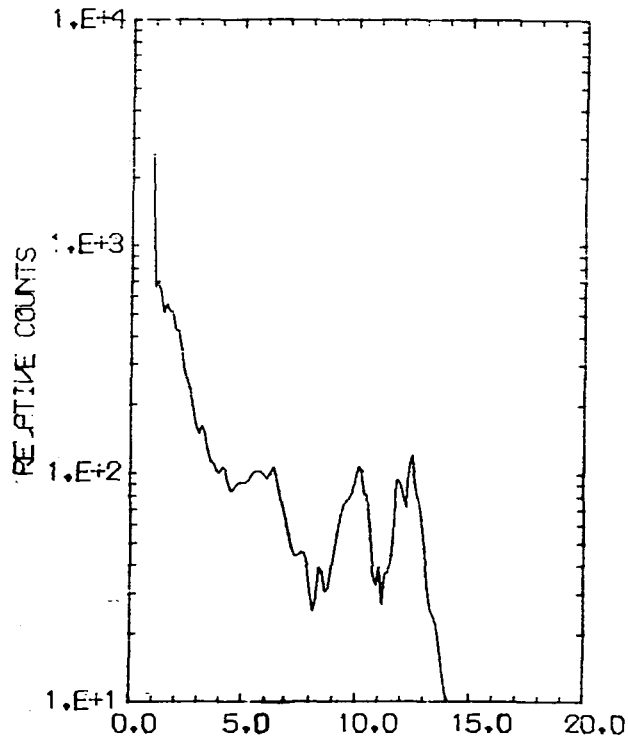

(f) θL=75 DEGREES

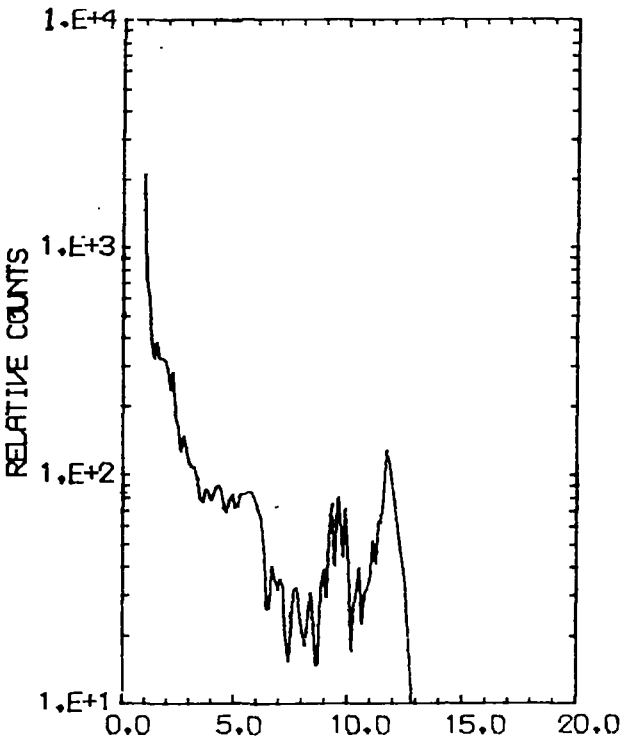

(g) θL=90 DEGREES

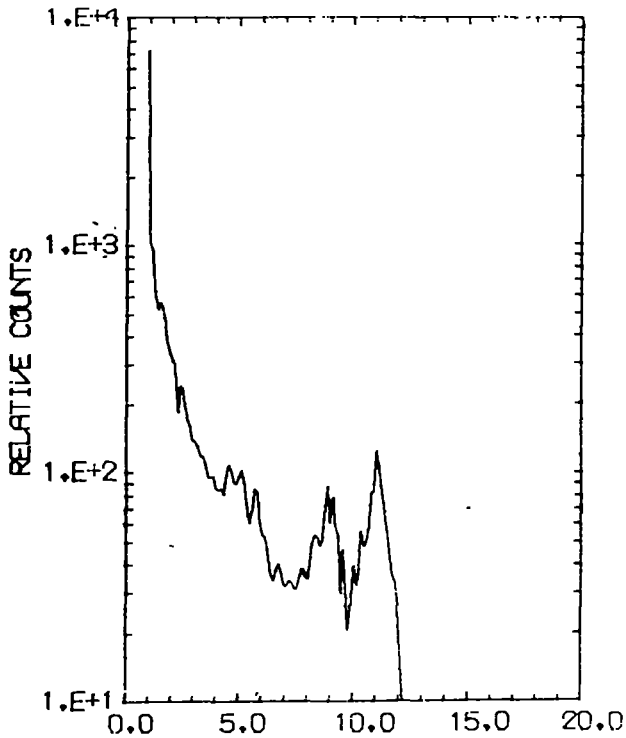

(h) θL=105 DEGREES

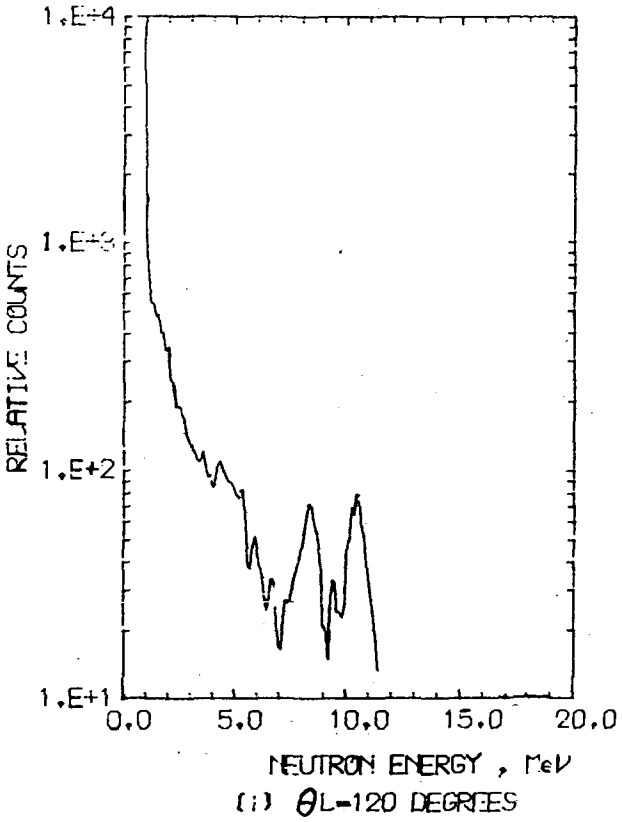

(i) θL=120 DEGREES

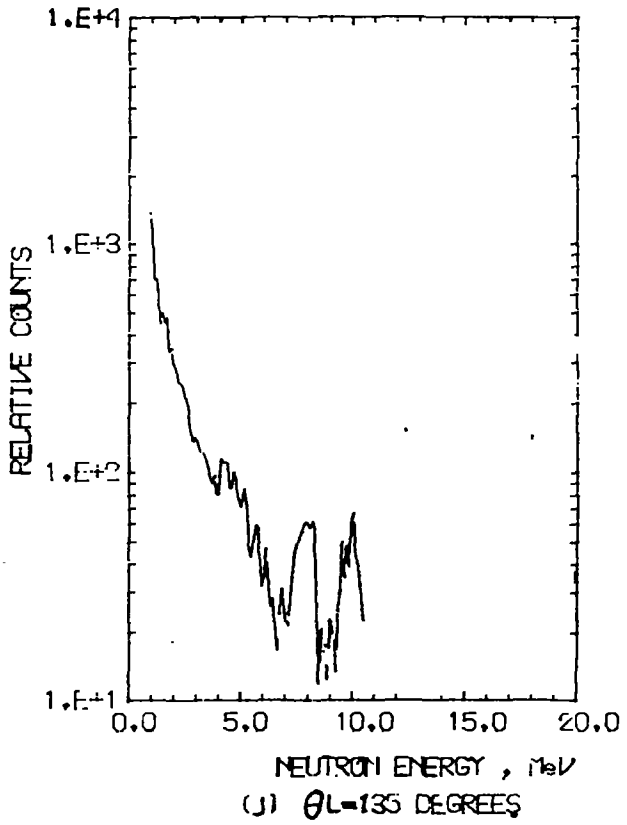

(j) θL=135 DEGREES

IV. RESULTS AND DISCUSSION

The energy-angluar neutron spectra for 14.7MeV incident neutron energy are shown in Figure 4. These spectra are given at 10 labortory angles. The error of the spectra is about 4% in the energy range of 1-5MeV, 7% in 5-8MeV and 10% in 8-14%MeV. It contains only statistical error, and the multiple scattering correction is not calculated yet. The statistical uncertainty of elastic peak is about 2.5% for small angles and 7.5% for large angles.

Some of the discrete levels have been acquired in our experiment such as 1.69-,2.43-,2.8-,3.06-,6.76-,7.94-MeV,which agreed with other experiement. In addition, we also obtained other levels such as .54-,.80-,1.06-,1.36-,1.94-,3.31-, 3.66-, 4.19-, 4.79-, 5.28-, 5.65-, 8.59-, 8.866-, 9.5-,10.18-,10.60-, 11.53-, 11.87-, 12.10-, 12.39-, 12.64-, 12.90-MeV, and so on. Usually, for these levels states in Be, the scattering cross section are too small to be measured. The levels above 9.5MeV at the angles large than 90 degrees and above 11.5MeV at the angles large than 60 degrees were not obtained because of the existence of the reaction threshold.

REFERENCES

<1> D. M. Drake et al.,Nuclear Science and Engineering. 63,401-412,(1977).

<2> B. Mamour et al., Nuclear Data For Science and Technology,1988MITO,209-212.

〈3〉 T. Akito et al.,Nuclear Data For Science and Techology, 1988MITO, 205-208.

〈4〉 G. Shen et al.,Chinese Journal of Nuclear Physics, Vol.3,No.4,288-297(1986).

DIFFERENTIAL NEUTRON EMISSION CROSS SECTIONS AND NEUTRON LEAKAGE SPECTRUM FROM BERYLLIUM AT 14 MeV.

B.V.Zhuravlev, A.A.Androsenko, P.A.Androsenko, B.V.Devkin, M.G.Kobozev, A.A.Lychagin, S.P.Simakov, V.A.Talalaev
A.S.Krivzov, S.I.Dubrovina
Institute of Physics and Power Engineering, Obninsk, USSR

Abstract

Differential neutron emission cross sections and neutron leakage spectrum from beryllium have been measured using time-of-flight technique at incident neutron energy 14.1 MeV. Comparison of our neutron emission spetra with experimental data known at the present time and with evaluation data from ENDF/B-V1 library demonstrates, that the agreement is unsatisfactory. Neutron leakage spectrum have been compared with calculation result on BRAND code with data file from ENDF/B-V1. Discrepancies are discussed.

1. INTRODUCTION

The energies and angular distributions of the neutron emission from beryllium are impotant for the transport and shielding calculation of fusion reactor, because of the beryllium is supposed to be used as a neutron multiplier material in conceptual design of fusion reactors. Several differential cross section measurements /1÷3/ and benchmark experiments on neutron leakage from sphere with a neutron source in center /4÷5/ have been performed, but the situation is not satisfactory. Famous neutron data libraries predict leakage spectrum with a considerable differences /6/. So we decided to contribute on measurement of double-differential neutron emission cross section from Be at incident energy 14.1 MeV. Neutron leakage spectrum have been measured on the same experimental technique earlier /4/. Here we compare this data with the calculation result obtained on BRAND code /7/ with neutron data file from ENDF/B-V1 /8/.

2. EXPERIMENT

The geometrical arrangement of fast neutron spectrometer is shown in fig.1. The neutron generator operated in a pulsed regime with the following parameters: energy of accelerated deutrons

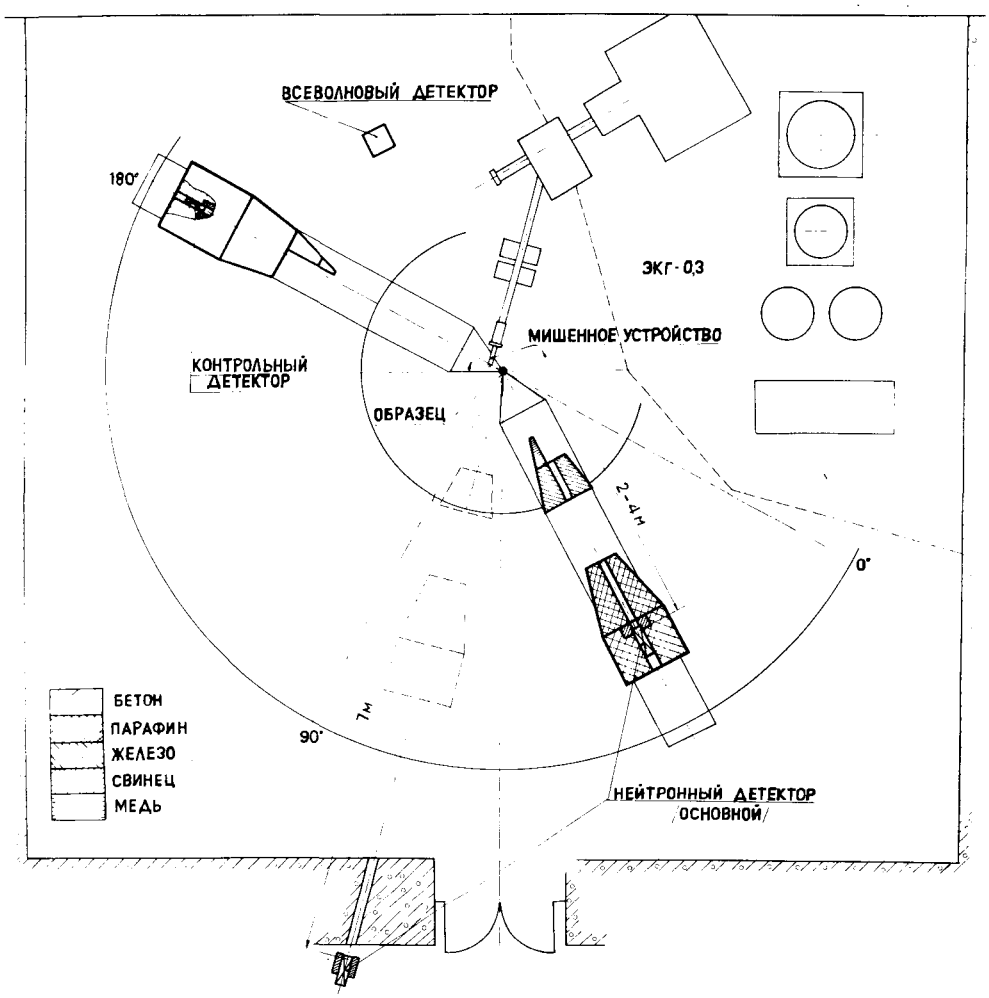

Fig.1 The geometrical arrangement of fast neutron spectrometer.

was 250 keV with pulse width 2.0 ns and 2.5 MHz repetition rate, the mean deutron current was 1.5 A. The neutron yield of about 10^8 neut./s was produced in a air cooled solid TiT target. A berillium sample allocated at 90^o relative to the deutron beam, at 12 cm of distance from the target had a hollow cylinder form with 2.81 and 4.0 cm inner and outer diameters, 5 cm height and 59.1 g of weight. The incident neutron energy was 14.1 $\pm$ 0.1 MeV.

Scattered neutrons were registered by a detector consisted of a NE-218 liquid scintillator of 10 cm diameter and 5 cm length coupled with a XP-2041 photomultiplier. The detector was placed in a massive shield composed of paraffin and LiH mixture. The direct neutron flux from the target was attenuated by shadow bar of iron and copper. The shield could be automatically rotated around the sample to perform the measurements at different angles from 30 to 150 in step of 30.

The spectrometer energy resolution with the flight path of 309 cm and 3 ns overall time resolution was 1.4 and 0.03 MeV at 14 and 1 MeV.

The generator pulse mode was controlled by a time-of-flight monitor consisted of fast plastic scintillator SPS-156 of Ø2xh2 cm and FEU-87 photomultiplier. The time resolution of this detector measured by $\gamma-\gamma$ coincidence technique was 0.4 ns at 0.5 MeV γ-energy threshold. The TOF Monitor measured the TOF spectrum of source neutron simultaneously with main detector. A Long Counter was used also for monitoring the neutron yield from target and making possible normalization of different runs.

The neutron detector efficiency was experimentally determined by two methods. In the first one, a specially designed ^{252}Cf ionization chamber ($2 \cdot 10^5$ fission rate) replaced the sample. Spectrum of prompt neutrons was measured by TOF method. The detector efficiency was then reduced from comparison of measured spectrum with standard one /9/. In the neutron energy range above (6-8) MeV, where the statistical accuracy of measurement on ^{252}Cf become poor, the efficiency was measured relative to (n-p) scattering cross section /10/. In this case we replaced a sample by the fast scintillate detector based on a stilbene crystal (Ø1 x h4 cm), which gave the stop pulses for the time-of-flight separation of hydrogen scattered neutrons. The efficiency measured relative to (n-p) scattering was normalized to californium one in overlapping energy interval. The energy threshold determined by extrapolation of the efficiency curve to zero was about 0.2 MeV.

The stability of the detectors and electronies was checked by long time measurements with radioactive sources. Moreover the main detector efficiency was measured several times during the whole experiment. The mean square deviations of different measurements estimated the unstability as (2÷3) %.

The acquisition procedure consisted of sequential measurements with the sample in and out, passing the selected angles several times. The cross-section was determined by comparison with (n-p) scattering cross-section (as described above) and by aluminum foil activation method. In later case, two Al foils (1.9 x 0.1cm) replaced the sample and were irrariated during the $T_{1/2}$=15 h period, the target neutron yield was monitoring by Long Counter. The activity of irradiated foils was then measured by $\beta-\gamma$ coincidences spectrometer. This data and the standard Al(n,α) reaction cross-section /10/ were used for calculation of the incident neutron flux at sample position.

3. DATA REDUCTION

In the data reduction at first the TOF spectra and corresponding monitor counts accumulated a teach definite angle were summed. Then the effect spectra were calculated as a difference of spectra obtained with the sample in and out taking into account the possible different counts of monitors. After that the TOF spectra were transformed into energy one ($N(E,\Theta)$) and double-differential cross-sections were calculated by expression

$$\frac{d^2\sigma}{dE\cdot d\Omega} = \frac{N(E,\Theta)}{\varepsilon(E)\cdot\Omega_D\cdot M\cdot F\cdot cor(E,\Theta)} \quad , \qquad (1)$$

where: $\varepsilon(E)$ - is the absolute neutron detector efficiency,
Ω_D - is the solid angle subtended by the detector,
M - is the total number of sample nuclei,
F - is the integral neutron flux, to which the sample was irradiated during the experiment,

$cor(E,\Theta)$ - is the correction for attenuation of in - and out - coming neutron fluxes and multiple scattering in the sample. It is obvious that there is a direct dependence between F and monitor counts N_M

$$F = k\cdot N_M \quad , \qquad (2)$$

where k - is unknown factor, that should be determined to make absolute normalization of measured spectra. It was mentioned above that it was performed experimentally by two methods.

In case of Al - foils activation method, the corresponding values F_{Al} and N_M^{Al} are measured directly, hence the factor k can be determined from

$$k = F_{Al}/N_M^{Al} \quad . \qquad (3)$$

Then $$\frac{d^2\sigma}{dE\cdot d\Omega} = \frac{N(E,\Theta)}{\varepsilon(E)\cdot\Omega_D\cdot M\cdot cor(E,\Theta)}\cdot\frac{N_M^{Al}}{N_M\, F_{Al}} \quad , \qquad (4)$$

In the second case the neutron flux or factor k were deduced from (n-p) scattering

$$F_H = k\cdot N_M^H = \frac{N_H}{\sigma_H/4\pi\cos(\Theta)\cdot\varepsilon(E_H)\Omega_D\cdot M_H\cdot cor_H(\Theta)} \quad , \qquad (5)$$

where: σ_H - cross-section of (n-p) scattering /10/,

N_H - number of neutrons in (n-p) scattering peak in TOF spectra,

M_H - number of hydrogen nuclei in stilbene crystal,

$cor_H(\Theta)$ - correction for neutron flux attenuation and recoil proton leakage in stylbene crystal,

$E_H = E_o \cdot \cos^2(\Theta)$ - energy of neutrons scattered by protons at the angle Θ_H.

From (1), (2), (5) in the case of (n-p) scattering normalization method we finally recieve

$$\frac{d^2\sigma}{dE \cdot d\Omega} = \frac{\sigma_H}{\pi} \cdot \cos(\Theta_H) \cdot \frac{N(E,\Theta)}{N_H} \cdot \frac{\varepsilon(E_H)}{\varepsilon(E)} \cdot \frac{N_M^H}{N_M} \cdot \frac{M_H}{M} \cdot \frac{cor(\Theta_H)}{cor(E,\Theta)} \quad , \quad (6)$$

In the present experiment the absolute scaling procedure was carried out by both methods, resulting to the normalization uncertainty of 2 %.

The neutron multiple scattering and flux attenuation corrections can be defined as the ratio of differential cross-section disturbed by the sample finite effects and the true one, the later corresponding to the infinite small sample

$$cor(E,\Theta) = \frac{(raw)}{(true)} \quad . \quad (7)$$

This function was calculated with the SSE Monte-Carlo computer code, using the evaluated and/or experimental neutron data /11/.

The statistical uncertainty of the measured spectra varies from 2 to 15 %, the overall error in determination of neutron detector efficiency was (3÷5)%, systematic uncertainty of absolute normalization was 2%. These factors contributed to the total uncertainty in the double-differential cross-section of (5÷15)%.

4. RESULTS AND DISCUSSION

The double-differential neutron emission cross-section from beryllium are shown in fig.2,3. We compared results of our measurements with the Drake et al data /1/, the Takahashi et al 56- and 120-deg data /3/, the Hermsdorf et al 89.8 - deg data /2/, the ENDF/B-V1 beryllium neutron emission spectra /8/. Our neutron emission spectra are in a good agreement with the Drake et al. and the Takahashi et al. data at 120 - and 150 - deg., but the data from ENDF/B-V1 essentially lower in low-energy part of

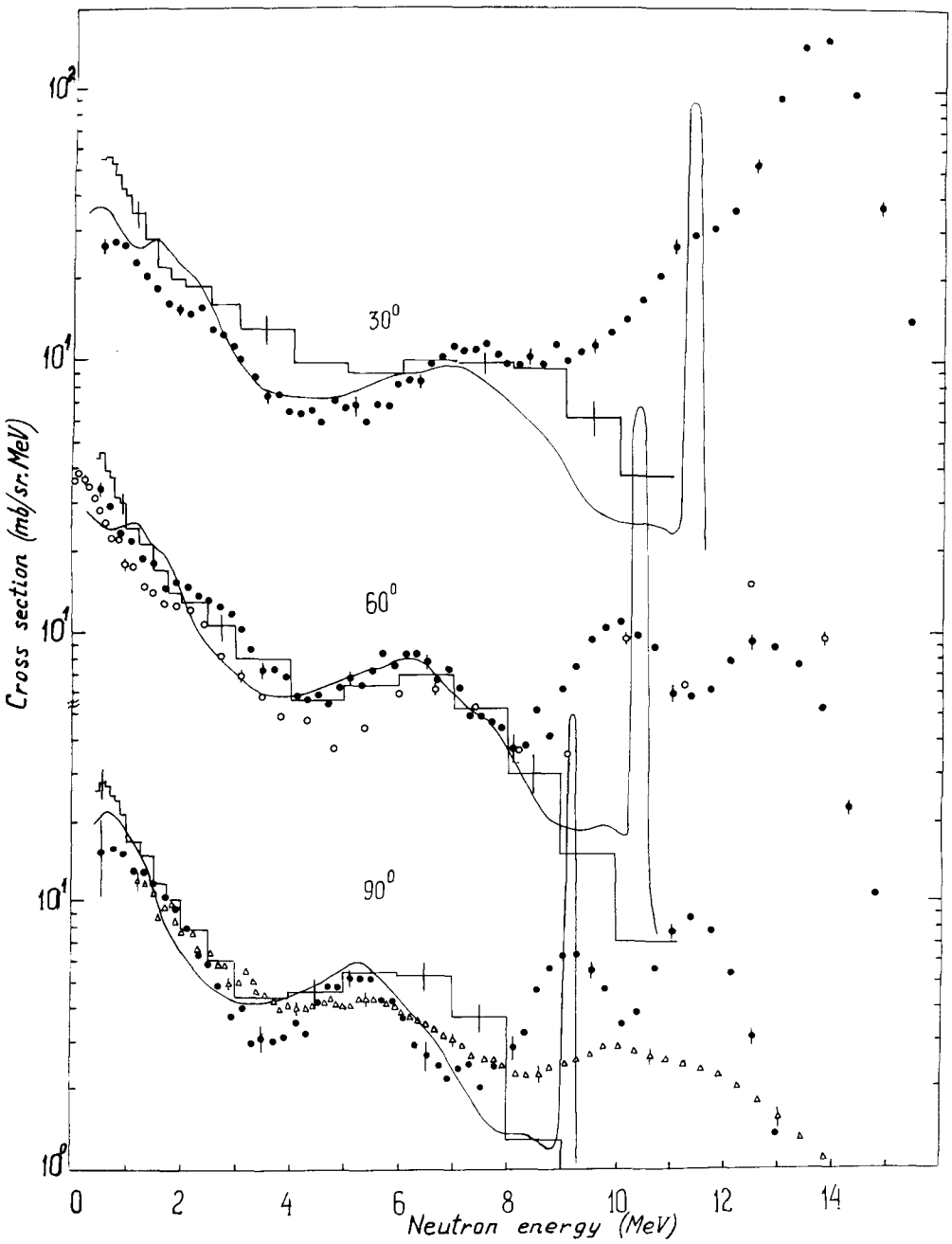

Fig.2. Neutron emission spectra from beryllium at 30, 60, 90 - deg. in the laboratory system.
● - our data,
⌙ - /1/, o - /3/, Δ - /2/, —— - ENDF/B-V1.

spectra. On the contrary at angle 30° there is the considerable discrepancy between our data and the Drake et al data, and the evaluation neutron spectrum from ENDF/B-V1 presents something the middle of these data. Only at angles 60° and 90° the agreement between various experimental data and evaluation neutron spectra from ENDF/B-V1 can be consider more or less satisfactory. Comparison of the angle-integrated neutron emission spectrum from our

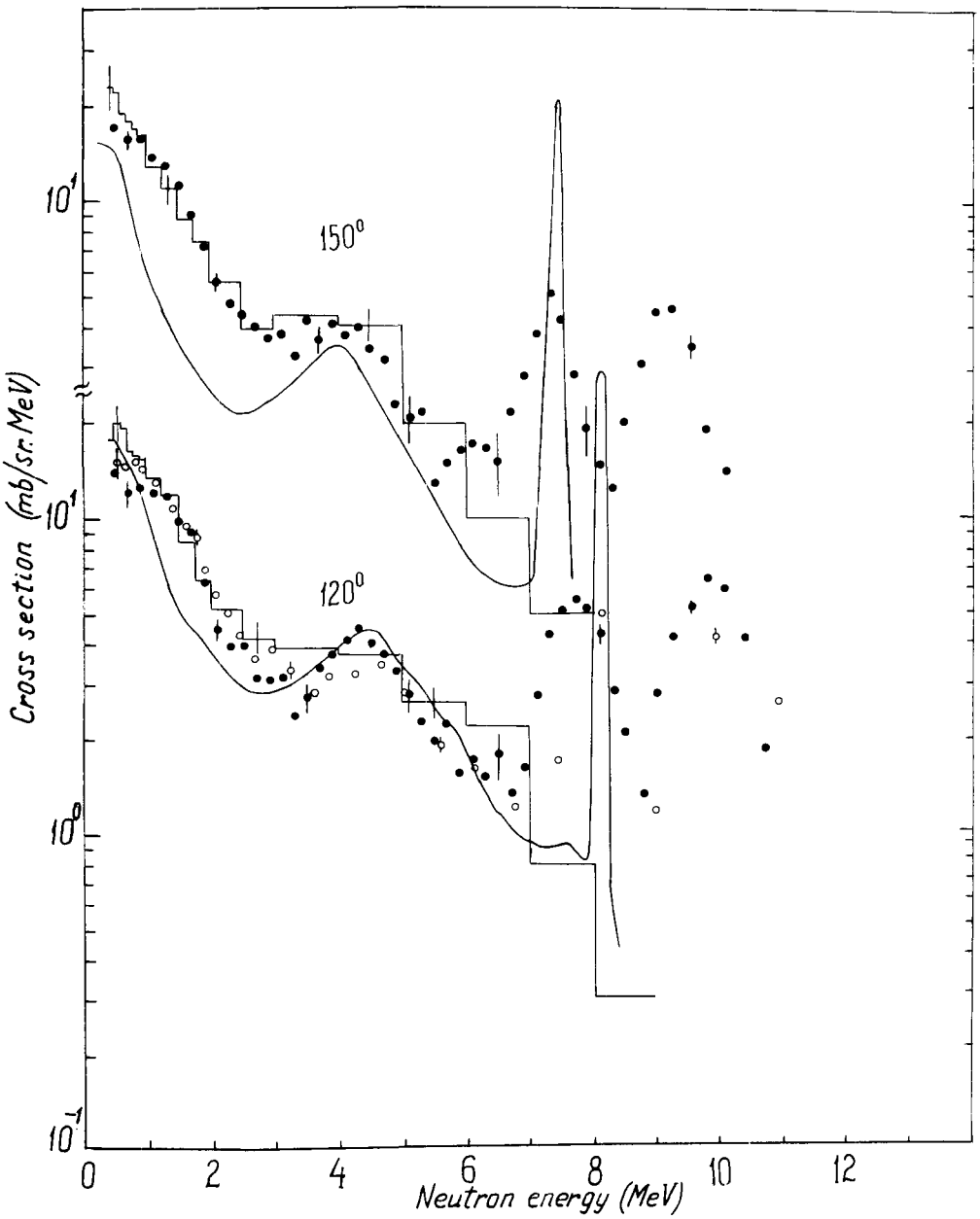

Fig.3. Neutron emission spectra from beryllium at 120 and 150 - deg. in the laboratory sistem. Designations are the same as in fig.2.

measurements with ENDF/B-V1 evaluation (see fig.4) demonstrates a good agreement in low-energy part (<6.5 MeV), but experimental data are higher (~ 20÷30%) for hard part of spectrum. The evaluation neutron emission spectrum was corrected on spectrometer resolution.

The neutron leakage spectrum measurements for Be sphere (R_{in}=6cm, R_{out}=11cm, ρ=1.85g/cm^3) with 14 MeV neutron source at centre were made on the same experimental technique at the angles 8°, 30°, 60° to the deutron beam direction /4/. The flight path was 3.35m. The absolute neutron yeild from the target was

determined by registration α-particles from T(d,n)α reaction by the surface-barrier selicon counter. Corrections for anisotropy of neutron source, sphere hole and method of measuring were estimated using the three dimensional BRAND code /7/. The uncertainty in the experimental values is no more than (6÷7)%. The results are presented in fig.4 and table.

table

Energy integrals of emergent neutrons from beryllium sphere.

Element	E_n, MeV	$N(E_n,\Theta)\cdot10^{-2}$, $\frac{n}{n\cdot source\cdot sr}$			A*	f_1*	f_2*	$N(E_n)$, $\frac{n}{n\cdot sour.}$	Cal./Exp.
		8°	30°	60°					BRAND ENDF/B-V1
Be	0.4÷1	0.94	0.90	0.88	0.02	1.08	1.05	0.120	0.78
	1 ÷ 3	1.21	1.19	1.13	0.02	1.03	1.03	0.157	0.88
	3 ÷10	1.54	1.54	1.42	0.05	1.01	0.97	0.178	0.92
	10 ÷15	5.89	5.66	5.57	0.05	1.01	0.99	0.690	1.014
	0.4÷15	9.58	9.29	9.00				1.145	0.96

* - A, f_1, f_2 - corrections for anisotropy of neutron source, sphere hole and method of measuring, respectively.

The calculated neutron leakage spectrum was received using three-dimensional Monte Carlo code BRAND with nuclear data module, adopted to the ENDF/B-V1 nuclear data file. Statistical accuracy was (0.5÷2)%. For the testing of code the calculation for thin sphere (=0.001cm) was performed, which had shown the reproducibility of the ENDF/B-V1 neutron emission spectrum.

The comparison of the data has shown, that discrepancies, observed between experimental data and ENDF/B-V1 evaluation in the neutron emission spectra, correlate with differences in the calculated and measured neutron leakage spectra. Underestimate of the neutron emission cross-section in ENDF/B-V1 in the (2÷3.5) MeV and (6.5÷12) MeV intervals leads to the differences in neutron leakage spectra in (0.4÷2) MeV, due to large multiply interaction, and in (5.5÷11) MeV respectively. With the excess of the evaluation neutron emission cross-section in (4.0÷5.5) MeV interval is connected the difference between calculation result and experimental data in neutron leakage spectra practically in the same energy interval. Integrated in the measured energy interval (0.4÷15) MeV the neutron leakage coincides within the

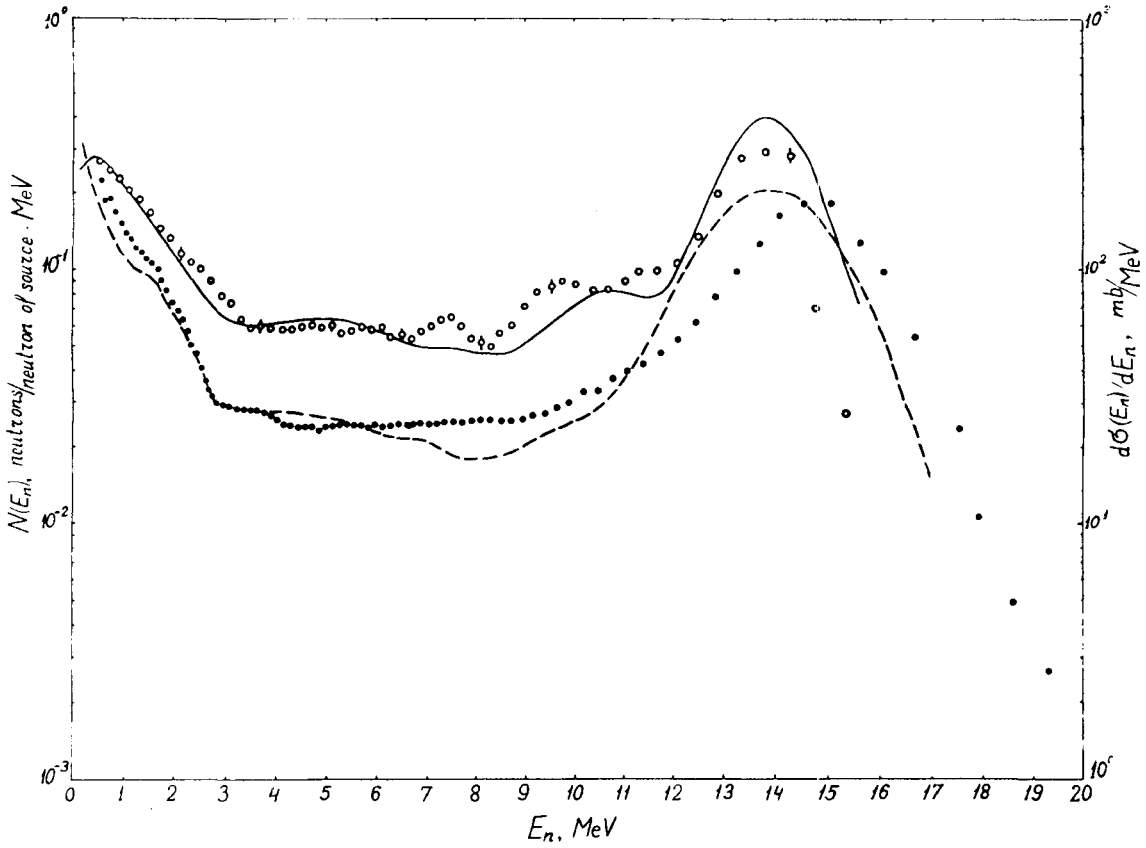

Fig.4. The angle-integrated neutron emission spectra (right scale - o - our data, solid line - ENDF/B-V1 data) and the neutron leakage spectra for 0.9-m.f.p. beryllium sphere (left scale - • - our data, dash line - calculation result of the BRAND code with data file from ENDF/B-V1).

accuracy of observation with calculation result (Cal/Exp =0.96), though the discrepancies in some energy intervals are mounting up ~ 20%.

CONCLUSIONS

New measurements of double-differential beryllium neutron emission cross-sections at incident neutron energy 14.1 MeV confirm discrepancy of the ENDF/B-V1 evaluation to the experimental data at backward angles. At angle 30 - deg are observed essential differences between our data and Drake et al. data. Angle-integrated neutron emission cross-section which we measured, are in a better agreement with ENDF/B-V1 evaluation.

The comparison of the measured and calculated neutron leakage spectra has shown, that observed discrepancies correlate with the differences between measured and evaluated angle-integrated neutron emission cross-sections.

Neutron leakage spectrum from beryllium sphere is little sensitive to the observed differences in angle-differential beryllium neutron emission cross-sections, therefore new measurements of differential cross-sections are imagine vital for the file correction.

REFERENCES

1. D.M.Drake, G.F.Aughampaugh, E.D.Arthur, C.E.Ragan, P.G.Young. Nucl.Sci. Eng. 63,401 (1977).
2. D.Hermsdorf, A.Meister, S.Sassonoff, D.Seeliger, K.Seidel, F.Shahin. ZFK-277,(1974).
3. A.Takahashi, J.Yamamoto, K.Ohshima, M.Fukazawa, Y.Yanagi, M.Veda, J.Miyaguchi, S.Kohno, K.Yugami, H.Nonaka,E.Ichimura, H.Sugimoto, K.Sumita. Oktavian report A-87-01,(1987).
4. A.A.Androsenko, P.A.Androsenko, B.V.Devkin, B.V.Zhuravlev, M.G.Kobazev, O.A.Salnikov, S.P.Simakov, V.A.Zagryadsij, D.V.Markovskij, D.Yu.Chuvilin. a) Neutron Physics. Proc. of Inter. Conf. on Neutron Physics, Kiev,14-18 Sept.1987. Moscow-1988, v.3,p.194. b) Kernenergie 31, 1988, 10, p.122-126..
5. L.F.Hansen. Neutron Physics. Proc. of Inter. Conf. on Neutron Physics, Kiev, 14-18 Sept. 1987. Moscow-1988, v.1, p.310.
6. FENDL. Proc. of the IAEA specialists meeting on fusion evaluated nuclear data library. Vienna, 8-11 May 1988. H.Vonach's comments to report of Working Group 11.
7. A.A.Androsenko, P.A.Androsenko et al. VANT(USSR),v.7, 1985,p.33.
8. S.T.Perkins, E.F.Plechaty and R.J.Howerton. Nuclear Science and Eng. v.90, 1, p.83-98, 1985.
9. W.Mannhart. Report IAEA-TECDOC-410. Vienna, 1987, p.158.
10. Data Standards for Nuclear Measurements. Report IAEA-TECDOC-227, Vienna, 1989.
11. Neutron Cross Section. Academic Press. INC. New York,1988,v.2.

EXPERIMENT OF NEUTRON MULTIPLICATION IN BERYLLIUM

YUAN CHEN, GANG CHEN, RONG LIU, HAIPING GUO,
WENJIANG CHEN, WENMIAN JIAN and JIAN SHEN
Southwest Institute of Nuclear Physics and Chemistry
P.O. Box 525-74, Chengdu 610003, P.R. China

ABSTRACT

Using the Total Absorption Method,the neutron multiplications in beryllium have been measured. A deionized water sphere with an outer radius of 75 cm and a polyethylene sphere with an outer radius of 69 cm were used as the total neutron absorbers. Neutron distributions in the spheres were measured using ^{235}U fission chambers. The relative and the efficiency-determined methods were compared. Important sources of experimental errors were analyzed in detail. 4 groups of neutron multiplications in beryllium up to 14.85 cm thick for two total absorbers and two methods of measurement have been obtained and agreement among them is satisfactory. Measured results have been compared with ANISN calculations using data based on ENDF/B-IV. It is shown that the measured results are 3% - 15% lower than the calculated ones.

INTRODUCTION

It is widely accepted to utilize beryllium to increase the tritium breeding ratio in a fusion reactor or a fusion-fission hybrid reactor blanket due to its relatively high cross-section for the (n, 2n) reaction and no fissionability. To have a satisfactory reliability of neutron multiplication which will be used in the conceptual blanket design, it is essential to get accurate beryllium (n, 2n) cross-section and its secondary neutron spectrum data. Several experiments have been carried out to measure the neutron multiplications.Julich experiments were about 25% lower than calculations[1]. Less-symmetric of the experimental system would be the important reason. V.A. Zagryadskij et al. have got rather consistent experimental data[2] using the "boron tank" method compared with the calculations, but the thickness of Be was lack and only up to 8 cm. Scientists at University of Texas[3] and Lawrence Livermore National Laboratory[4] performed the measurements on the same beryllium assembly and were estimated that the experimental errors are large. A review of the nuclear data status and requirements was made by E.T. Cheng[5].

To clarify the inconsistences of these experiments we have undertaken a project to measure the neutron multiplication in Be. The thickness of beryllium was up to 14.85 cm.

EXPERIMENT METHOD

The method utilized in the experiment is "Total Absorption Detector(TAD)" method. A deionized water sphere and a polyethylene sphere were used as neutron moderators and absorbers. Beryllium sphere was placed in the center of the

absorber. A TiT target system was located in the Be sphere and 14 MeV neutrons were produced by T(D,n)^{4}He reaction. Neutrons leaking from the Be sphere were moderated and absorbed by water or polyethylene. The neutron distributions in the region of the moderator were measured with ^{235}U fission chambers.

Integrating the neutron distributions over the whole space of the moderator and normalized with the associated alpha particle counts, we get the numbers of neutrons detected by ^{235}U fission chambers, N and N^0, for the case of with and without beryllium in the system. We denote the quantities with superscript "0" for the absence of Be from the absorber. The ratio of N/N^0 is equal to the ratio of A_H/A_H^0 quite accurately. Where A_H and A_H^0 are the neutron absorption rates by hydrogen in moderator. We can get the apparent neutron multiplication, M_{app}, as,

$$M_{app}=A_H/A_H^0=N/N^0 \tag{1}$$

When the Be sphere is removed from the system and a 14 MeV neutron comes out of the neutron source, we have the relation of,

$$1=A_H^0+A_X^0+L^0 \tag{2}$$

But when the Be sphere is located at the center of the moderator and also a 14 MeV neutron comes out of the neutron source, the number of neutrons leaking from Be sphere is,

$$M_L=A_H+A_X+L \tag{3}$$

A_X and A_X^0 are the neutron absorptions by non-hydrogen nuclei in absorber. In the water sphere they are the absorptions by O and for polyethylene sphere they are the ones by C. L^0 and L are the neutrons leaking out of the absorber.

From relations (1) to (3) we also have,

$$\begin{aligned} M_L&=(1-A_X^0-L^0)A_H/A_H^0+A_X+L \\ &=(1-A_X^0-L^0)M_{app}+A_X+L \end{aligned} \tag{4}$$

Where the four correction factors, A_X, A_X^0, L and L^0 can be obtained by calculations. M_L is defined as the neutron leakage multiplication and we call the relation (4) the relative method (RM).

The leakage neutron spectrum from beryllium sphere can be separated into two groups. One group contains the neutrons, N_t, with the energy higher than 10 MeV and another one contains the neutrons, N_{scc}, with the energy lower than 10 MeV. We use the first group of neutrons to represent the neutrons leaking from D-T source directly into the moderator and the second group as the secondary, nonelastic-reaction neutrons. We define ε_{14MeV} and ε_{Cf} as the parameters which are proportional to the detective efficiencies of TAD for the case of 14 MeV neutrons and ^{252}Cf neutrons. ε_{14MeV} can be measured when the Be sphere is removed and 14 MeV neutrons go into moderator directly and ε_{Cf} can be obtained when the D-T source was replaced by a ^{252}Cf neutron source. ε_{14MeV}

and ε_{cf} are approximately equal to the detective efficiencies of ^{235}U fission chambers for the two groups of neutrons, and thus we can get the integral neutron count,N, within the region of the TAD when the beryllium is put in the absorber and one 14 MeV neutron comes out from the D-T neutron source as,

$$N=\varepsilon_{14MeV}N_t+\varepsilon_{cf}N_{scc} \tag{5}$$

N_t can be obtained by calculation and

$$N_t=e^{-\Sigma d} \tag{6}$$

where Σ is the nonelastic scattering cross section and d is the thickness of Be. We can also get the leakage neutron multiplication as,

$$M_L=N_t+N_{scc}=N_t+(N-\varepsilon_{14MeV}N_t)/\varepsilon_{cf} \tag{7}$$

When the Be sphere is removed from the TAD and one 14 MeV neutron goes directly into the absorber, the number of neutron detected by fission chamber is ε_{14MeV}. So the apparent neutron multiplication can be expressed as $M_{app}=N/\varepsilon_{14MeV}$,and we also have

$$M_L=N_t+(M_{app}-N_t)\varepsilon_{14MeV}/\varepsilon_{cf} \tag{7a}$$

We call the relation (7) or (7a) the efficiency-determined method (EDM).

EXPERIMENTAL SETUP

The diameter of the water sphere is 1.5 m and the outer shell was made of steel with 0.7 mm thick. The Be sphere was put in the center of the water sphere and isolated from water with a polyethylene spherical shell which the inner and outer radii are 20 and 21.7 cm respectively. Five detector holes in which the neutron detectors were inserted were made at the directions of 0°, 40°, 80°, 120° and 150° to the deutron beam. The spatial distributions of neutron count rates were measured with ^{235}U fission chambers at these five directions. The sphere is filled with about 1.7 tons of pure water. Fig.1 shows the diagram of the water sphere system.

The structure of polyethylene sphere is similar to that of the water sphere and shown in Fig.2. The sphere consists of 8 blocks and the outer diameter is 1.38 m. It has three regions of density as listed in Table 1.

Table 1. Densities of polyethylene sphere

R (cm)	20-21.7	21.7-28	28--69
Density (g/cm^3)	0.92	0.56	0.94

The positions of detector channels are the same as that of the water sphere. The vacant parts of the channels in front of and behind the detectors are filled with polyethylene columns. The length of the columns are precisely adjusted while the detectors are moved along the channels.

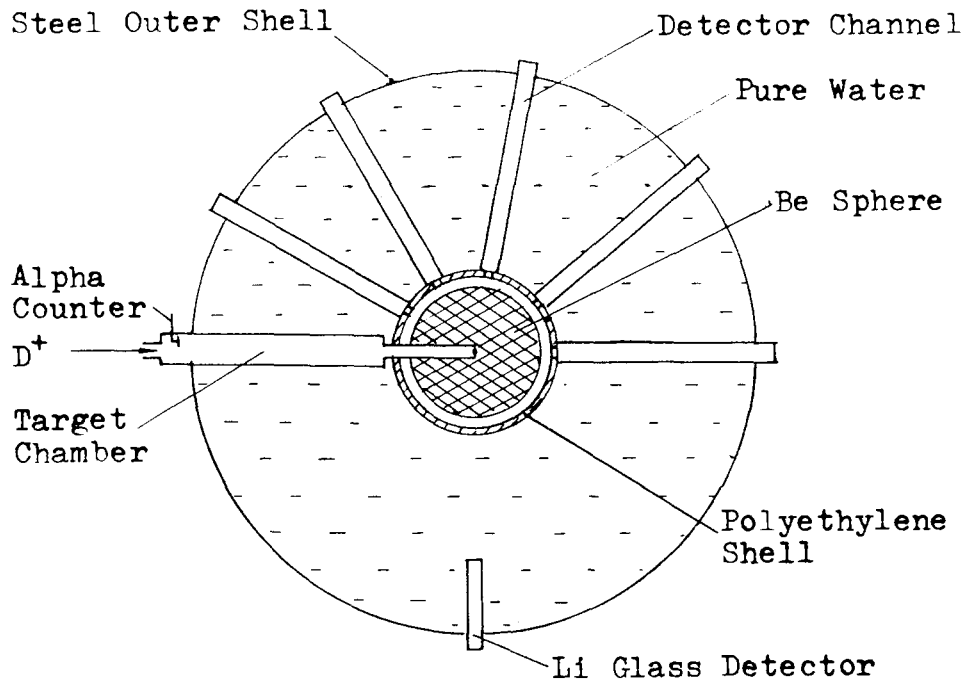

Fig.1. Diagram of the Water Sphere System (TAD)

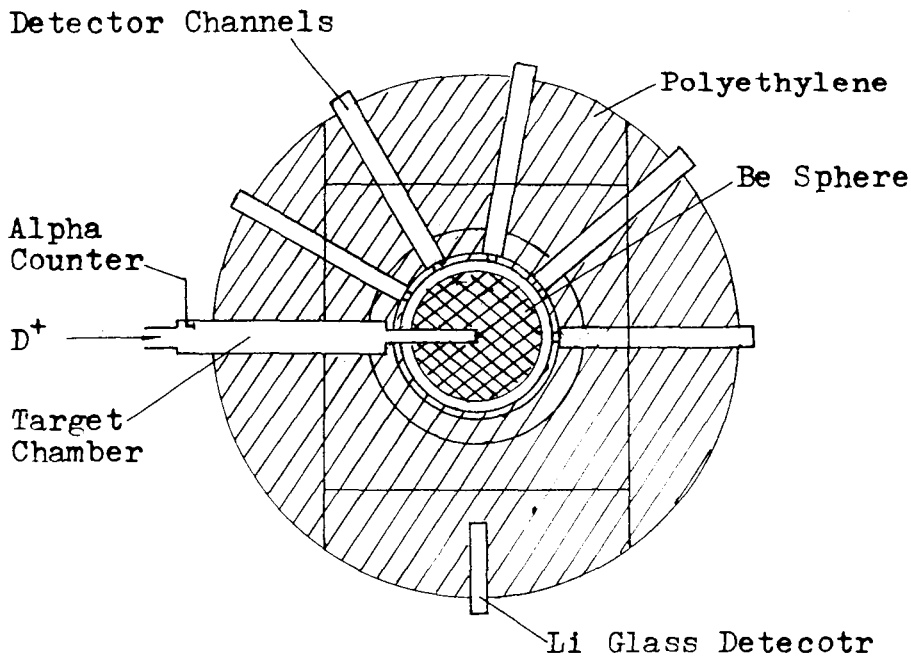

Fig.2. Diagram of the Polyethylene Sphere System (TAD)

The target chamber used as the 14 MeV neutron source consists of a beam drift tube which is made of Al as shown in Fig.3. The wide part of the drift tube is about 620 mm in length and the thickness of the wall is 1.5 mm. The thin part is 230 mm long and has 1 mm thick of the wall. A TiT target is fixed at the front of the drift tube. A GM5ⅢA Si(Au) surface-barrier detector is also set in the target chamber at the angle of 178.2° to the deuteron beam line and used to monitor the yield of neuteron source by associated alpha particles. The distance between the detector and the TiT target is 935±1 mm, and the

aperture of the detector is 2.634±0.007 mm, To discriminate the protons which generate from (D,D) reaction, a 5μm thick of Al foil is placed in front of the alpha detector. It can also shut out the scattered D^+ particles come from deuteron beam.

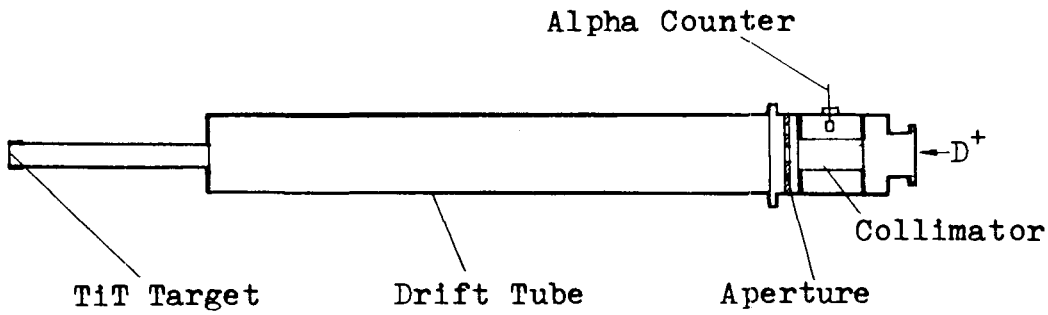

Fig.3. Structure of the Target Chamber

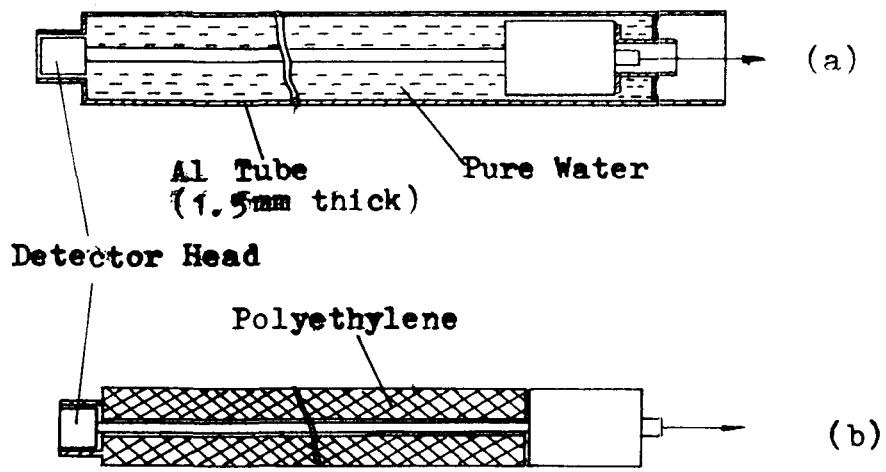

Fig.4. Structures of the Fission Chambers
(a) used in water system
(b) used in polyethylene system

The structures of ^{235}U fission detectors used in the experiment are shown in Fig.4. It has been investigated that the fission chambers can measure the ratio of H(n,γ) reaction rate accurately. The head of the chamber has the shape of the cylinder. The outer case of the cylinder is made of copper with 3 cm in diameter and 2 cm high. The nickel foil plated with ^{235}U is placed in the front of the cylinder and the U layer is in round shape with 0.35 mg/cm² in thickness and 2.4 cm in diameter. The chamber is filled with argon. To test the effect of the copper case, several copper caps with different thicknesses were put onto the detector respectively and some of the measurements were performed with the capped detectors. It has been found from the results that the absorptions of neutron by copper can be quite large, but the changes of measured neutron multiplications caused by the case of detector are small and negligible.

A Cockcroft-Walton accelerator was used in the experiments as the source of deuteron beam and operated in continuous current mode. The energy of deutron is 150 Kev. Average neutron yield was about $1x10^9$ n/s.

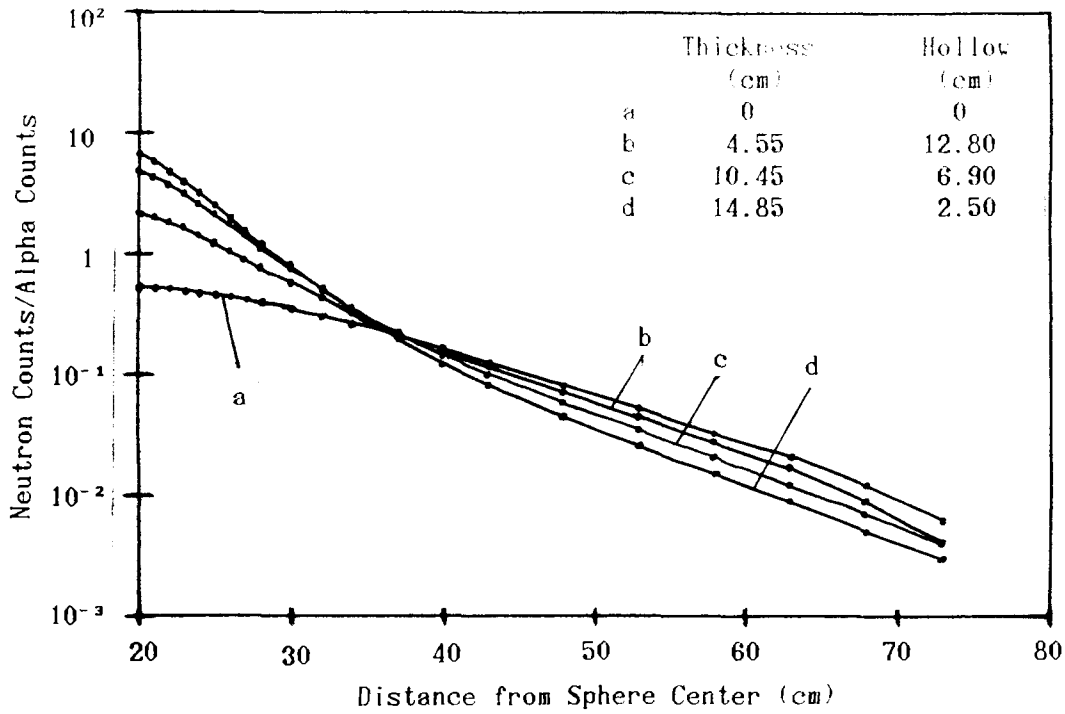

Fig.5. Neutron Distributiond in Water Sphere

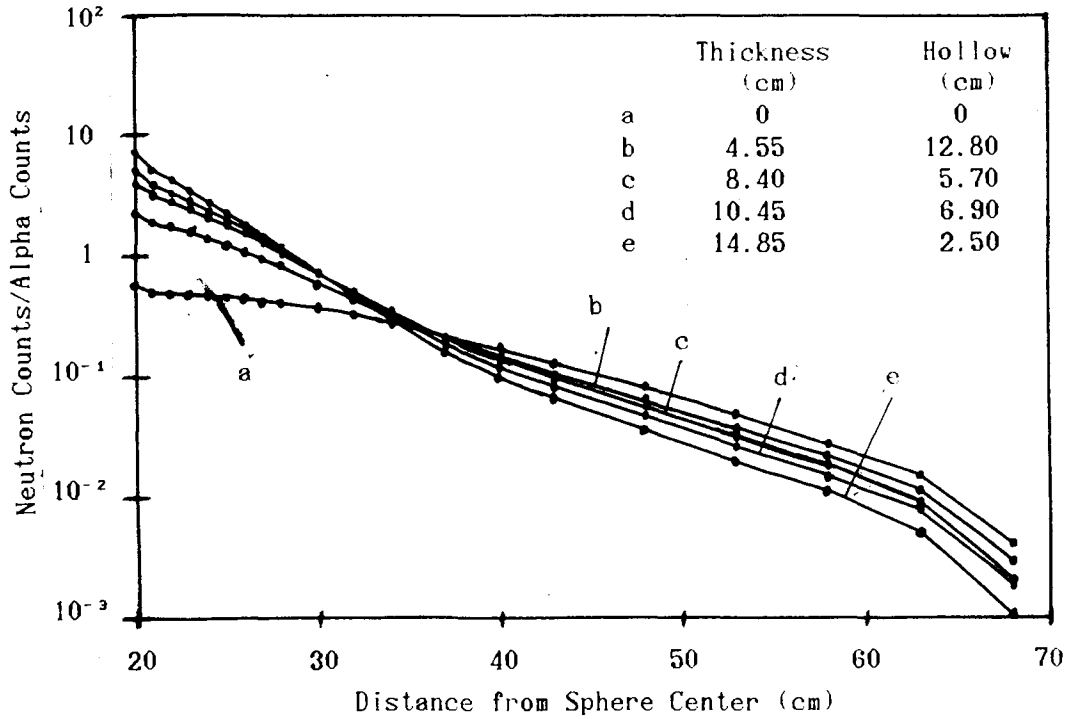

Fig.6. Neutron Distributions in Polyethylene Sphere

EXPERIMENT PROCEDURE

The beryllium assembly was made up of 6 spherical shells which three ones came from USA and three from China. The inner and outer radii of the shells are 2.5/5.7/6.9/9.7/12.8/15.2/17.35 cm respectively. Also an other shell with 12.8/14.1 (IR/OR) cm was used. The shells were used to combine into several hollow spheres with different thicknesses. Leakage neutron multiplications

with three thicknesses have been measured on the water sphere and four on the polyethylene sphere.

Both relative and efficiency-determined methods were employed. For relative method, the neutron distributions in the moderator were measured at the five angles mentioned previously when the beryllium sphere was located in and then removed from the center of the moderator respectively. Measured counts were normalized with associated alpha particle counts and integrated over the region of the moderator. Non-hydrogen absorptions and leakage rates in Equation (4) were obtained by calculations with ANISN code and the data based on ENDF/B-IV. Results are listed in Table 2. Neutron distributions at the angle of 80° to the beam line are also shown in Fig.5-6.

To determine the parameters of ε_{14MeV} and ε_{Cf}, the beryllium sphere was removed from the moderator sphere. D-T source or ^{252}Cf neutron source was located in the center of the sphere. Source neutrons went directly into the moderator and were measured. ε_{14MeV} or ε_{Cf} was the number of neutrons detected by the fission chambers in the TAD and normalized to one source neutron. The leakage multiplications were got from relations of (6) and (7a).

RESULTS AND DISCUSSIONS

Experimental Results

The apparent neutron multiplications in Be were obtained and tabulated in Table 2.

Table 2. Apparent neutron multiplications in Be

Be (cm)	14.85	10.45	10.30	8.40	4.55	4.40
Water sphere	1.990	1.845	-	-	1.401	-
PE sphere	1.936	1.798	1.785	1.695	1.428	1.373

For the relative method, the parameters of non-hydrogen absorptions, A_x and A_x^*, and the leakage rates, L and L^*, are calculated by Lian-yan Liu[6] as listed in Table 3.

Table 3. Neutron absorptions and leakage rates

Be (IR/OR) cm	Absorptions		leakage rate	
	Water	Polyethylene	Water	Polyethylene
0	0.11739	0.06916	0.06654	0.07638
2.50/17.35	0.04720	0.03523	0.02202	0.02469
6.90/17.35	0.06167	0.04241	0.03021	0.03418
5.70/14.10	0.07172	0.04729	0.03653	0.04131
12.80/17.35	0.08990	0.05620	0.04707	0.05393
2.50/12.80	0.06458	0.04399	0.03243	0.03662
2.50/6.90	0.09302	0.05781	0.05033	0.05748

For the efficiency-determined method, it was known from experiment[7] that Σ is equal to 0.0644 cm^{-1}, and we can obtain N_t from relation (6) as the function of the thickness of Be and shown in Table 4.

Table 4. Neutron leakage rates directly from Be spheres

Be (IR /OR) cm	2.50 17.35	6.90 17.38	5.70 14.10	12.80 17.35	2.50 12.80	2.50 6.90
N_t	0.384	0.510	0.582	0.746	0.515	0.753

ε_{14MeV} and ε_{cf} were measured using the method mentioned above and shown in Table 5.

Table 5. Detective efficiencies of ^{235}U fission chamber in TAD

	ε_{14MeV}	ε_{cf}
Water Sphere	0.0585±0.0011	0.0728±0.0011
PE Sphere	0.0510±0.0010	0.0605±0.0009

The measured neutron leakage multiplications from beryllium and a group of calculations are tabulated in Table 6. It is found that agreement between the results obtained by two methods on each absorber sphere is about 1%. It demonstrates that the relative and the efficiency-determined methods are self-consistent and valid. Results from two absorber systems are quite consistent with each other. It is also shown in Table 4 that experimental results are 3% to 15% lower than calculated values with ENDF/B-IV evaluations.

Table 6. Neutron leakage multiplications in beryllium

Method	Moderator	Thickness of beryllium (cm) 14.85	10.45	8.40	4.55
Relative	Water sphere	1.690	1.599	-	1.282
	PE sphere	1.714	1.605	1.537	1.331
Efficiency-determined	Water sphere	1.674	1.582	-	1.273
	PE sphere	1.692	1.595	1.520	1.321
Calculated	Water sphere	1.9426	1.7468	-	1.3605
	PE sphere	1.9429	1.7473	1.6225	1.3610

The effect of the inner hollow of the Be sphere on the neutron leakage multiplication was also observed. For the near same thickness of Be, it has been found the multiplication increases slightly with the inner radius of the beryllium sphere increases as shown in Table 7.

Table 7. Effect of inner hollow of Be

Be thickness(cm) Inner radius(cm)	4.40 2.50	4.55 12.80	10.30 2.50	10.45 6.90
M_L	1.275	1.321	1.585	1.595

The neutron distributions for the near same thickness of Be are shown in Fig.7. It can be found the leakage spectrum becomes softer when the inner

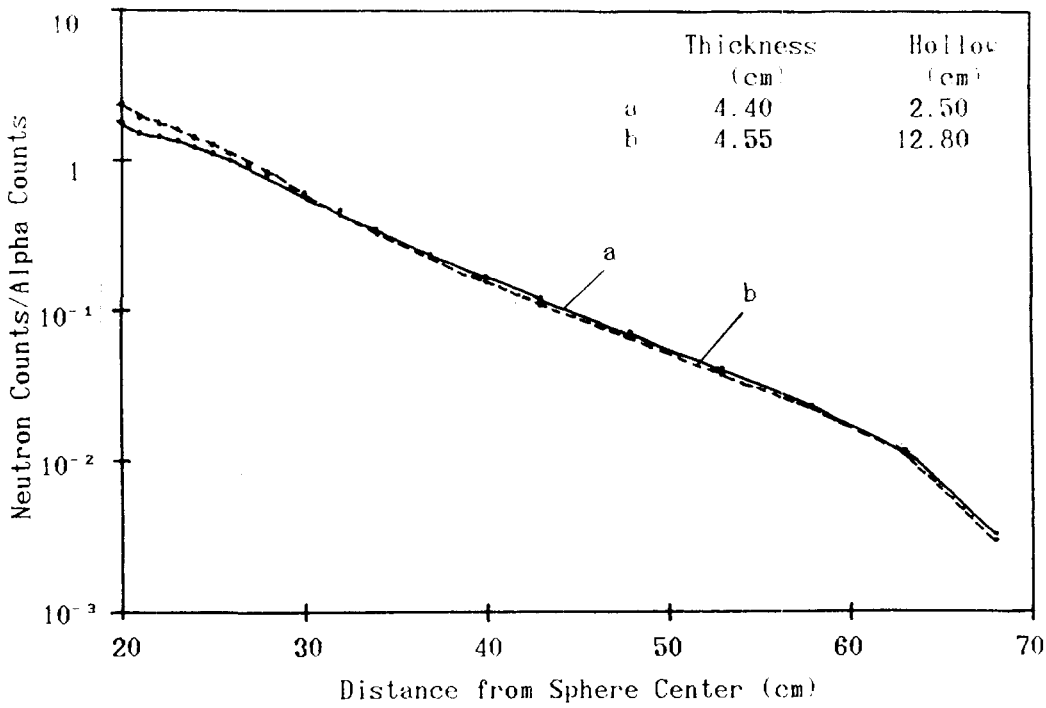

Fig.7. The Effect of Beryllium Hollow

hollow becomes larger. The facts are agree to the predictions of the calculation and the effects was small.

Experimental Errors

In the case of practical usage, when the detectors are put in the detector channels, the vacant parts of the channels in front of and behind the detectors are filled with the same materials as that of the moderators. In order to estimate the perturbations attributed to the Ar chambers, the fillers behind the detectors were all removed. Only a very small deviation was observed, and the changes of detector response caused by the Ar chamber is smaller than 1%.

Neutrons come out from the beryllium are partly absorbed by non-hydrongen nuclei in moderator. In the water sphere, oxygen nucleus is not a standard one and the neutron data of the oxygen are not accurate enough. This bring about up to 2.4% of error to the leakage multiplication when the four correction factors rates are calculated. On the contrary, non-hydeogen absorption is smaller in the polyethylene sphere and the absorptions by hydrogen and carbon can be calculated quite accurately. Overall error in the calculations of the absorptions and leakage rates was given[6] as better than 1%.

A small-sized ^{6}Li glass detector was inserted into the moderator sphere to measure the neutron flow and the results were compared with the measurement of associated alpha particle counter and analyzed in detail. It is found the stability of the neutron yield monitor was better than 2% during the whole period of the experiments.

The statistical error of neutron counts is smaller than 1%. The unstability of the experimental instruments is about 1%. Experimental errors are listed in

Table 8. Overall error of the experiments on the water sphere system was obtained as 3.7% and on the polyethylene sphere system was 2.8%.

Table 8. Experimental Errors

	Water Sphere	PE Sphere
Non-hydrogen Absorption	2.4%	-
Neutron Monitor Stability	2%	2%
Effect of Detector Chamber	1%	1%
Calculational Error	1%	1%
Statistics	1%	1%
Unstability of Instruments	1%	1%
Overall Error	3.7%	2.8%

CONCLUSIONS

Neutron reflection from moderator back to the beryllium assembly will influence the Be(n,2n) process. It was calculated[6] that the leakage multiplications from bare beryllium will decrease 0.3%-2.5% for the neutron reflection. The results given in this article are the leakage multiplications of the "Be+moderator" systems.

The experiments of neutron multiplication in Be have been carried out. The leakage multiplications have been obtained with 2.8% of experimental error for polyethylene sphere and 3.7% for water sphere. We can confirm good consistency among the methods of measurements used in the experiments. The measured results are 3% to 15% lower than the calculated ones. Further studies of the integral experiment are required.

ACKNOWLEDGEMENTS

Our thanks are due to International Atomic Energy Agency for the support under the research contract No.5828/RB. We thank E.T. Cheng from G.A. of USA for his kindly help to join the beryllium assembly of China to the one from USA and the valuable discussions with us. We also thank Li-jian Qiu of IPP of China for his continuous concerns to the experiments. We thank Lian-yan Liu and Yu-quan Zhang from IAPCM of China for their sincerely cooperations with us. We are also very pleased to thank Shaojie Duan, Yuqing Zhou, Guoliang Liu and other scientists at SWINPC for their helps to prepare for the work.

REFERENCES

1. T.K. BASU, V.R. NARGUNDKAR, P. CLOTH, D. FILGES and S. TACZANOWSKI, "Neutron Multiplication Studies in Beryllium for Fusion Reactor Blankets," NUCL.SCI. ENG. 70,309 (1979).

2. V.A. ZAGRAYADSKIJ, M.I. KRAJNEW, D.V. MARKOVSKIJ, V.M. NOVIKOV, D.Yu CHUVILIN and G.E. SHATALOV, "Measurement of Neutron Leakage from U,Th and Be Spherical

Assemblies with a Central 14-MeV Source," INDC(CCP)-272/G, IAEA, Vienna, Austria, 1987.

3. R.S. HARTLEY, "Neutron Multiplication in Beryllium," PHD Dissertation, Univ. of Texas, Austin, Texas, 1987.

4. CALVIN WONG, E.F. PLECHATY, R.W. BAUER, R.C. HAIGHT, L.F. HANSEN, R.J. HOWERTON, T.T. KOMOTO, J.D. LEE, S.T. PERKINS and B.A. POHL, "Measurements and Calculations of the Leakage Multiplication from Hollow Beryllium Spheres," FUSION TECHNOL., 8,1165 (1985).

5. E.T.CHENG, "Review of the Nuclear Data Status and Requirements for Fusion Reactor," Proc. Int. Conf. on Nuclear Data for Sci. Tech., Mito, Japan, 30 May - 3 June, 1988.

6. LIAN-YAN LIU. YU-QUAN ZHANG, "Analysis of SWINPC Beryllium Neutron Multiplication Integral Experiment," Beijing, 1990, to be published.

7. UCRL-51663(1974).

ANALYSIS OF SWINPC BERYLLIUM MULTIPLICATION INTEGRAL EXPERIMENT

Liu Lian-yan and Zhang Yu-quan

Institute of Applied Physics and Computational Mathematics
P.O. Box 8009, Beijing 100088, P.R. China

ABSTRACT

In order to check the nuclear data of beryllium, which is known as one of the most promising neutron multipliers for fusion reactor blanket, beryllium multiplication integral experiment is performed at SWINPC, Chengdu. Analysis work is done involving this experiment. The experiment scheme is fully examined. Calculation corrections are made to measured results. The experimental beryllium multiplications have been compared with calculated ones. It is shown that ENDF / B-IV data predict higher multiplication capability by 14%, while ENDF / B-VI and Los Alamos evaluation give a 10% larger multiplication for beryllium thickness 14.85 cm.

INTRODUCTION

Beryllium is a very important candidate as neutron multiplier for fusion blanket because of its large (n,2n) cross-section and low threshhold energy. However, beryllium data are still a controversial issue [1]. There are discrepancies among evaluations and experimental data. The recently-released ENDF / B-VI evaluation decreases the Be(n,2n) cross-section at neutron energy 14-MeV by 8% compared to previous version ENDF / B-IV.

Facing the dilemma of beryllium data, people are strongly motivated to study the effectiveness of current beryllium data. Efforts have been devoted to beryllium integral multiplication experiment, which is a powerful means for checking nuclear data.

Table 1. Summary of beryllium integral experiments

Institution	Be thickness(cm)	Geometry	Error(%)
Julich [2]	8, 12, 20	rectangular	3.8, 3.2, 12.
Kurchatov [3]	1.5, 5, 8	spherical	3.2, 2.9, 2.8
U. of Texas [4]	4.6, 13.8, 19.9	spherical	9., 9., 9

Julich experiment suggested that the multipication capability of 20cm thick beryllium is 25% overestimated by ENDF / B-IV calculation, while Kurchatov obtained rather consistent results with B-IV prediction. U. of Texas also showed large differences between experimental and calculated values. Considering the drawbacks of the experiments mentioned above, it is advisable to carry out further integral experiment with simple geometry, thick beryllium and high accuracy. The integral experiment at South West Institute of Nulcear Physics and Chemistry (SWINPC) is a response to this need.

BRIEF DESCREPTION OF THE EXPERIMENTS

The neutron multiplications of beryllium spheres are measured by total absorption method. 14-MeV neutron source, located at the center of the assemblies, was generated by bombardment of deuteron beams on a TiT target. Beryllium spheres are surrounded by a large volume of spherical moderator (see Fig.1).

Table 2. Beryllium samples measured in the experiment

Rin (cm)	Rout (cm)	Thickness (cm)
12.8	17.35	4.55
6.9	17.35	10.45
2.5	17.35	14.85

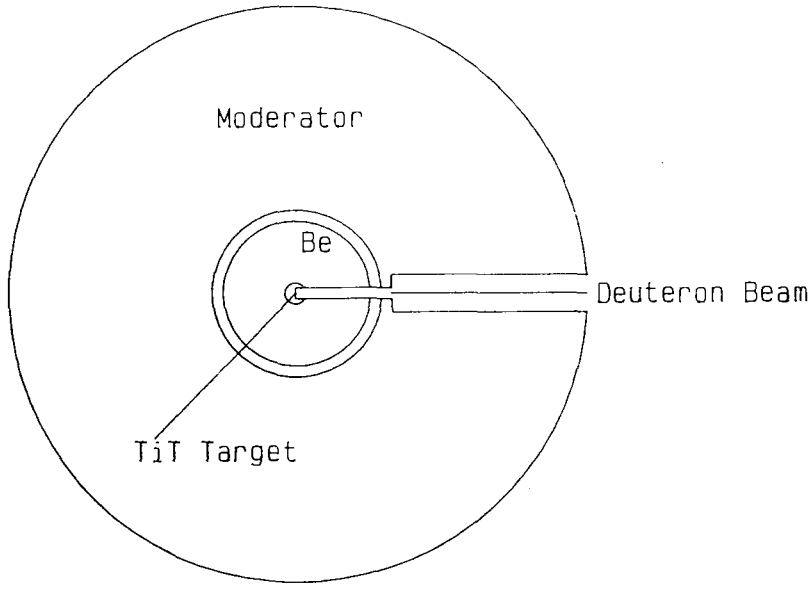

Fig.1 The Experiment Set-up

Table 3. Dimension of the moderators

Moderator	Zone	Rin (cm)	Rout(cm)	Material	Density(g / cm^3)
water	PE1	20.0	21.7	CH_2	0.92
	water	21.7	75.0	H_2O	1.0
polyethylene	PE1	20.0	21.7	CH_2	0.92
	PE2	21.7	28.0	CH_2	0.56
	PE3	28.0	69.0	CH_2	0.94

The source neutrons are multiplied in the beryllium sphere via Be(n,2n). The major part of neutrons from the beryllium sample is absorbed by hydrogen in the moderator, which can be obtained by measurement. The minor part is absorbed by non-hydrogen nuclides in the moderator and leaks from the moderator sphere, which is to be determined by calculation. To avoid detector efficiency calibration, relative measurement is adopted: H-1 neutron absorption rates in the moderator are measured for systems with and without beryllium sample, respectively. Then the beryllium neutron leakage multiplication can be expressed as,

$$M_L = M_{app} F_C \tag{1}$$

where $M_{app} = A_H^M / A_H^0$

$$F_C = \frac{1 + \frac{A_C^M}{A_H^M} + \frac{A_O^M}{A_H^M} + \frac{L^M}{A_H^M}}{1 + \frac{A_C^0}{A_H^0} + \frac{A_O^0}{A_H^0} + \frac{L^0}{A_H^0}}$$ for water-moderator system;

or $$F_C = \frac{1 + \frac{A_C^M}{A_H^M} + \frac{L^M}{A_H^M}}{1 + \frac{A_C^0}{A_H^0} + \frac{L^0}{A_H^0}}$$ for polyethylene-moderator system.

In the above expressions, the superscript "M" and "0" denote with-sample and without-sample system. A_H, A_C and A_O are the total neutron absorption rates of H-1, C-12 and O-16 in the moderator, L the neutron leakage from the moderator. M_{app} is called apparent multiplication, measured with U-235 fission chamber detector; Fc is a correction factor, determined by calculation.

VERIFICATION OF EXPERIMENT SCHEME

The experiment scheme is examined thoroughly in this part, so as to ensure the experimental results. The following issues is to be covered: geometry and impurities of Be samples, DT neutron source, validity of the detector measurement, neutron reflection of moderator. 1–D ANISN [5] and Monte Carlo code MCNP [6] are employed. The calculated results below are normalized to one source neutron.

Geometry and Impurities of Beryllium Samples

As is shown in Fig.1, the Be samples is not rigorous spherical because of the deuteron beam duct of diameter 3.0 cm. MCNP was used to investigate the deviation of beryllium neutron multiplications due to the geometric defect.

Table 4. Be multiplications for rigorous and ducted spheres
(MCNP, LASL data)

Be thickness	Rigorous sphere	Ducted sphere
12.8 / 17.35	1.333	1.332
6.9 / 17.35	1.693	1.691
2.5 / 17.35	1.875	1.854

The above table shows the duct in the Be samples results in about 1% or less differences to beryllium multiplications. Therefore, the Be samples measured can be treated as rigorously one–dimensional.

There are some impurities in the Be samples (see Table 5). As a consequence of neutron absorption by impurities, the Be multiplication may be affected. Table 6 gives the calculated results, which demonstrate the impurities in the Be samples produce negligible changes in Be multiplications.

Table 5. Compositions of Be samples (w%)

Isotope	P.R.C. shell (5.7 / 12.8)	U.S.A. shells (2.5 / 5.7, 12.8 / 17.35)
Be	98.9	98.82
O	0.5	0.72
Fe	0.6	0.13
C	—	0.11
others	—	0.12

Table 6. Neutron absorption in beryllium by impurities
(MCNP, Be C—LASL data, others—B–IV data)

Be sample	12.8 / 17.35	6.9 / 17.35	2.5 / 17.35
Absorption rate	0.0005	0.003	0.005

DT Neutron Source

The neutron source used in the experiments was generated based on the T(d,n)α reaction. The incident deuterons ($E_d^0 = 150$keV) are slowed down to zero energy in the TiT target. In this process neutron generation reactions are possible at various energies. Before emitting from the target, the D–T neutrons may interact with target material and structure material.

A subroutine SOURCE was programmed and embeded to MCNP so as to simulate the whole process. Deuteron energy, E_d, was sampled under the probability distribution $\sigma_{D-T}(E_d)$ [7] (unnormalized) between $0-E_d^0$, the emission angle θ_C in CM system sampled under the expression:

$$f(\theta_C) = 0.998 + 0.213COS\theta_C - 0.019COS^2\theta_C$$

Then the emitted neutron energy is determined by

$$E_n = 0.08E_d + 0.8(0.6E_d + 17.6) + 1.6\sqrt{0.1E_d(E_d + 17.6)}\,COS\theta_C$$

and the emission angle in Lab system by

$$COS\theta_L = \frac{\gamma + COS\theta_C}{\sqrt{1 + 2\gamma COS\theta_C + \gamma^2}}$$

where $\gamma = \sqrt{\frac{E_d}{10(0.6E_d + 17.6)}}$

The angle–integrated spectrum is shown in Fig.2, which indicates that almost all of source neutrons have their energies between 13.5–15.0 MeV.

Comparison has been made in Table 7 to ascertain the differences of beryllium multiplications between the calculations with actual source (SOURCE subroutine used) and simplified source, an isotropic point source with neutron energies evenly distributed from 13.5 to 15.0 MeV. Results show the actual source can be substituted by the simplified source within a good pricision.

Table 7. Beryllium multiplications with different sources (MCNP, LASL data)

Be sample	Actual source	Simplified source
12.8 / 17.35	1.313	1.333
6.9 / 17.35	1.681	1.693
2.5 / 17.35	1.860	1.875

Validity of Detector Measurement

In the experiment, H–1(n,γ) reaction rates in moderator sphere are measured by U–235 fission chamber detector. It is of primary interest to verify if the detector can measure the H–1(n,γ) rates accurately.

Table 8 assures that, if only the ratioes of reaction rates are concerned, H–1(n,γ) can be given out by U–235(n,f) reaction perfectly in the whole moderator region. This is because most of the H–1(n,γ) and U–235(n,f) reactions occur in the thermal neutron energy range, where the cross–sections for both reactions obey the same 1 / V law versus neutron energy.

Table 8. Total H–1(n,γ) and U–235(n,f) rates in the moderator region (ANISN, B–VI)

Moderator	Be sample	H–1(n,r)	Rela.Value	U–235(n,f) ★	Rela. Value
water	0.0	0.7715	1	1.258E–12	1
	12.8 / 17.35	1.1468	1.486	1.867E–12	1.484
	6.9 / 17.35	1.5490	2.008	2.520E–12	2.003
	2.5 / 17.35	1.7606	2.282	2.863E–12	2.276
polyethylene	0.0	0.8329	1	1.580E–12	1
	12.8 / 17.35	1.1932	1.433	2.261E–12	1.431
	6.9 / 12.8	1.5787	1.895	2.988E–12	1.891
	2.5 / 17.35	1.7810	2.138	3.370E–12	2.133

★ — obtained by weightedly summing values of all zones

What should be pointed out is that the U–235(n,f) rates in the table are calculated by weightedly summing the U–235(n,f) rates in all zones with H–1 atomic density in corresponding zone as weighting factor, because there are different H–1 atomic densities in various zones of the moderator while the atomic density of the detector media U–235 keeps constant.

Neutron Reflection of Moderator

In order to measure the neutron leakage multiplication of naked beryllium samples, moderator was placed outside the samples. The beryllium multiplications are subject to changing, owing to neutron reflection from moderator to beryllium samples.

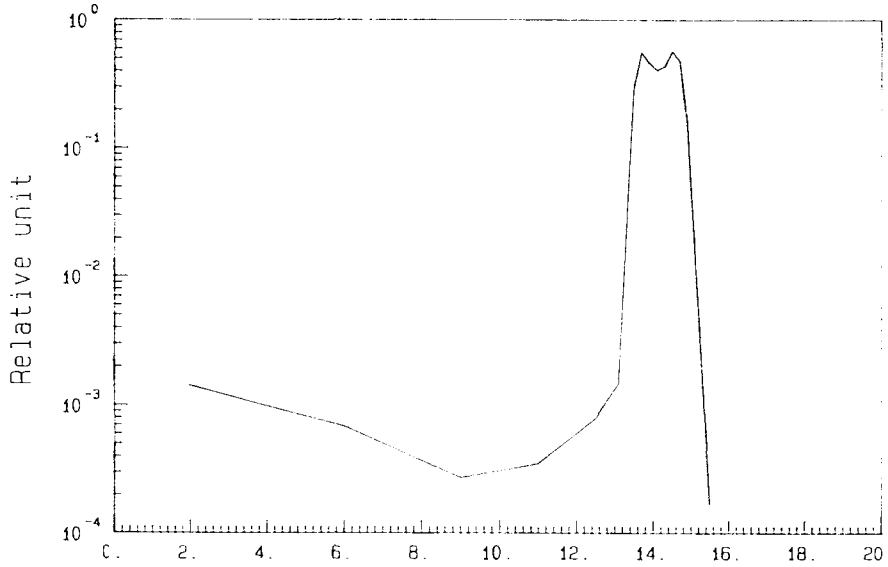

Fig.2 D-T source neutron spectrum

Table 9. Infuence of neutron reflection to Be multiplications (ANISN, B–VI)

Be sample	Be process	Naked Be	Be+water	Be+ polyethylene
12.8 / 17.35	(n,2n)	0.349	0.356	0.357
	absorption	0.030	0.036	0.036
	leakage	1.319	1.320	1.321
6.9 / 17.35	(n,2n)	0.758	0.764	0.764
	absorption	0.080	0.097	0.096
	leakage	1.678	1.667	1.668
2.5 / 17.35	(n,2n)	0.984	0.987	0.987
	absorption	0.114	0.137	0.136
	leakage	1.870	1.850	1.851

As is shown in Table 9, the presence of the moderator sphere has little influence on Be(n,2n), but considerable changes in neutron absorption occur as a result of soft spectrum of reflected neutrons. On the whole, there are only 1% or less deviations from the multiplications of naked beryllium samples.

CORRECTION FACTORS AND EXPERIMENTAL RESULTS

In Eq.(1), to obtain the multiplication M_L, correction factor F_C needs to be given by calculation. One–dimensional discrete ordinate code ANISN was used for this purpose. Group constants were processed from ENDF / B–VI by NJOY [8]. Neutron source was assumed to be an isotropic point source with neutron energies between 13.5–15.0 MeV.

Table 10 lists the calculated correction quantities. We are much concerned with the uncertainty of the factor F_C. Generally, uncertainty induced by calculation comes from three parts: calculation method, physical modeling and nuclear data. Because the weak dependence of F_C on A_H,A_C,A_O and L, and the former two parts are much less important than the third in our case, nuclear data are the main source of the uncertainty. For water–moderator system, O–16 data may be a disastrous problem to the experimental precision. The uncertainty of O(n,α) is up to 30% according to Evaluation Files, which can lead to 4% uncertainty of corretion factor F_C. For polyethylene–moderator system, the correction factor F_C is far more accurate, because the nuclear data of H and C have satisfactory accuracies.

Table 10. Calculated Correction Factors
(ANISN, B–VI)

Moderator	Be sample	M_L	A_H	A_C	A_O	L	F_C
water	0.0	1.0	0.772	0.005	0.137	0.087	—
	12.8 / 17.35	1.320	1.147	0.005	0.105	0.064	0.888
	6.9 / 17.35	1.667	1.549	0.004	0.071	0.044	0.831
	2.5 / 17.35	1.850	1.761	0.004	0.053	0.033	0.811
polyethylene	0.0	1.0	0.833	0.062	—	0.105	—
	12.8 / 17.35	1.321	1.193	0.052	—	0.077	0.922
	6.9 / 17.35	1.668	1.579	0.039	—	0.051	0.880
	2.5 / 17.35	1.851	1.781	0.033	—	0.038	0.865

From the measured apparent multiplication M_{app} and calculated correction factor F_C, the neutron leakage multiplications are achieved.

Table 11. Experimental results of beryllium multiplication

Moderator	Be sample	M_{app}	F_C	M_L
water	12.8 / 17.35	1.401	0.888	1.244
	6.9 / 17.35	1.845	0.831	1.533
	2.5 / 17.35	1.990	0.811	1.614
polyethylene	12.8 / 17.35	1.428	0.928	1.325
	6.9 / 17.35	1.798	0.880	1.582
	2.5 / 17.35	1.936	0.865	1.675

Table 12. Be neutron leakage multiplications by calculation and experiment

Be sample	Cal. B–IV ANISN	Cal. B–VI ANISN	Cal. LASL MCNP	Exp.
12.8 / 17.35	1.361	1.320	1.333	1.325
6.9 / 17.35	1.747	1.667	1.693	1.582
2.5 / 17.35	1.943	1.850	1.875	1.675

The experimental results results are compared with the calculated values by ENDF / B–IV, ENDF / B–VI and Los Alamos evaluations in Table 12. The multiplications by B–IV are much higher than experimental values. Although calculations with B–VI and LA data give a consistent prediction to neutron multiplication for thin beryllium sample, there are large discrepancies between calculated and experimented values, up to 10% for 14.85 cm thick beryllium sphere.

CONCLUSIONS

Experiment Scheme

The Berullium assemblies can be regarded as pure, rigorously spherical. The D–T neutron source can be represented by an isotropic point source with energies between 13.5 and 15.0 MeV. U–235 fission detector enjoys good precision in measuring H–1(n,γ) rates in the whole moderator region. Neutron reflection of moderator gives rise to negligible changes in beryllium multiplications.

Correction Factors

The poor quanlity of oxygen nuclear data puts doubts over the correction factors for water–moderator system. Polyethylene–moderator system shows its advantage in getting accurate experimental results.

Beryllium Data

ENDF / B–VI and LA data predict the beryllium multiplication capability better than ENDF / B–IV. Still, B–VI and LA data can not reproduce the Be multiplication for thick beryllium sample. They over estimated beryllium multiplication of thickness 14.85 cm by 10%.

ACKNOWLEDGEMENT

This work is supported by IAEA under research contract No. 5740 / RB. The authors would like to express their thanks to Dr. E. T. Cheng for his constructive instructions and suggestions.

REFERENCES

[1] E.T. Cheng, "Review of the Nuclear Data Status and Requirements for Fusion Reactor", Proc. Int. Conf. on Nucl. Data for Sci. Tech., (Mito, Japan, 30 May–3 June, 1988)

[2] T.K. Basu, et al., NSE, 70, 309 (1979)

[3] V.A. Zagryadsdij, et al., INDC(CCP)–272 / G, IAEA,Vienna,Austria(1987)

[4] R. S. Hartley, Neutron Multiplication in Beryllium, PhD Dissertation, University of Texas, Austin, Texas (1987)

[5] W.W. Engle, Jr. "A User's Manual for ANISN, A One–Dimensional Discrete Ordinate Transport Code with Anisotropic Scattering", K–1693, ORNL(1957)

[6] "MCNP–A General Monte Carlo Code for Neutron and Photo Transport", LA–7396–M (1981.4)

[7] J. Benveniste, et al., "Information on the Neutrons Produced in the T(d,n)^{4}He Reaction", UCLA–4266 (1954)

[8] R. MacFarlane, et al., "The NJOY Data Processing System", Vol. II , LA–9303–M, Los Alamos National Laboratory (1982)

Calculation of the INEL Beryllium Multiplication Experiment*

J.W. Davidson and M.E. Battat
Los Alamos National Laboratory
and University of California
U.S.A.

* was presented at the meeting orally, and the main conclusions were included in the Summary Report of the meeting, published as report INDC(NDS)-264/G. The paper was also submitted to the Ninth Topical Meeting on the Technology of Fusion Energy, Oak Brook, Illinois, 7-11 October 1990. Proceedings published in Fusion Technology, Vol. 19, No. 3, Part 2B, (May 1991), pp. 2007-2015.

Beryllium Integral Experiment at EG & G/Idaho Using a Manganese Bath Detector*

J. Richard Smith
Idaho National Engineering Laboratory
EG & G Idaho, Inc.
Idaho Falls, Idaho 83415
U.S.A.

* was presented at the meeting orally, and the main conclusions were included in the Summary Report of the meeting, published as report INDC(NDS)-264/G. See also a) J. Richard Smith and John J. King, "Neutron Multiplication in Bulk Beryllium, Proc. Ninth Topical Meeting on the Technology of Fusion Energy, Oak Brook, Illinois, 7-11 October 1990, published in Fusion Technology, Vol. 19, No. 3, Part 2B, (May 1991), pp. 1925-1930 and b) J.R. Smith and J.J. King, "The INEL Beryllium Multiplication Experiment: Final Report", Idaho National Engineering Laboratory report EGG-PHY-9615 (March 1991).

A paper presented at the IAEA Advisory Group Meeting on the Nuclear Data for Neutron Multiplication in Fusion Reactor First Wall and Blanket Materials, Chengdu, P.R. China, November 19-21, 1990 and at the Ninth ANS Topical Meeting on the Technology of Fusion Energy, Oak Brook, Illinois, USA, October 17-11, 1990. Also, to appear in Fusion Technology Journal.**

STUDY ON THE ACCURACY OF SEVERAL BERYLLIUM EVALUATIONS AND COMPARISON OF MEASURED AND CALCULATED DATA ON REACTION RATES AND TRITIUM PRODUCTION DISTRIBUTIONS

M. Z. Youssef, Y. Watanabe*
School of Engineering and Applied Science
University of California of Los Angeles
Los Angeles, CA 90024, U.S.A.
(213) 825-2879

ABSTRACT

The accuracy of beryllium data, particularly the $^{9}Be(n,2n)$ cross-section and the associated secondary neutrons energy distribution has direct impact on the prediction accuracy of important neutronics parameters such as in-blanket neutron spectra, tritium production and other reaction rates distributions. The measured values for these parameters obtained within the U.S./JAERI Collaborative Program on Fusion Integral Experiments were compared to the calculated ones with three evaluations for beryllium data. The ENDF/B-V, LANL, and ENDF/B-VI evaluations for beryllium (denoted Be5, (LANL)Be, and Be6, respectively) were processed, along with ENDF/B-V data of other materials, into 80-group neutron structure of the MATSX6 library. The processed library was used to calculate tritium production rate, neutron spectrum, and several foil activation reaction rates along the central axis of a Li_2O test assembly in which a 5 cm-thick beryllium zone precedes the Li_2O zone and acts as a neutron multiplier. The test assembly itself is located at one end of a Li_2CO_3 enclosure where the D-T neutron point source is located inside the inner cavity. Examination of the Be data indicates that the total Be(n,2n) cross-section of B6 is lower than that of B5 and (LANL)Be by ~ 10-15% at high incident energies and that this cross-section is very similar in the case of B5 and (LANL)Be evaluation. However, the secondary energy distribution (SED) from this reaction is noticeably different among the three evaluations; the SED in Be6 evaluation does not extend down below ~ 1KeV while the (LANL)Be evaluation extends down below ~ 1 KeV, but the cross-section in this energy range is negligible. On the other hand, in the Be5 evaluation, the SED extends down to very low energies. The impact of these differences on tritium production from $^{6}Li(T_6)$ and $^{7}Li(T_7)$ is that the calculated-to-measured values (C/E) for T_6 have improved with the Be6 by ~ 3-5% (C/E = 1.05) as compared to those obtained by the Be5 and (LANL)Be evaluations in the bulk of the Li_2O zone. The C/E values for the high threshold reactions [e.g., $^{58}Ni(n,2n)$] have also improved by 3-7%. By comparing the calculated spectra to the measured ones at various locations, it was noticed that the 14 MeV peak is better predicted by the Be6 evaluation.

I. INTRODUCTION

Three evaluations for the beryllium cross-sections were used to study their impact on the neutronics characteristics in the beryllium-front system with First Wall (BEFWFW) of Phase IIB experiments of the USDOE/JAERI Collaborative Program on Fusion Neutronics[1-3] for which measured parameters exist.[4-5] This particular system was chosen for the present study because an appreciable amount of beryllium was used in this experiment. In this system (See Fig. 1), a Li_2O test assembly (86.2 cm x 86.2 cm x 55.7 cm) is preceded by a 5 cm-thick beryllium zone (with a SS First wall of thickness 5 mm) and the assembly is located at one end of a 20 cm-thick Li_2CO_3 rectangular enclosure whose outer dimensions are 136 x 136 x 235 cm. The rest of the cavity's inner surface is also covered by a 5 cm-thick Be layer. The outer surface of the enclosure is covered by a 5 cm-thick polyethylene layer to isolate the assembly from the surroundings (details of the configuration can be found in Refs. 1-5) The neutronics characteristics studied are the tritium production rate (from ^{6}Li and ^{7}Li), several activation reactions, and in-system neutron spectrum.[4-5] The three evaluations used for Be are

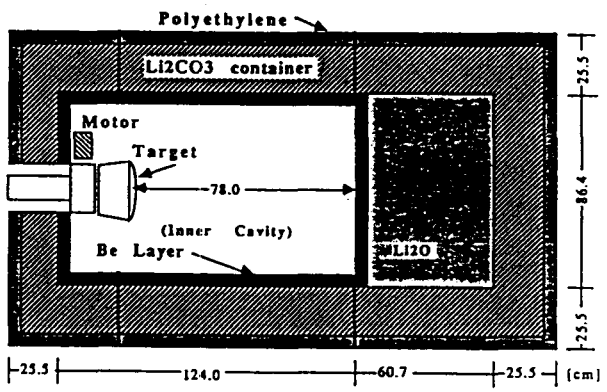

Figure 1: Geometrical configuration for the Beryllium front with first wall (BEFWFW) experiment.

the ENDF/B-V evaluation, the LANL evaluation and the ENDF/B-VI evaluation. The ENDF/B-V evaluation has been modified to obtain a better prediction of neutron multiplication since it was published about fifteen years ago.[6] The LANL evaluation was proposed by Young and Stewart in 1979 while the ENDF/B-VI evaluation is based on the original work of Perkins, Plechaty, and Howerton[8] of ENDL-86 (from LLNL) where modifications were made to account for the recent results of the differential cross-section measurements for $^{9}Be(n,2n)$ reaction.[9-10] The above evaluations are denoted ENDF/B5, LANL(Be), and ENDF/B6 in the present study. The calculations were performed by using the 2-D Sn code DOT 5.1 along with the

* Present address: Innovative Nuclear Power Institute, College of Engineering, University of Florida, Gainsville, FL 32611.

** Vol. 19, No. 3, Part 2B, (May 1991), pp. 1967-1973

first collision code, RUFF[11],used to mitigate the ray effect. The MATXS6[12] library (80-g) was used in P_5S_8 approximation. Except for beryllium, the cross-sections of other materials are based on ENDF/B-V (version 2). Details of the 2-D R-Z calculational model used can be found in Ref. 1.

II. THE STATUS OF BERYLLIUM DATA

The integrated (over energy and angle) cross-section for the ^{9}Be(n,2n) reaction is known to a better accuracy than the secondary energy (SED) and Angular (SAD) distributions of neutrons emitted from this reaction. This has direct impact on the neutronics characteristics in the test assembly since subsequent interactions with various nuclides of the transport media depend on the incident neutron energy and direction of these secondary neutrons. In ENDF/B-V, the ^{9}Be(n,2n) cross-section is represented by four inelastic excitation levels in ^{9*}Be at 1.68, 2.43, 6.76, and 11.28 MeV, each having zero width and with the energy-angle correlation between the emitted neutrons ignored. In the LANL evaluation, this cross-section is represented by 33 inelastic levels that were chosen to fit the neutron emission spectrum measurements of Drake, et. al[13]. The ^{9}Be(n,2n) cross-section is then based on data for a cluster of real levels near E_x = 2.429 MeV and 32 excitation energy bins to represent the (n,2n) continuum levels. The energy-angle correlation for the secondary neutrons was considered in this evaluation. The total integrated cross-section for the ^{9}Be(n,2n) reaction is very similar in ENDF/B-V and LANL evaluation; the difference being in the SED/SAD distribution of the secondary neutrons. In ENDF/B-VI data evaluated at LLNL, improvement has been made in the total integrated ^{9}Be(n,2n) cross-section, mainly being reduced by ~ 10-15% at high incident neutrons energies. Also, the energy/angle correlation for the secondary neutrons was considered.

Fig. 2 shows the total integrated cross-section for the ^{9}Be(n,2n) reaction above 2 MeV processed [in 30 neutron group of MATXS5 group structure[12]] from ENDF/B-V, LANL, and ENDF/B-VI (LLNL) evaluations. In the case of LANL evaluation, two processing systems were used, namely, the AMPX processing system[14], and the NJOY processing system[15]. One can notice from Fig. 2 that the ENDF/B-V and LANL data (processed either with AMPX or NJOY processing systems) are very similar. Also, the ENDF/B-VI data are lower than ENDF/B-V and LANL data (by ~ 10-15%) at high energies, as pointed out earlier. As for the SED of the ^{9}Be(n,2n) cross-section, Figs. 3 and 4 show this distribution for several incident energies (incident energy group in 30-group structure) for the ENDF/B-V and LLNL evaluations. In these figures, the notations E-in and E-out, represent the incident and emitted energy, respectively (10** - 1.0 eV means 10^{-1} eV). As shown, the SED in LLNL evaluation does not extend down below ~ 1 KeV. In the LANL evaluation, the cross-section (not shown) extends down below 1 KeV, but the cross-section in this energy range is negligible. However, in the ENDF/B-V evaluation, the SED extends down to very low energies.

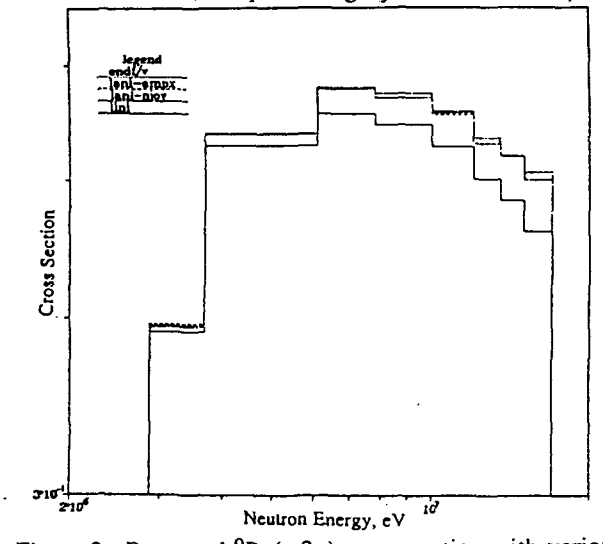

Figure 2: Processed ^{9}Be(n,2n) cross-section with various evaluations.

For the purpose of illustration, the transfer cross-section for ^{9}Be (n,total) and ^{9}Be(n,2n) reactions were prepared directly for the three evaluations. The 80-g cross-section set of the MATXS6 group structure we collapsed into 6-g cross-section sets in P_3 approximation. The lower energy boundaries for this group structure are 14 MeV, 10 MeV, 1.738 MeV, 0.11 MeV, 0.00109 MeV, and 1.39 x 10^{-10} MeV for group 1 to 6, respectively. The upper energy boundary is 20 MeV. Table 1 shows the P_0 component of the transfer matrix $\sigma gg'$ for the ^{9}Be(n,2n) cross-section of the three evaluations. It can be seen that the cross-sections for group 1 and 2 (corresponds to energy above 10 MeV) have been reduced by a 3-7% for ENDF/B-VI data over the other evaluations. The cross-section from group 1 to group 2, $\sigma_{1\text{-}2}$, is ~ 27% larger in ENDF/B-V than the other evaluations, i.e., there is an overestimation in the number of the secondary neutrons going into the energy range 10-14 MeV for reactions above 14 MeV in ENDF/B-V cross-section for ^{9}Be(n,2n) as compared to other evaluations. On the other hand, LANL evaluation has the largest cross-section for neutron transfer from group 1 (above 14 MeV) to group 3 (2-10 MeV) and group 4 (0.1-2 MeV). Notice also from Table 1 that the ENDF/B-VI and LANL cross-sections are much smaller for neutron transfer from group 1 (above

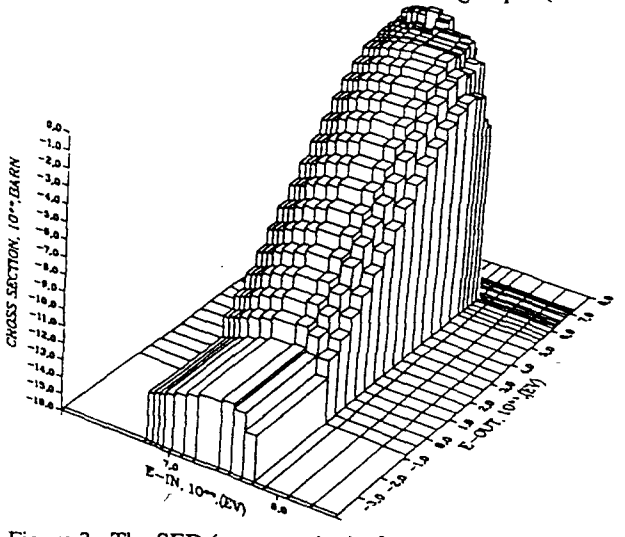

Figure 3: The SED (cross-section) of neutrons emitted from the ^{9}Be(n,2n) reactions (ENDF/B-V).

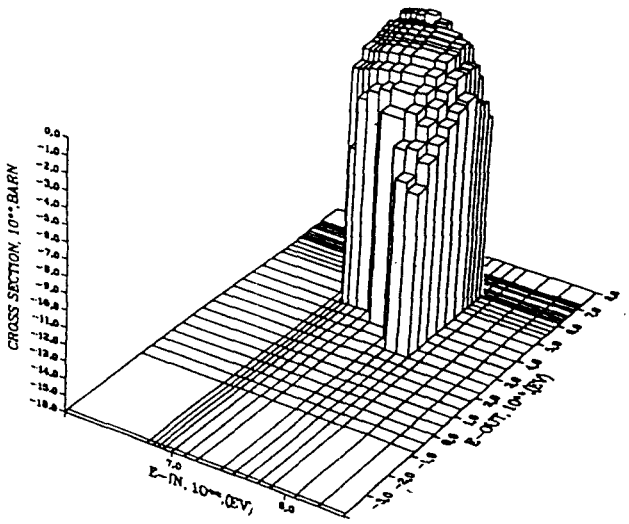

Figure 4: The SED (cross-section) of neutrons emitted from the $^{9}Be(n,2n)$ reactions (ENDF/B-VI).

14 MeV) to group 5 (1 KeV-0.1 MeV) and group 6 (below 1 KeV) than ENDF/B-V, as was pointed out in regard to Figs. 3-4. In fact, no neutron transfer from group 1 to group 6 (below 1 KeV) in ENDF/B-VI. The impact of those differences on the calculated values for the in-system spectrum and other reactions are discussed below.

Table 1: The P_0 Transfer Cross-Section, $\sigma_{gg'}$, for the $^{9}Be(n,2n)$ Cross Reaction in 6-Group Structure for the ENDF/B-V, LANL, and ENDF/B-VI Evaluations

	Energy Group g					
σ	1	2	3	4	5	6
total	5.139-1*	5.571-1+	2.964-1	0.0	0.0	0.0
	5.146-1	5.583-1	2.940-1	0.0	0.0	0.0
	4.769-1	5.276-1	2.881-1	0.0	0.0	0.0
$\sigma_{g\to g}$	1.664-3	1.147-1	1.779-1	0.0	0.0	0.0
	7.821-4	6.978-2	1.555-1	0.0	0.0	0.0
	1.444-3	6.350-2	1.082-1	0.0	0.0	0.0
$\sigma_{g-1\to g}$	0.0	2.364-1	5.242-1	3.437-1	0.0	0.0
	0.0	1.829-1	5.533-1	4.215-1	0.0	0.0
	0.0	1.915-1	5.142-1	4.253-1	0.0	0.0
$\sigma_{g-2\to g}$	0.0	0.0	4.053-1	4.180-1	7.124-2	0.0
	0.0	0.0	4.495-1	4.808-1	1.127-2	0.0
			3.937-1	4.497-1	4.264-2	0.0
$\sigma_{g-3\to g}$	0.0	0.0	0.0	3.562-1	5.727-2	5.475-5
	0.0	0.0	0.0	3.872-1	1.269-2	1.209-5
	0.0	0.0	0.0	3.505-1	2.772-2	0.0
$\sigma_{g-4\to g}$	0.0	0.0	0.0	0.0	2.818-2	2.316-5
	0.0	0.0	0.0	0.0	9.132-2	1.702-5
	0.0	0.0	0.0	0.0	1.680-2	0.0
$\sigma_{g-5\to g}$	0.0	0.0	0.0	0.0	0.0	9.370-6
	0.0	0.0	0.0	0.0	0.0	9.364-6
	0.0	0.0	0.0	0.0	0.0	0.0

* Reads as 5.139×10^{-1}

\+ Upper entry: ENDF/B-V, Middle: LANL, Lower: ENDF1B-VI

III. IMPACT OF DIFFERENCES IN BERYLLIUM CROSS-SECTIONS ON VARIOUS NEUTRONICS PARAMETERS

III.A In-System Neutron Spectrum

The neutron spectrum at five locations was examined with the three evaluations in the BEFWFW system, and the intercomparison to the NE 213 measurements [2-3,16] was made. These locations are at depth Z = 1.15, 3.68, 6.21, 11.27, and 31.51 cm. The first two locations are inside the front Be layer while the third is at 1.21 cm behind this layer. Figs. 5 and 6 show this comparison for Z = 3.68 cm and 11.27 cm. In these figures, the NE213 measurements below 2 MeV have large experimental errors (not shown) and should be disregarded. From these figures and for other locations (not shown) the following can be observed:

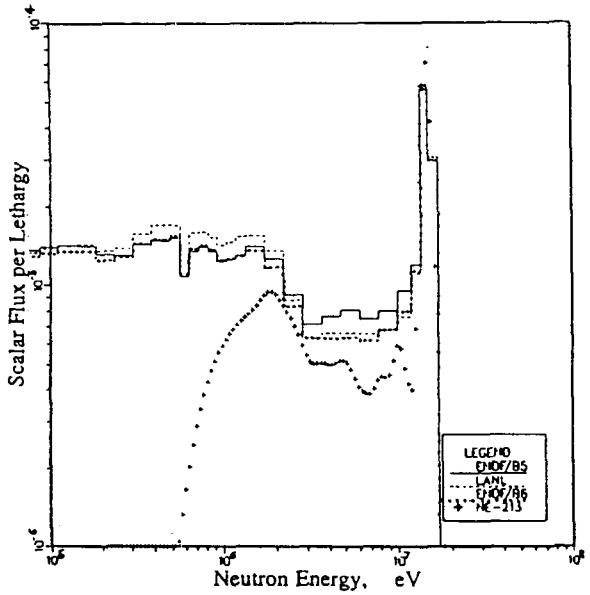

Figure 5: Neutron spectrum at depth Z = 3.68 cm with various Be evaluations.

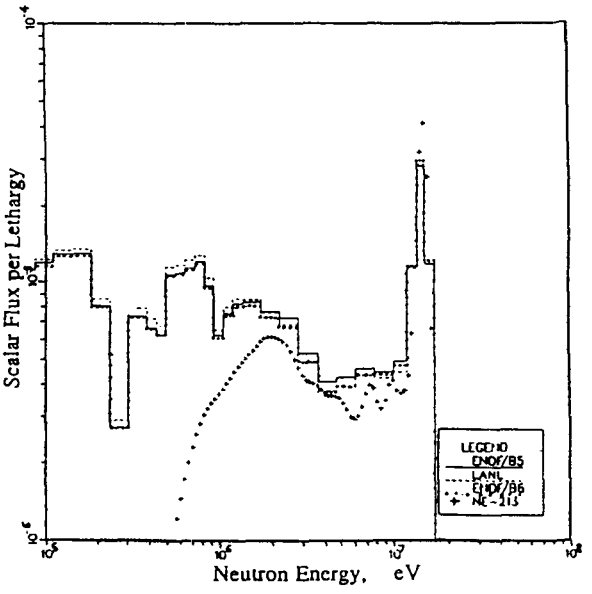

Figure 6: Neutron spectrum at depth Z = 11.27 cm with various Be evaluations.

(1) At the five locations selected, the 14 MeV peak is much smaller than the measured value obtained by the NE213 detector.

(2) The 14 MeV peak obtained by the ENDF/B6 evaluation is larger than that obtained by the ENDF/B5 and LANL evaluations where this peak is basically the same.

(3) The computed spectrum with the three evaluations in the energy range 2-13 MeV is larger than the measurements. The ENDF/B5 evaluation gives the largest spectrum in this energy range while the spectrum is comparable with the ENDF/B6 and LANL evaluation.

(4) In the energy range 0.1 - 2 MeV, the neutron spectrum calculated by the LANL evaluation is the largest; ENDF/B6 results are similar (but slightly less) to the ENDF/B5 results in this energy range.

(5) The differences in the spectrum calculated by the three evaluations decrease outside the Be layer, particularly at locations far from this layer (at Z = 31.51 cm).

The above intercomparison among the calculated spectrum with the three evaluations for energies below 1 MeV was carried out and comparison was made to the measurements performed by the Proton Recoil Counter, PRC [16], in the energy range 1 KeV-1MeV. The spectrum calculated by the ENDF/B5 evaluation is always larger than that obtained by ENDF/B6 and LANL evaluations below 0.1 MeV. This could be due to the observation that the SED from the ^{9}Be(n,2n) reaction extends to very low energies in comparison to the two other evaluations, as was discussed in Section II. Good agreement with the PRC measurements was obtained in the energy range 10 - 100 KeV but larger spectra are obtained by calculations in the energy range 1 KeV - 10 KeV.

Figs. 7 and 8 show the Calculated-to-Experimental values (C/E) for the integrated spectrum, in the energy ranges En>10MeV and 1.01 MeV<En<10 MeV, respectively. Inside the Be layer, the C/E values for the integrated spectrum above the 10 MeV is lower than unity by ~ 5% with the three evaluations at depth Z = 1.15 cm, but slightly larger than unity at depth Z = 3.68 cm. These two locations are inside the Be layer. From Fig. 5 and the similar fig. at Z = 1.15 cm (not shown), one can observe that the underprediction at Z = 1.15 cm is mainly due to the underprediction in the neutron spectrum above 13 MeV which dominates the over prediction in the energy range 10 - 13 MeV. At Z = 3.68 cm, however, the overpredicted part of the spectrum in the energy range 10 - 13 MeV dominates and this leads to the C/E value that is larger than unity (by ~ 5%). Behind the Be layer and in the bulk of the Li_2O, the integrated spectrum above 10 MeV is underpredicted by the three evaluations by 5-10%, and this underprediction is less pronounced in the case of the ENDF/B6 data for Be. Since the integrated cross-section for the ^{9}Be(n,2n) reaction is less in the ENDF/B6 data, particularly at high energies (see Fig. 2), this leads to an improvement in the prediction of the integrated spectrum above 10 MeV, although this component is still underpredicted with the ENDF/B6 data.

The integrated spectrum in the energy range 1.01 MeV <En <10 MeV is overpredicted by three evaluations at all locations. In the Li_2O zone, the overprediction is ~ 20% but it is larger (by ~ 60%) inside the Be layer. In the Be region and at Z = 3.68 cm, the overprediction with the ENDF/B5 data is similar to that with the LANL data (by examining Fig. 5, we can see that the spectrum between 1 MeV - 2MeV is larger with the LANL data while it is smaller in the energy range 2 - 10 MeV as compared to results obtained with the ENDF/B5 data; and this leads to compensation in the integrated spectrum in the energy range 1 - 10 MeV). With the ENDF/B6 data, the integrated spectrum is better predicted since the spectrum in the energy range 1 - 10 MeV is the closest to the experimental values, up to a depth of ~ 15 cm.

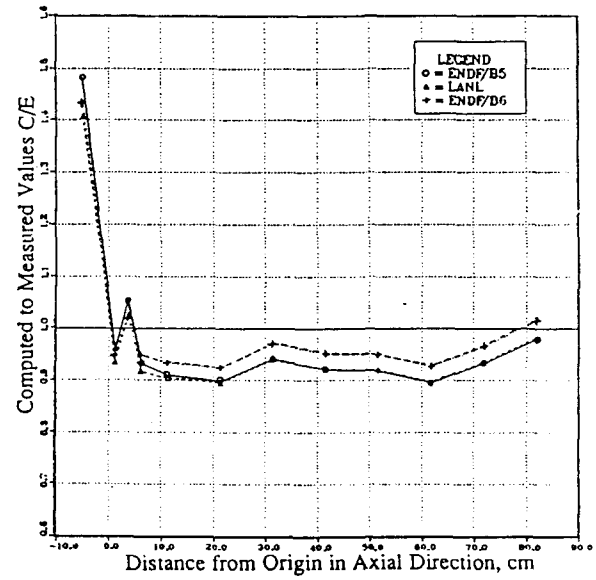

Figure 7: Integrated spectrum (E > 10 MeV) Measured by NE213 in the Central Drawer.

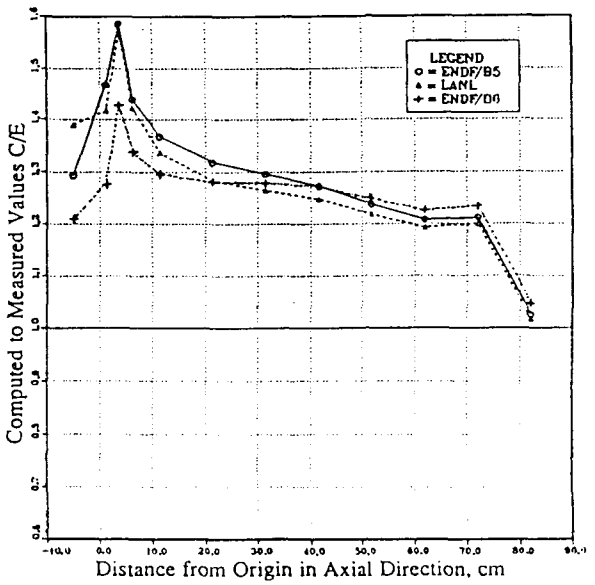

Figure 8: Integrated Spectrum (10 MeV < E < 1.01 MeV) measured by NE213 in the central drawer.

III.B Activation Reaction Rates

Threshold reactions can give a measure of the differences in the integrated spectrum over a certain range of energy. The C/E values for the $^{93}Nb(n,2n)^{92m}Nb$ reaction (E_{th} ~ 8 MeV) are shown in Fig. 9. At the front face of the assembly, and inside the Be layer, the C/E values are larger than unity, but their values drop below unity behind that layer. The ENDF/B6 evaluation for Be gives larger values (by ~ 3%) in comparison to the other evaluations. This was also found in the C/E curves for $^{58}Ni(n,2n)$ (E_{th} ~ 12.5 MeV) where improvement of that order was obtained although it was shown that the cross-section for $^{58}Ni(n,2n)$ of ENDF/B-V should be increased by ~ 25-30%. In the bulk of the Li_2O zone, the C/E values are less than unity. This could be partly attributed to an overestimation in the total $^{9}Be(n,2n)$ cross-section itself at high energies (which leads to lower neutron spectrum around the 14 MeV peak) and partly to an underestimation in the SED of the emitted neutrons from the $^{9}Be(n,2n)$ reactions above 10 - 13 MeV. The ENDF/B6 evaluation for Be has lower total (n,2n) cross-section (see Fig. 2) and thus an improvement in the C/E curves for the high-threshold reactions takes place.

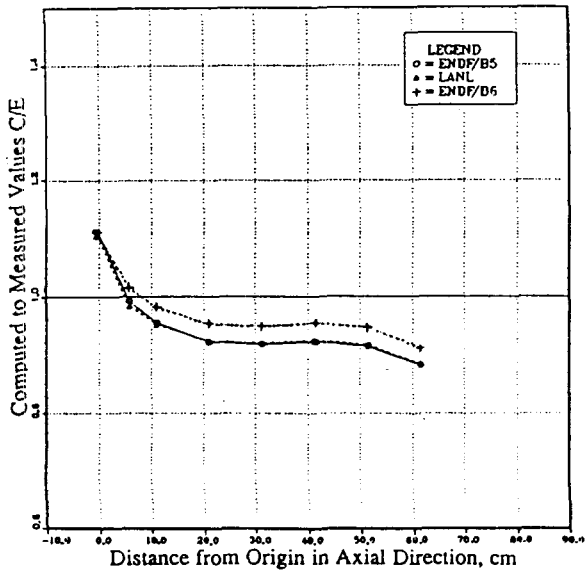

Figure 9: The C/E values for the $^{93}Nb(n,2n)^{92m}Nb$ reaction in the central drawer.

For lower threshold reactions, the characteristics of the C/E curves are different. The C/E curves for $^{27}Al(n,\alpha)^{24}Na$ reaction (Eth ~ 6 MeV) were examined and found to be larger than unity inside the Be zone (by ~ 5-10%) but fall below unity thereafter. As was shown in Fig. 5, the neutron spectrum inside the Be layer is the largest with the ENDF/B5 evaluation in the energy range 2 - 13 MeV, where the threshold energy of this reaction lies. Also, the integrated spectrum in the energy range 1 - 10 MeV is overpredicted with this evaluation than others, as can be seen from Fig. 8. This is reflected on the C/E value inside the Be zone, where the values are the largest with the ENDF/B5 evaluation followed by the ENDF/B6 and LANL data. In the Li_2O zone, the LANL values approach those calculated by the ENDF/B5 (C/E ~ 0.95) while the C/E values obtained by ENDF/B6 evaluation are the largest (by ~ 5%) and closest to unity (C/E ~ 1.0).

Trends similar to those discussed above were observed in the C/E curves for the $^{58}Ni(n,p)^{58}Co$ and $^{115}In(n,n')^{115m}In$ reactions. The overprediction of the neutron spectrum in the energy range 2 - 13 MeV by the ENDF/B5 data shows up as the largest C/E values inside the Be layer, as shown in the C/E curves for $^{58}Ni(n,p)$ reactions (E_{th} ~ 2 MeV) depicted in Fig. 10. At deeper locations, such overprediction in the spectrum is less pronounced, hence the larger neutron spectrum above 13 MeV predicted by the ENDF/B6 data leads to the largest C/E values. The threshold energy for the $^{115}In(n,n')^{115m}In$ reaction is low (~ 1 MeV) and neutron flux below 2 MeV also makes contribution to this reaction. In the Be zone, the overprediction of this spectrum component (in the energy range 0.1 - 2 MeV) by the LANL data (see Figs. 5 and 6) leads to medium values between those obtained by ENDF/B5 and B6 data. This is also shown in Fig. 8, where the integrated spectrum between 1 and 10 MeV, as predicted by LANL data, tends to be between the ones obtained by the ENDF/B6 and ENDF/B5 data.

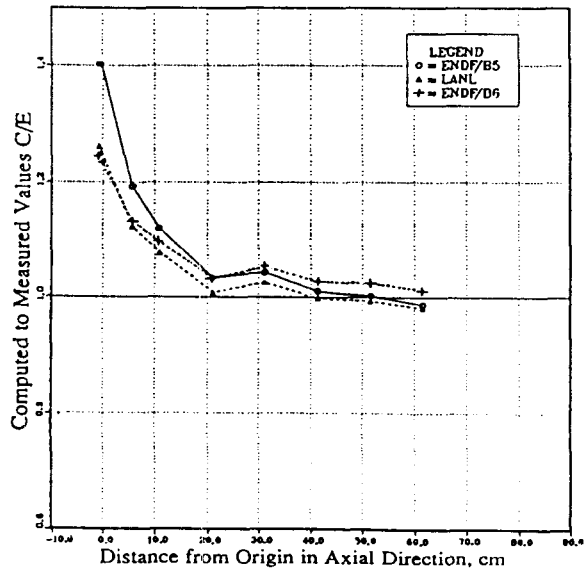

Figure 10: The C/E values for $^{58}Ni(n,p)^{58}Co$ reaction in the central drawer.

III.C. Tritium Production Rates

The C/E curves for T_7 is shown in Fig. 11. Note that the measured values for T_7 are obtained by folding the neutron spectrum measured by the NE213 detector with the $^{7}Li(n,n'\alpha)t$ cross-section of the JENDL3-PR1 data.[17] The threshold energy for this cross-section (~ 2.8 MeV) is similar to the $^{58}Ni(n,p)$ reaction and, therefore, the C/E curves have similar trends. The C/E values obtained by LANL evaluation approach the values obtained by the

ENDF/B5 at deep locations, and the C/E values obtained by the ENDF/B6 are the largest at these deep locations. Note that the last trend is due to the fact that the $^{9}Be(n,2n)$ cross-section is the smallest at high incident energies in the ENDF/B6 evaluation as compared to the other two evaluations. Cross-section Sensitivity analysis (see Ref. 2) has indicated, as expected, that T_7 has negative integrated sensitivity coefficients for variation in the $^{9}Be(n,total)$ cross-section. That is, decreasing the total (elastic + nonelastic) cross-section leads to an increase in T_7, and that increase is more noticeable as one proceeds towards the back end of the test assembly. Also, it was shown that the main contribution to the sensitivity coefficient comes from variation in the $^{9}Be(n,2n)$ cross-section. Since the $^{9}Be(n,2n)$ cross-section in ENDF/B6 evaluation is smaller (by ~ 15%) than those of ENDF/B5 and LANL, the T_7 will consequently increase, particularly at deep locations, as shown in Fig. 11. In addition, by examining the relative sensitivity profile for variation in the $^{9}Be(n,2n)$ cross-section, it was shown [2] that any reduction in this cross-section at high energies above 13 MeV leads to the largest impact (increase) on T_7.

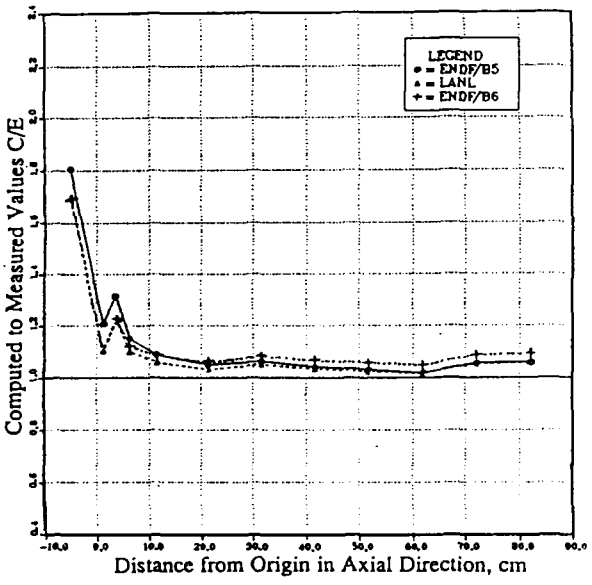

Figure 11: The C/E values for T_7 measured by NE213 detectors in the central drawer.

The C/E curves for T_6 shown in Fig. 12 are very different from those seen for other threshold-type reactions. The lower energy component of the neutron flux plays a significant role on T_6 values. It can be seen from Fig. 12 that the C/E values in the Be layer are as large as 1.6. When corrections due to the self-shielding by the Li-glass scintillator itself and the flux perturbation effect of the detector structure materials are made, it was shown that the C/E values inside the Be region decrease to about unity (see Ref. 10 and 18). It is clear without such corrections that the magnitude of the C/E values inside the Be layer is in the order, ENDF/B5, ENDF/B6, and LANL, from the largest to the smallest. Just behind the Be layer the sudden drop in the C/E values (to below unity) is more noticeable with the ENDF/B6 evaluation followed by those obtained with the LANL and ENDF/B5, in that order. As was shown in the spectrum calculations at various locations in the test assembly that both the ENDF/B6 and LANL data lead to smaller low-energy component in the spectrum than in the case with the ENDF/B5 evaluation. In addition, it was shown in Figs. 3 and 4 that the SED of neutrons emitted from the $^{9}Be(n,2n)$ reactions does not extend below ~ 1 KeV in the ENDF/B6 evaluation while the LANL evaluation extends below this energy but with insignificant cross-section. On the other hand, the SED in the ENDF/B5 case has the largest component at very low energies as compared to ENDF/B6 and LANL data. The difference in the low-energy component in the neutron spectrum shows up in Fig. 12 as smaller C/E values with the ENDF/B6 and LANL data than those obtained with the ENDF/B5 data at all locations in the Li_2O region. Thus, it can be said from Fig. 12 that the C/E values for T_6 in the bulk of the Li_2O zone have generally improved upon using the ENDF/B6 data for beryllium, except at locations just behind the Be layer.

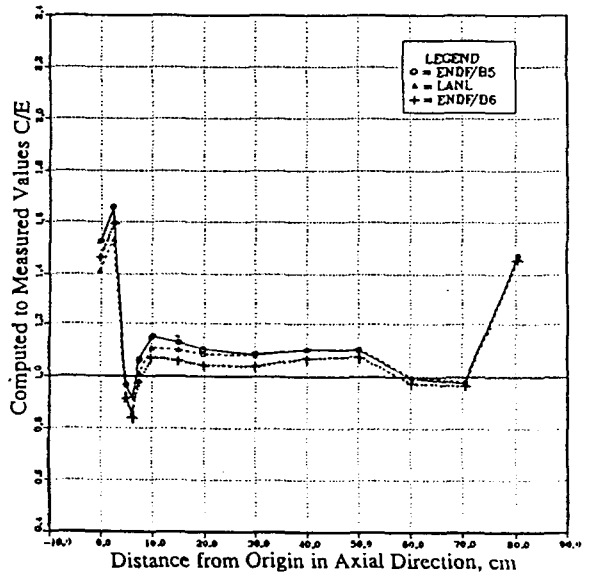

Figure 12: The C/E values for T_6 measured by Li-glass detectors in the central drawer.

IV. SUMMARY

Three evaluations for beryllium data (ENDF/B-V, LANL, and ENDF/B-VI) were used to calculate in-system spectrum, tritium production and other reaction rates inside a test assembly of Li_2O (55 cm thick) that has a 5 cm-thick beryllium front zone. By comparing the calculations to spectrum measurements it was shown that the integrated spectrum above 10 MeV has been improved with the ENDF/B-VI data due to the improvement in the total $^{9}Be(n,2n)$ cross-section (~ 10-15% less than in the other evaluations) and to the improvement in secondary energy distribution (SED) from this reaction. In ENDF/B-VI, the emitted neutrons from $^{9}Be(n,2n)$ reactions has harder SED (larger component above 10 MeV and lower component in the energy range 2-10 MeV) than in other evaluations and this led to noticeable improvements (3-7%) in the high-

threshold reactions such as $^{58}Ni(n,2n)$ and $^{93}Nb(n,2n)^{92m}Nb$. Improvement in the order of ~ 5% has also been noted for tritium production from ^{6}Li (T_6) in the bulk of the Li_2O) zone although the drop in the Calculated-to-Experimental (C/E) values below unity (C/E ~ 0.9) just behind the beryllium layer has increased by ~ 5% (C/E ~ 0.85) when the ENDF/B-VI data were applied. As for T_7 larger values were obtained with ENDF/B-VI data inside the Li_2O zone and that is due to the reduction in the total $^{9}Be(n,2n)$ cross-section at high incident energies. Nevertheless, the integrated spectrum above 10 MeV (particularly around the 14 MeV peak) tends to be lower than measurements in the Li_2O zone. Perhaps increasing the SED of the emitted neutron from the $^{9}Be(n,2n)$ reaction above 10 MeV could improve this discrepancy.

ACKNOWLEDGEMENT

Special thanks to Dr. D. Muir from Los Alamos National Laboratory for processing ENDF/B-VI for beryllium in MATXS6 multigroup format. This effort is supported by the United States Department of Energy, Office of Fusion Energy under Grant No. DE-F603-86ER52124.

REFERENCES

(1) M. Z. YOUSSEF, et al, "Comparative Analysis for Phase IIA and IIB Experiments of the U.S./JAERI Collaborative Program on Fusion Breeder Neutronics", Fusion Technol., 15, 2, Part 2B, 1299-1308, 1989.

(2) M. Z. YOUSSEF, et al, "The U.S./JAERI Collaborative Program on Fusion Neutronics; Phase IIA and IIB Fusion Integral Experiments, The U.S. Analysis: UCLA-ENG-90-14, University of California at Los Angeles, December, 1989.

(3) M. NAKAGAWA, et al, "JAERI/U.S. Collaborative Program on Fusion Blanket Neutronics, Analysis of Phase IIA and IIB Experiments, JAERI-M-89-154, Japan Atomic Energy Research Institute, October, 1989.

(4) Y. OYAMA, et al, "Phase IIB Experiments of JAERI/USDOE Collaborative Program on Fusion Blanket Neutronics, Fusion Technol., 15 Number 2, Part 2B, 1293-1298, 1989.

(5) Y. IKEDA, et al, "Determination of Neutron Spectrum in D-T Fusion Field by Foil Activation Technique, Fusion Technol., 15, 2, Part 2B, 1287-1292, 1989.

(6) R. J. HOWERTON, S. J. PERKINS, "Evaluated Neutron-Interaction and Gamma-Ray-Production Cross-Sections of ^{9}Be for ENDF/B-IV, MAT No. 1289," UCRL-51603, Lawrence Livermore National Laboratory, July, 1974.

(7) P.G. YOUNG, L. STEWART, "Evaluated Data for n + ^{9}Be Reactions," LA-7932-MS(ENDF-283). Los Alamos Scientific Laboratory, July, 1979.

(8) S. T. PERKINS, E. F. PLECHATY, R. J. HOWERTON, A Re-Evaluation of the $^{9}Be(n,2n)$ Reaction and its Effect on Neutron Multiplication in Fusion Blanket Applications," Nucl. Sci. Engr., 90, 83-98, 1985.

(9) A. TAKAHASHI, Y. SASAKI, H. SUGIMOTO, "Double Differential Neutron Emission Cross-Sections at 14.1 MeV for Be, V, and Fe," Proc. of the International Conference on Nuclear Data for Science and Technology," pp. 205-208, May 30-June 3, 1988, Mito, Japan. S. Igarashi, ed., Japan Atomic Energy Research Institute, 1988.

(10) M. BABA, M. ISHIKAWA, T. KIKUCHI, H. WAKABAYASHI, N. HIRAKAWA, "Double-Differential Neutron Scattering Cross-Sections of Beryllium, Carbon, Oxygen." Proc. of the International Conference on Nuclear Data for Science and Technology," pp. 209-212, May 30-June 3, 1988, Mito, Japan. S. Igarashi, ed., Japan Atomic Energy Research Institute, 1988.

(11) L. P. KU and J. KOLIBAL, "RUFF-A Ray Tracing Program to Generate Uncollided Flux and First Collision Source Moments for DOT 4, A User's Manual, EAD-R-16, Plasma Physics Laboratory, Princeton University, 1980.

(12) R. A. MACFARLANE, "TRANSX-CTR: A Code for Interfacing MATXS Cross-Section, Libraries to Nuclear Transport Codes for Fusion Systems Analysis," LA-9863-MS, Los Alamos National Laboratory, February, 1984.

(13) D. M. DRAKE, G. F. AUCHAMPAUGH, E. D. ARTHUR, C. E. RAGAN, and P. G. YOUNG, "Double-Differential Beryllium Neutron Cross-Sections at Incident Neutron Energies of 5.9, 10.1, and 14.2 MeV," Nuc. Sci. Engr., 63, 401-412, 1977.

(14) N. M. GREEN, et al, "AMPEX: Modular Code System for Generation Coupled Multigroup Neutron-Gamma-Ray Cross-Section Library from Data in ENDF Format," PSR-063/AMPXII, ORNL/TM-3706, Radiation Shielding Information Center, Oak Ridge National Laboratory, 1980.

(15) R. MACFARLANE, D. MUIR, and R. BOICOURT, "The NJOY Nuclear Data Processing System," Vol. I and II ((ENDF-9303-M, Vol. I, LA-9303-M, Vol. II (ENDF-324), Los Alamos National Laboratory, May, 1982.

(16) Y. OYAMA, et al, "Phase IIA and IIB Experiments of JAERI/U.S.DOE Collaborative Program on Fusion Blanket Neutronics - Neutronics Experiment on Beryllium Configuration - in a Full Coverage - Blanket Geometry," Part I & II, JAERI-M-215, Japan Atomic Energy Research Institute, November, 1989.

(17) K. SHIBATA, et al, "Evaluation of Neutron Nuclear Data for ^{6}Li, ^{7}Li, and ^{12}C for JENDL3," JAERI-M-84-198, JAERI-M-84-204, JAERI-M-83-221, Japan Atomic Energy Research Institute, 1984.

(18) M. Z. YOUSSEF et al, "Analysis of Neutronics Parameters Measured in Phase II Experiments of the JAERI/U.S. Collaborative Program on Fusion Blanket Neutronics, Part II: Tritium Production and In-System Spectrum, Fusion Engr. and Design, 9, 323-332, 1989.

Neutronic Integral Experiments for Evaluation on Tritium Breeding in s Fusion Blanket. -- Li,Pb,Be and C sphere systems with OKTAVIAN -

Kenji Sumita, Akito Takahashi,
Junji Yamamoto, Ken Yamanaka
Osaka University, Department of Nuclear Engineering,
Faculty of Engineering,
and
Chen Yuan
Southwest Institute of Nuclear Physics and Chemistry.
(SWINPC). P.O. Box 525-74. Chengdu, Sichuan, PRC.

Abstract:

For T breeding blanket design, a series of integral measurements to evaluate neutron multipliers, Pb and Be, have been carried out by using OKTAVIAN and a large natural lithium sphere with/without a graphite reflector. The preliminary measurement results of TBR and Time dependent reaction rate of Li are compared with the calculated values to investigate the existing evaluated cross section library and calculational code. Our experimental results raised the questions to the evaluated cross section data of 9Be in lower energy range.

1. Introduction

In the beginning stage of the design works for a fusion reactor blanket, it was commonly misunderstood that the tritium breeding ratio (TAR) over 1.0 would be easily achieved by using simple blanket structures consisted of natural lithium. However, such misunderstanding was revised after the remarkable progress of analytical and computational methods of neutron transport calculations as well as the reevaluations of nuclear data in fusion neutronics field. Now enrichment of 6Li and/or adoptions of neutron multipliers (Be or Pb) are considered to override the uncertainly of TBR. It might be very useful to use a graphite reflector, too. So far, the TBR values from 1.02 to 1.05 are also demanded with the high accuracy within a few percent in the present design works.

To make clear guide lines for resolving such problems, a fusion neutronics research group had been organized from 1983 by Japanese inter-universities under the support of Grant in Aid for Fusion Research of the Ministry of Education, Science and Culture. The group, which was headed by Prof. K. Sugiyama of Tohoku University, consists of researchers and post-graduate students of Tohoku University, the University of Tokyo, Tokyo technology, Nagoya University and Osaka University. The OKTAVIAN facility(1) of Osaka University was supplied as a 14 MeV neutron source or experiments.

Before 1983, the research subjects to improve the accuracy of nuclear data, i.e. DDX, especially relevant to neutron multiplication of Pb, to tritium production reactions as 7Li(n,n'α)T and to establish the calculation methods of neutron transport have been investigated at the OKTAVIAN(2)(3). As the inter-

---

*The preliminary version of this paper was presented to Japan-US Workshop on Fusion Neutronics at UCLA. Oct. 15-17, 1990, under the title of "Integral Experiments to Improve Tritium Breeding Ratio". Here, the latest experimental results, which contain uncorrected tentative values, have been newly include in section 5 in addition to rhetoric rewrittening generally.

university experiments, we started the basic experiments to investigate the neutron transport phenomena in blanket materials using a lithium sphere of 120 cm-diam. Metallic natural lithium is contained with stainless steel vessel and the sphere has a cavity of 40 cm-diam at the center of the sphere as a test region of neutron multipliers. During last 7 years, various experiments were undertaken for three categories of systems, as explained in the following;

2. The system of Li(10)+Li(40) (bare natural lithium sphere)

The central cavity was filled with only natural lithium and the total thickness of lithium layer was 50cm. The radial distributions of tritium production rate (TPR) from 6Li(n,α)T and 7Li(n,n'α)T were measured and the respective TBR's by 6Li(T6) and 7Li(T7) could be obtained from the integrations of the TPR distributions. The total TBR (T6+T7) was 0.73. In such geometrical arrangement, nearly one half of neutrons injected was estimated to leak from the sphere. The measured T7 was smaller by 20 % than the value calculated using the ENDF/B-IV library(4)-(6).

3. The system of Pb(5) or Pb(10)+Li(40)

The assembly is shown in Fig. 1. Neutrons in the lithium sphere were multiplied by (n,2n) reactions of lead which was positioned at the central cavity. However, the total TBR decreased in both cases of Pb(5) and Pb(10). The value was observed as 0.67 for the Pb(5) shell and as 0.62 for the Pb(10) shell, respectively(7). It was understood the neutron energy softening by adding Pb(n,2n) reaction effected remarkably on the TBR reduction of 7Li(T7), though the effective neutron multiplication were attained.

4. The system of Pb(10)+Li(40)+C(20)

The experiments results using a graphite reflector of 20 cm in thickness with lead multipliers is now at the final review stage. The total measured TBR is nearly 1.16 by the preliminary analyses of irradiated TLD(8),(9). Neutron multiplication factors which are predicted by calculation for various evaluated nuclear data sets as shown in Table 1. Corresponding TBR values for the Pb+Li+C systems are shown in Table 2 and 3. With a graphite reflector, it became very difficult by time of flight method to measure the lower energy parts of spectrum, which were very effective on T6 determination. Then, for TBR estimation, we introduced a new method based on the time-dependent neutron balance(10). The time-dependent reaction rates of 6Li(n,α)T reaction were measured using a 6Li-glass scintillator, with the correction of γ-ray background using a 7Li-glass scintillator. Example of time- dependent measurement is shown in Fig.2 for the fore ground and background runs. This method improves the S/N ratio in the time region after the burst of 14 MeV neutron, and provides the information about the energy profile of T6. Time dependent reaction rates (P6(t)) were measured at several points along the radial direction in the spheres. By integrating the time-dependent reaction rates over the whole sphere, we obtain the time variation of T6 in the whole systems. Result are shown in Fig. 3 though Fig. 5, respectively for the Li, Pb+Li and Pb+Li+C systems. Predictions by calculation give good agreement for the pure Li system, but not so good for the systems including a Pb multiplier. It means the under estimation is remarkable for the Pb(n,2n) reaction.

Table 1

Comparisons of calculational results by four nuclear data libraries in a Pb(10cm) assemblies.

	ΔM		Leakage	
JENDL-3	0.513	(1.000)	1.510	(1.000)
JENDL-3T	0.470	(0.916)	1.467	(0.972)
ENDF/B-IV	0.563	(1.097)	1.559	(1.032)
EFF-1	0.486	(0.947)	1.484	(0.983)

* For leakage, in a bare Be (11.65cm) system. JENDL-3 gives 1.734, JENDL-3T gives 1.742 & ENDF/B-IV gives 1.769.

Table 2

Comparisons of calculational results by the four nuclear data libraries in a Pb(10cm)+Li(40cm) assemblies.

	T 6		T 7		T t		ΔM		Leakage	
JENDL-3	0.318	(1.000)	0.183	(1.000)	0.501	(1.000)	0.551	(1.000)	1.218	(1.000)
JENDL-3T	0.301	(0.947)	0.188	(1.027)	0.489	(0.976)	0.509	(0.924)	1.165	(0.956)
ENDF/B-IV	0.349	(1.097)	0.193	(1.055)	0.542	(1.082)	0.604	(1.096)	1.238	(1.016)
EFF-1	0.311	(0.978)	0.193	(1.055)	0.504	(1.006)	0.527	(0.956)	1.174	(0.964)

Table 3

Comparisons of calculational results by the four nuclear data libraries in a Pb(10cm)+Li(40cm)+C(20cm) assemblies.

	T 6		T 7		T t		ΔM		Leakage	
JENDL-3	0.924	(1.000)	0.187	(1.000)	1.112	(1.000)	0.551	(1.000)	0.570	(1.000)
JENDL-3T	0.886	(0.956)	0.193	(1.032)	1.079	(0.970)	0.509	(0.924)	0.566	(0.993)
ENDF/B-IV	0.979	(1.060)	0.198	(1.059)	1.177	(1.058)	0.604	(1.096)	0.533	(0.935)
EFF-1	0.907	(0.982)	0.198	(1.059)	1.105	(0.994)	0.527	(0.956)	0.561	(0.984)

Table 4

Calculational results by the nuclear data library JENDL-3 in a Be(11.65cm)+Li(40cm)+C(20cm) assemblies.

	T 6	T 7	Tt	△M	Leakage
JENDL-3	1.174	0.250	1.424	0.830	0.499

Fig.1 The Pb+Li system

Fig.2 Time dependent count rates in Pb-Li sphere;
a) by ^{6}Li glass. b) by ^{7}Li glass.

Fig.3 Time-dependent ^{6}Li(n,α)T reaction rates in a 120cm φ spherical assembly (vacuum[10cm]+Li[50cm])

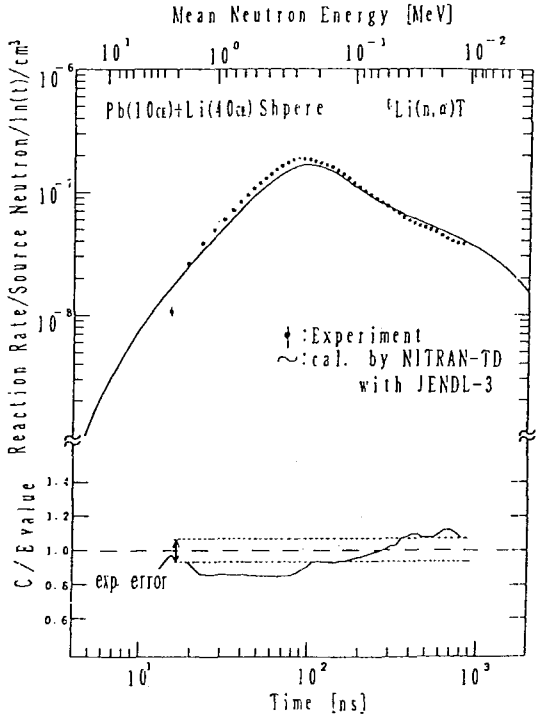

Fig.4 Time-dependent ^{6}Li(n,α)T reaction rates in a 120cm φ spherical assembly (vacuum[10cm]+Pb[10cm]+Li[40cm])

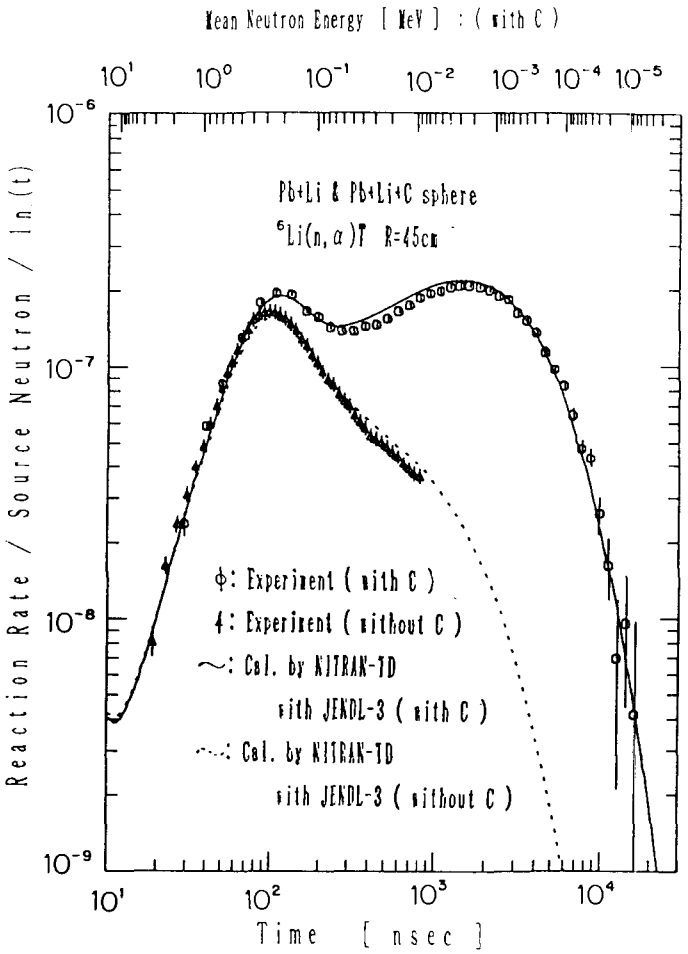

Fig.5 Time-dependent ^{6}Li(n,α)T reaction rate for the Pb+Li+C assembly, compared with that for Pb+Li assembly

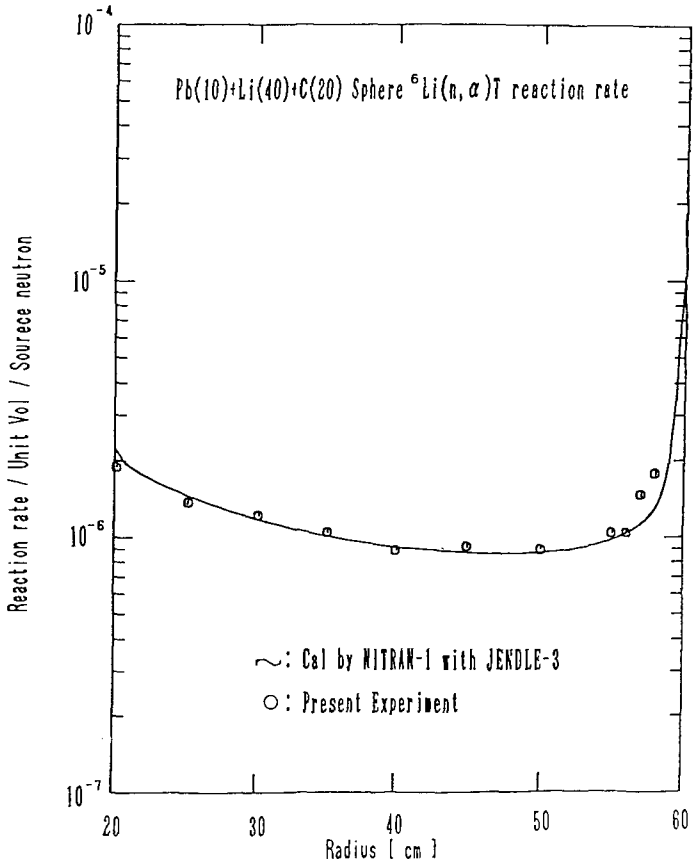

Fig.6 Radial distribution of ^{6}Li(n,α)T reaction rates for the Pb+Li+C assembly

The effect of a graphite reflector is separately observed in the experiment as shown the rise of P6(t) at the later time in Fig. 5. By integrating measured space-time dependent 6Li(n,α)T rates over time, we obtain the radial distribution of steady 6Li(n,α)T rates, as shown in Fig. 6. Agreement with the calculated curve using the cross section of JENDL-3 is fairly well. However, we still need further improvement of experimental technique to make the space resolution higher for the region very near graphite reflector. The spatial integration of measured points of 6Li(n,α)T rates in Fig. 6 can give the overall T6 in the assembly with in reasonable error, but not yet attained to meet the required experimental accuracy within a few percent.

5. The system of Be(11.65)+Li(40)+C(20)

In order to support the nuclear design studies for the next stage of D-T burning fusion facility like as a ITER, a series of experiment on Be multipliers with a Li sphere and a graphite reflector at OKTAVIAN are planned for TBR. The project is carried out now at OKTAVIAN site as a Japan/U.S./China collaboration work since the summer of 1990. The main subject is to evaluate the available gain of TBR by the help of Be(n,2n) reaction, which is expected that the values from 1.3 to 1.5 will be finally achieved. This should be also a good benchmark experiment for the improvement of Be nuclear data. To accurately determine the neutron multiplication performance of Be-9, three type experiments are planned.

The 1st one is the measurement of leakage neutron multiplication for bare Be sphere with various thickness, based on the neutron T.O.F. method. To cover the wide energy range from 14 MeV to thermal (0.025 eV), 2 detection systems (NE213

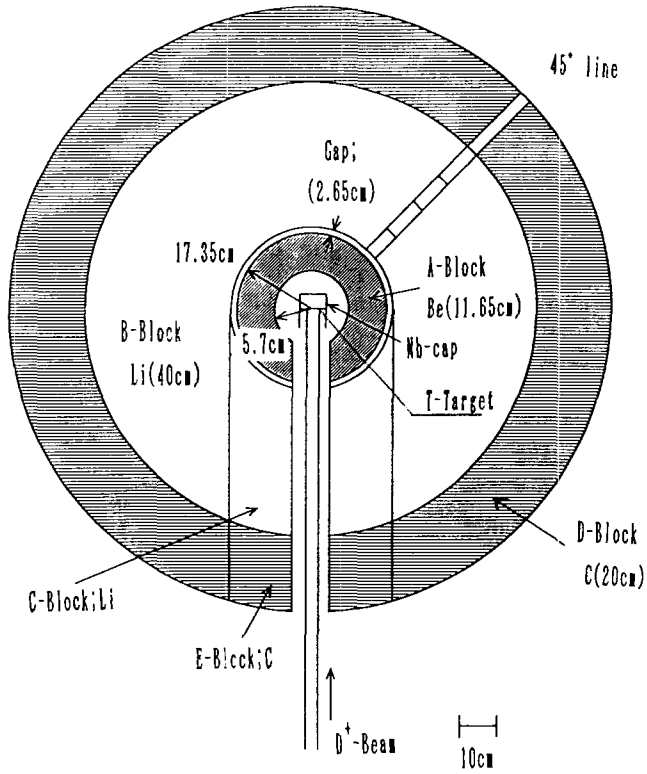

Fig 7 The Be-Li-C System

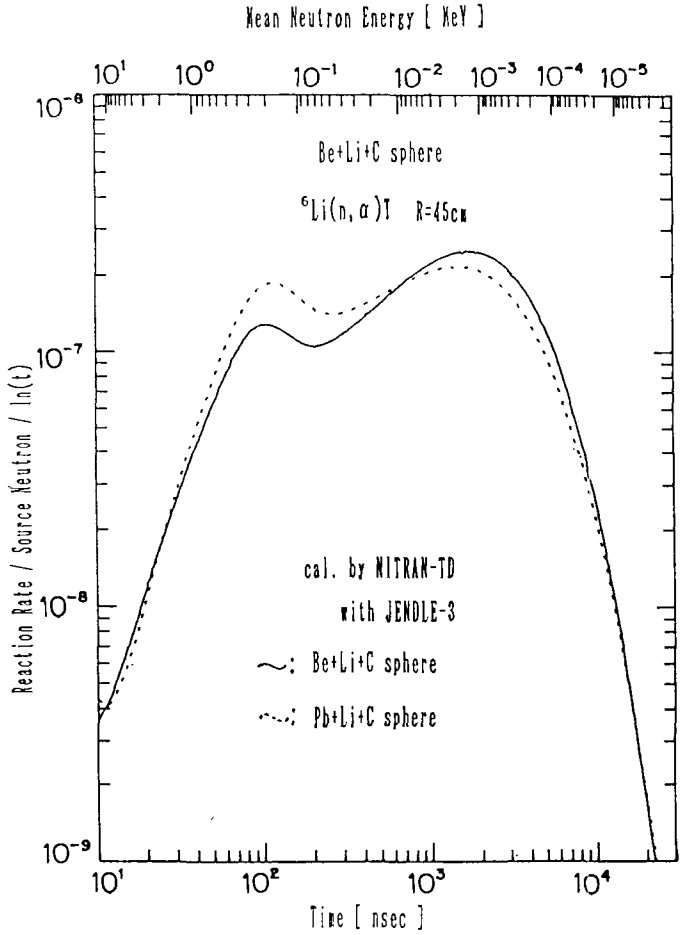

Fig.8 Time Dependent $^{6}Li(n,\alpha)T$ reaction rates for the Be+Li+C assembly, compared with that for Pb+Li+C assembly

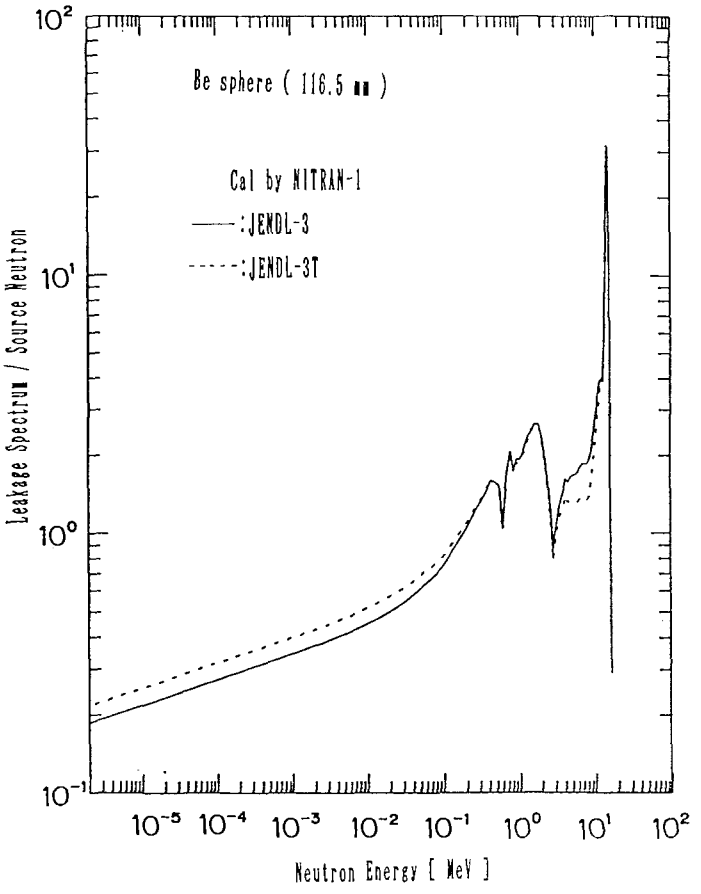

Fig.9 Calculated Neutron Leakage Spectrum from bare Be sphere

and 6Li-glass detectors) with the short (nsec) and long ($\sim\mu$sec) pulsed operation of neutron source are needed. The 2nd type is of using a Be+Li sphere in which 40 cm thickness outer Li shell absorbs low energy neutron component from a inner Be shell to result of 6Li (n,α)T reactions. Leakage (L) neutron spectrum distributes from 14 MeV to about 1 keV, which can be measured by the T.O.F. method. By adding T6 and L which are separately measured, the multiplication factor is given to be T6+L with correction for parasitic absorptions. The 3rd type of experiments is a total absorption method by using a Be+Li+C assembly to measure T6. See Fig. 7.

Preliminary predictions for the experimental results have been also prepared with JENDL-3 data and 1-D NITRAN code (see Table 4). Calculated time dependent reaction rate (P6(t)) for the Be+Li+C assembly were shown in Fig. 8, compared with that for the Pb+Li+C assembly, and leakage spectrum from Be sphere were shown in Fig. 9.

The experiments of the 3rd type had been finished firstly and now the 2nd type have been carried on. The experiments on a bare Be sphere is expected to be finished before the end of 1990. The final authorized experimental data of whole experiments shall be reported after several corrections on raw measurement values, however we shall open the preliminary experimental results of the 3rd type experiments for discussions on evaluation of cross section of Be, especially on (n,2n) reaction. From Figures 10-12, the fairly good agreement are observed between the calculated and measured time dependent reaction rate of 6Li in high energy parts, but not so well in lower energy side, especially at near position of Be sphere. Those results raise the questions to the 9Be cross section in low energy and the calculated method.

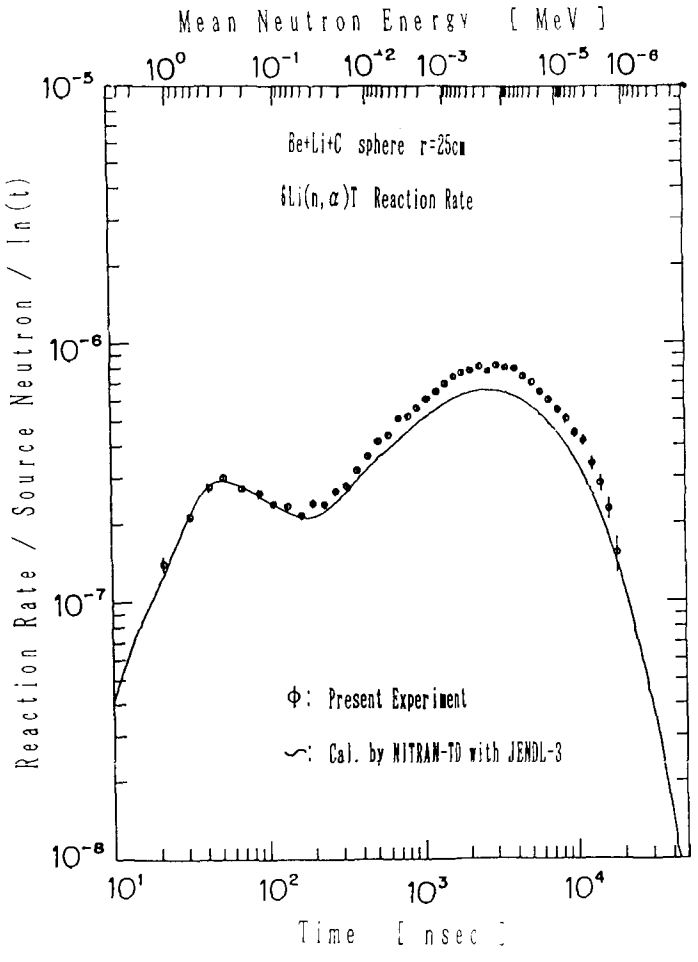

Fig.10 Time-dependent $^{6}Li(n,\alpha)T$ reaction rate for the Be+Li+C assembly

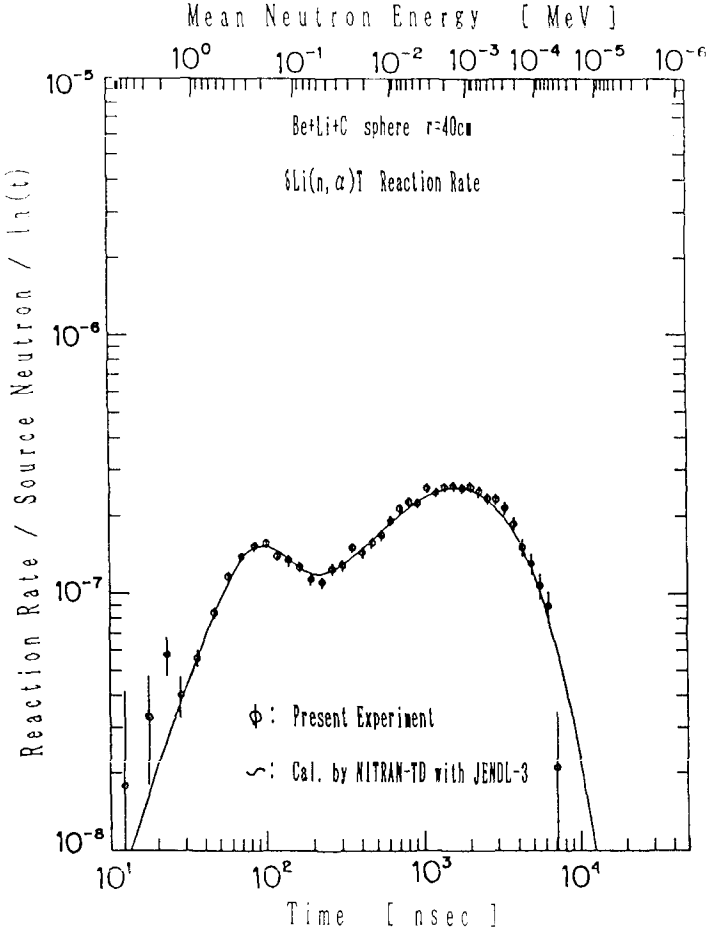

Fig.11 Time-dependent $^{6}Li(n,\alpha)T$ reaction rate for the Be+Li+C assembly

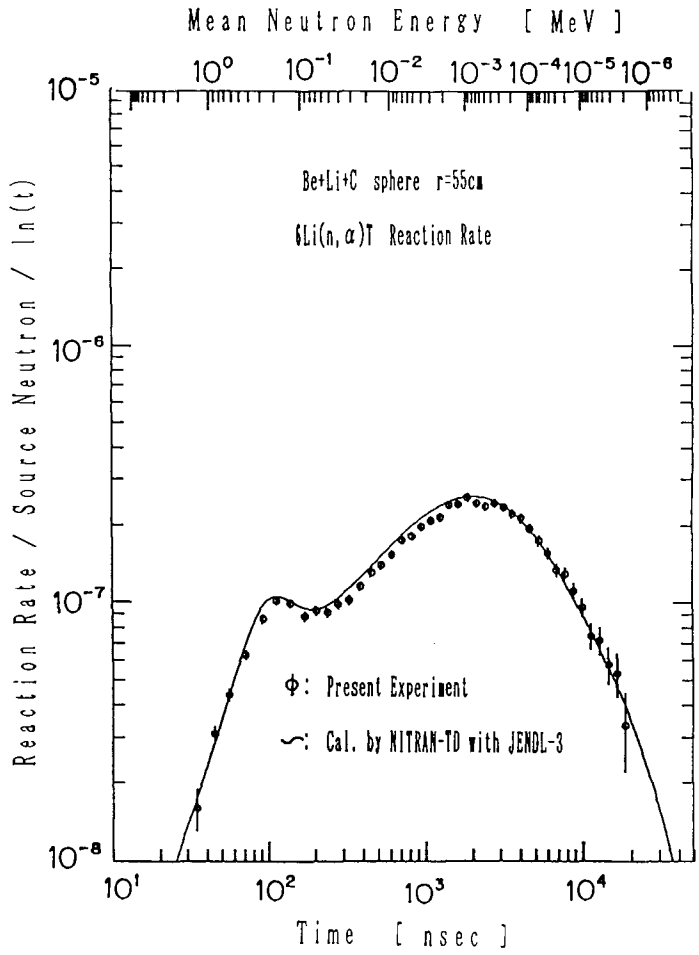

Fig.12 Time-dependent $^6Li(n,\alpha)T$ reaction rate for the Be+Li+C assembly

And also we are informed from other group(11) on TBR measurements results on this system using TLD. The tentative reported value of Tt is estimated as 1.4 and its experimental error are about 10 %.

Acknowledge

The authors wish to show their thanks for the courtesy of U.S. DOE and SWINPC of P.R.C. on kind renting arrangements of Be spheres and also the personal endeavor of Dr. E.T. Cheng (TSI. Research) for his promoting action on such international collaboration.

References

(1) K. Sumita, et al. ; Nucl. Sci. and Eng. 106, 249-265 (1990)
(2) A. Takahashi, et al.; J. Nucl. Sci. and Tech. 16 1-15 (1979)
(3) A. Takahashi, et al.; J. Nucl. Sci. and Tech. 25 215-232 (1988)
(4) K. Sugiyama, et al. ; Proc. 13th Symp. on Fusion Tech. at Verese, Vol. 2, 1375 (1984)
(5) K. Sugiyama, et al. ; Fusion Tech. 8, 1491 (1985)
(6) K. Sugiyama, et al. ; Proc. Meet. Nucl. Data for Fusion Neutronics July 1985, Tokai, JAERI-M-86029, p141 (1986)

(7) K. Sugiyama, et al. ; Proc. 14th Symp. on Fusion Tech. at Avignon, (1986)
(8) T. Iguchi, et al. ; Private Communication for Summary Rep. of JPN-US WS on Fusion Neutronics, at UCLA. (1990)
(9) J. Yamamoto, et al. ; Fusion Engineering and Design, 10 169-174 (1989)
(10) K. Yamanaka, et al. ; Proc. of 1990 Fall Meeting of Atomic Energy Soc. Jpn. B-19, (1990), in Japanese.
(11) T. Iguchi, et al. ; Private Communication on TBR BE-LI-C sphere. (1990)

Benchmark analyses on the 14 MeV neutron transport in beryllium

U. Fischer, A. Schwenk-Ferrero, E. Wiegner
Kernforschungszentrum Karlsruhe
Institut für Neutronenphysik und Reaktortechnik
P.O. Box 3640, D-7500 Karlsruhe 1
Federal Republic of Germany

Abstract

The 14 MeV neutron transport in beryllium is analyzed on the basis of a S_N-transport procedure with rigorous treatment of the neutron scattering and double-differential cross-section data from the European Fusion File EFF-1. Comparisons with conventional computational techniques show the validity of the applied procedure for one- and two-dimensional transport problems. Comparisons with existing one- and two-dimensional 14 MeV neutron benchmark experiments show good agreement for the neutron multiplication factors and, with some restrictions, for the neutron leakage spectra.

1. Introduction

Beryllium is the superior neutron multiplier candidate for fusion reactor blankets: due to its low (n, 2n)-reaction threshold it has the greatest potential of all nonfissionable nuclides for multiplying 14 MeV neutrons. For this reason beryllium is used in nearly all solid breeder blanket designs for "next step" fusion machines (NET/ITER) and demonstration power reactors. Consequently it is necessary to have a reliable assessment of its multiplication power. This can be achieved by means of beryllium multiplication experiments performed in simple geometrical configurations (e.g. spherical shell assemblies with a central 14 MeV neutron source) and their theoretical analysis with appropriate computational techniques and data.
In this work we analyze the 14 MeV neutron transport in beryllium on the basis of double-differential cross-section (DDX) data from the European Fusion File EFF-1. Various computational techniques are used for the description of the neutron transport and are applied for the calculation of one- and two-dimensional benchmark experiments. This proceeding allows us to draw conclusions on the quality of both the applied calculational procedures and the used nuclear data.

2. Methodical treatment of the neutron transport

2.1 Data

The neutron transport in beryllium is determined by elastic and inelastic scattering processes. Elastic scattering is a two-particle process and can be described by single-differential cross-sections (SDX-data), i.e. angular distributions of the scattered neutrons. Elastic scattering of beryllium is strongly forward directed: in the Legendre approximation a high number of moments is needed to describe its angular dependence. The inelastic scattering of beryllium is given by the (n, 2n)-reaction; this is a three-particle process necessitating the use of DDX-data, i.e. correlated angle-energy distributions of the scattered neutrons. The EFF-1 data file contains the beryllium evaluation of P. Young et al. /1/. It uses the so-called "pseudo-level" representation of the Be-DDX-data: for a series of excitation energy bins the excitation cross-sections and the angular distributions are given on the file. These data can be handled like SDX-data for discrete excitation energies.

2.2 Data processing

Conventional data processing (e.g. using the NJOY83 code /2/) can be applied to generate scattering matrices of Legendre order ℓ from the Be-data (SDX and DDX) on the EFF-1 file. These scattering matrices can be used in conventional S_N/P_ℓ-transport calculations.

At KfK we use a rigorous S_N-procedure that describes the anisotropic neutron transport through the use of angle-discretized scattering matrices (see below). We developed a special version of the NJOY83 code to generate these matrices from the Be-data on the EFF-1 file /3/. Both SDX- and DDX-data on the EFF-1 file are given in the Legendre representation in the centre-of-mass (CM) system. We transform them to the laboratory (LAB) system by avoiding there the Legendre representation. Thus we obtain the Be-DDX-data in a pointwise energy-angle representation in the LAB-system. They are further processed into angle-discretized scattering matrices. The angular discretization is performed according to the angular segmentation scheme of the S_N-transport calculation.

2.3 Transport procedure with rigorous treatment of the neutron scattering

The forward directed elastic and inelastic scattering processes result in an anisotropic neutron transport in beryllium. The rigorous S_N-procedure is appropriate to treat the anisotropic neutron transport: it avoids the usually applied Legendre ap-

proximation of the scattering kernel through the use of angle-discretized scattering matrices. In this procedure the scattering integral is numerically integrated following a theory that had been suggested by A. Takahashi et al. for one-dimensional spherical geometry /4/. At KfK this method has been incorporated into the ONETRAN-transport code /5/ and has been validated in the framework of the lead benchmark analyses /6/. For the treatment of azimuthally dependent transport problems an advanced numerical method using the Gauss-Tchebychev quadrature for the integration of the scattering integral has been developed /7/. This method has been incorporated into both the ONETRAN- and the TWOTRAN-code. Both newly developed transport programmes, called ANTRA1 and ANTRA2, serve as computational tools for the benchmarking of methods and data describing the anisotropic neutron transport.

3. Beryllium benchmark calculations

Benchmark calculations using the rigorous S_N-transport technique, the conventional S_N/P_ℓ-procedure and the Monte Carlo method (MCNP-code) have been performed in one- and two-dimensional geometry. In all cases the beryllium nuclear data from the EFF-1 file are used.

3.1 Spherical geometry

A spherical shell configuration with a central 14 MeV neutron source, an inner shell radius of 6 cm and an outer radius of 11 cm is used. It corresponds to the configuration of the beryllium multiplication experiment performed at Kurchatov Institute Moscow (KIM) /8/.

Fig. 1 shows the neutron leakage spectra, i.e. the neutron leakage current at the outer surface of the beryllium spherical shell normalized to one source neutron, obtained by the rigorous ANTRA1-calculation in S_{20} angular segmentation and conventional ONETRAN-calculations in S_{20}/P_1-, P_3- and P_5-approximations. Obviously the calculated neutron leakage spectra in all cases agree very well.

The anisotropic neutron transport therefore is very weak in this configuration: it is sufficient to use the P_1-approximation in the S_N-calculation. However, this is due to the small thickness of the beryllium spherical shell of 5 cm, whereas the mean free path of the 14 MeV neutrons in beryllium is 5.8 cm. Therefore the neutron leakage spectrum approximately gives the angle-integrated neutron emission spectrum at 14 MeV.

If we increase the thickness of the beryllium spherical shell up to 30 cm, neutron transport effects will become important. Fig. 2 shows the corresponding neutron leakage spectra. It can be seen that the P_1-calculation underestimates the forward

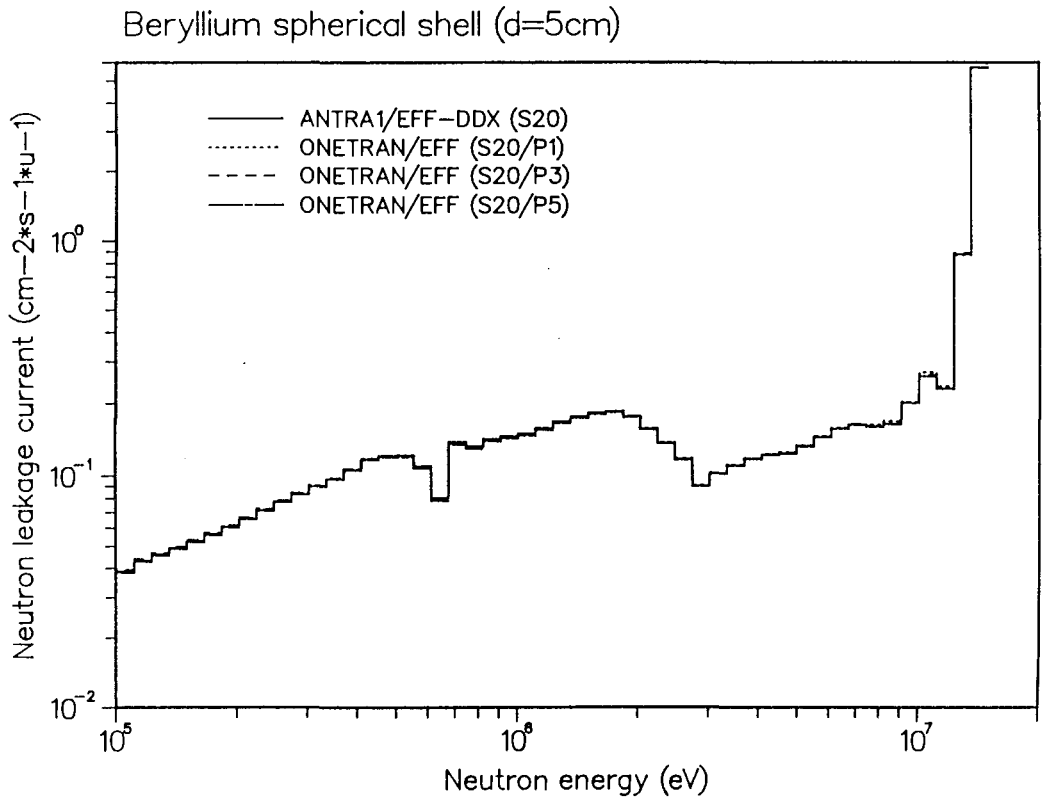

Fig. 1 : Neutron leakage spectra of a 5 cm thick beryllium spherical shell : Comparison between various calculations.

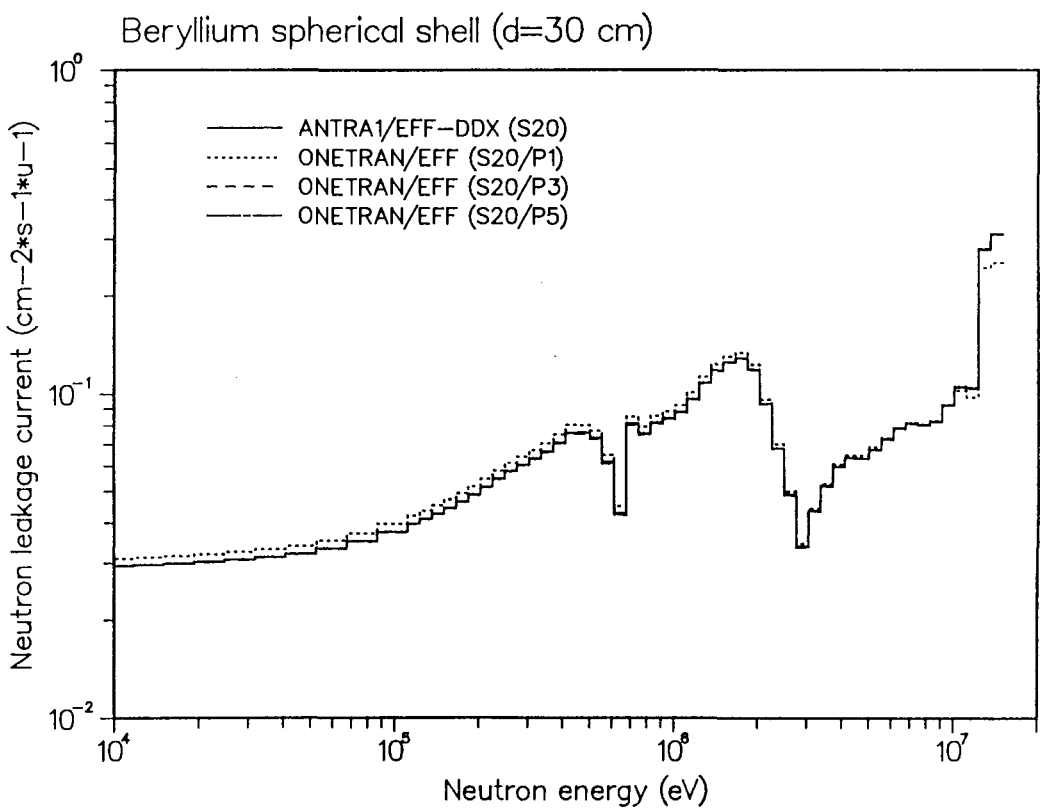

Fig. 2 : Neutron leakage spectra of a 30 cm thick beryllium spherical shell : Comparison between various calculations.

directed neutron scattering (i.e. the elastic peak); thus more neutrons are being backscattered, resulting in an enhanced neutron multiplication and consequently in an enhanced leakage of low energy (E < 1 - 2 MeV) neutrons. But actually it is sufficient to use a P_3-approximation in the S_N-calculation: it agrees already with the P_5-approximation and the rigorous S_N-calculation.

Several conclusions can be drawn from these observations:

i) The rigorous S_N-procedure in spherical geometry is validated for the light element beryllium.

ii) The conventional S_N/P_ℓ-procedure is sufficient to describe the 14 MeV neutron transport in beryllium.

iii) It is sufficient to use a low order Legendre approximation of the scattering kernel in the S_N/P_ℓ-transport calculation, although the angular distribution of the scattering cross-section requires a high order Legendre approximation.

Note that these conclusions are based on the use of the EFF-1 beryllium data. The good agreement between the rigorous S_N-calculation and the S_N/P_ℓ-calculation may be traced back to the use of the Legendre representation for the basic cross-section data (although they are given in the CM-system). On the other hand it is obvious, that the strong angular dependence of the scattering cross-sections does not necessarily result in strong anisotropic neutron transport effects in the beryllium spherical shell. This, of course, would be the case in a heterogeneous configuration of beryllium and some neutron absorbing material.

3.2 Two-dimensional geometry

The beryllium slab configuration of the FNS-experiment /9/ is used for these calculations. Fig. 4 shows the two-dimensional calculational model used for the S_N-calculations. They are performed in cylindrical (r, z)-geometry with the TWOTRAN and the ANTRA2-code, respectively.
Fig. 5 shows the leakage spectra at an angle of 41.8^0 obtained by the rigorous ANTRA2-calculation in S_{16} angular segmentation and conventional TWOTRAN-calculations in S_{16}/P_1-, P_3- and P_5-approximations. Obviously the angular neutron spectrum is sensitive to anisotropic neutron scattering processes: TWOTRAN-calculations of low Legendre order disagree with rigorous ANTRA2-calculations, but the TWOTRAN results converge towards the ANTRA2-results as the Legendre order increases. Again this behaviour can be interpreted as validation of the ANTRA2-procedure. It can be taken from fig. 5, however, that a conventional S_N-calculation

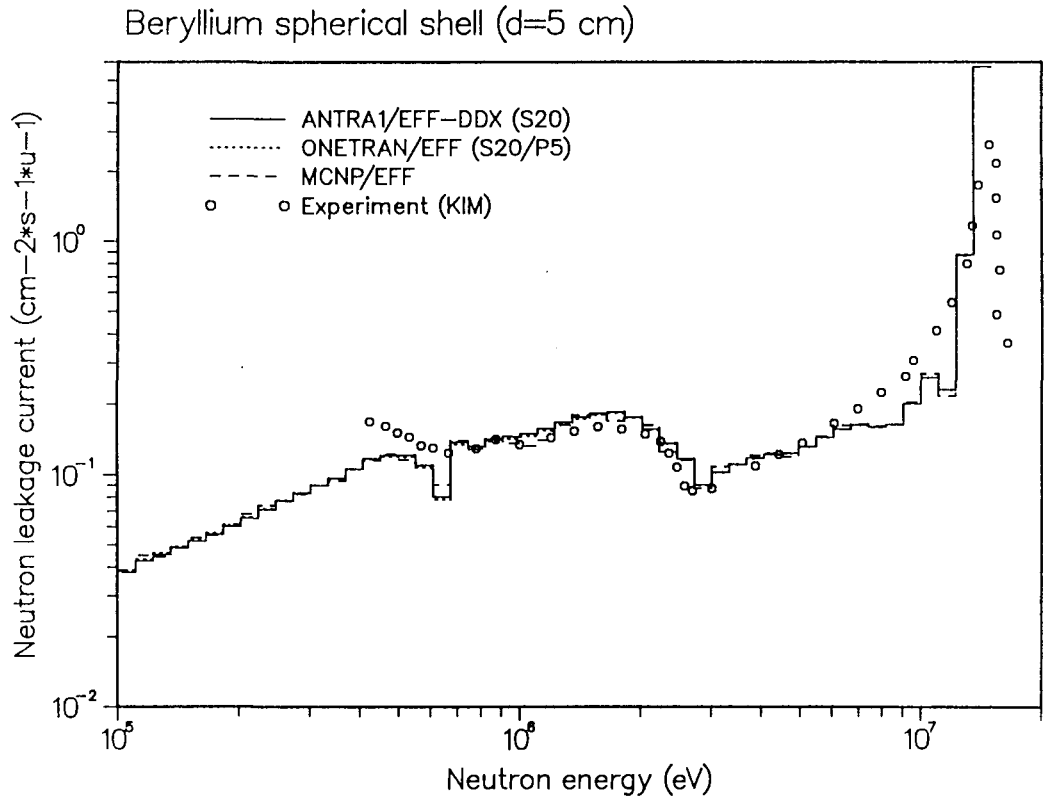

Fig. 3 : Neutron leakage spectra of a 5 cm thick beryllium spherical shell : Comparison between calculations and experiment.

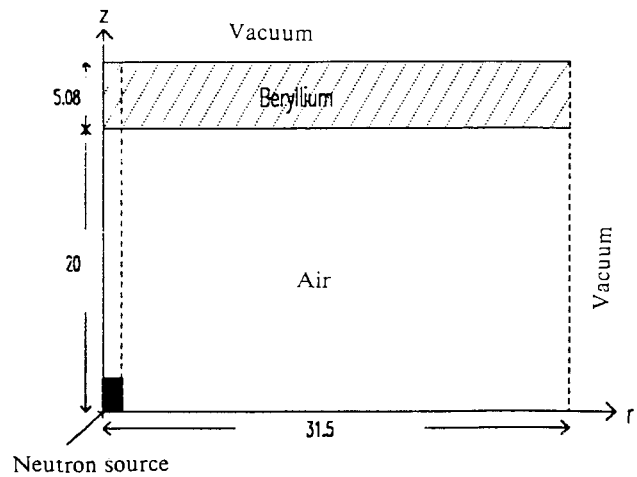

Fig. 4 : Two-dimensional model of the FNS/JAERI beryllium experiment.

in P_5-approximation is sufficient for describing the 14-MeV neutron transport through the beryllium slab.

4. Comparison to experimental results

At the Kurchatov Institute Moscow (KIM) the neutron multiplication factors of several beryllium shell configurations have been measured by the total absorption method /8/. Table I compares the experimental values with the calculated ones.

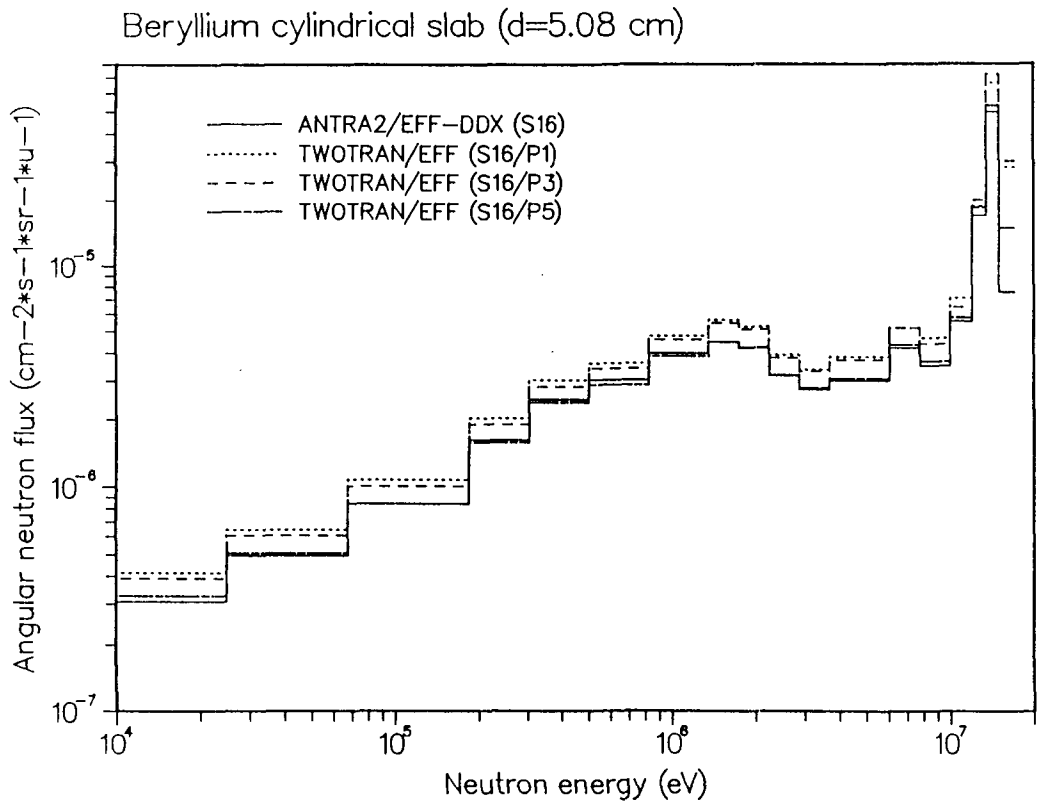

Fig. 5 : Neutron leakage spectra of a 5.08 cm thick beryllium cylindrical slab : Comparison between various calculations at an angle of 41.8 °.

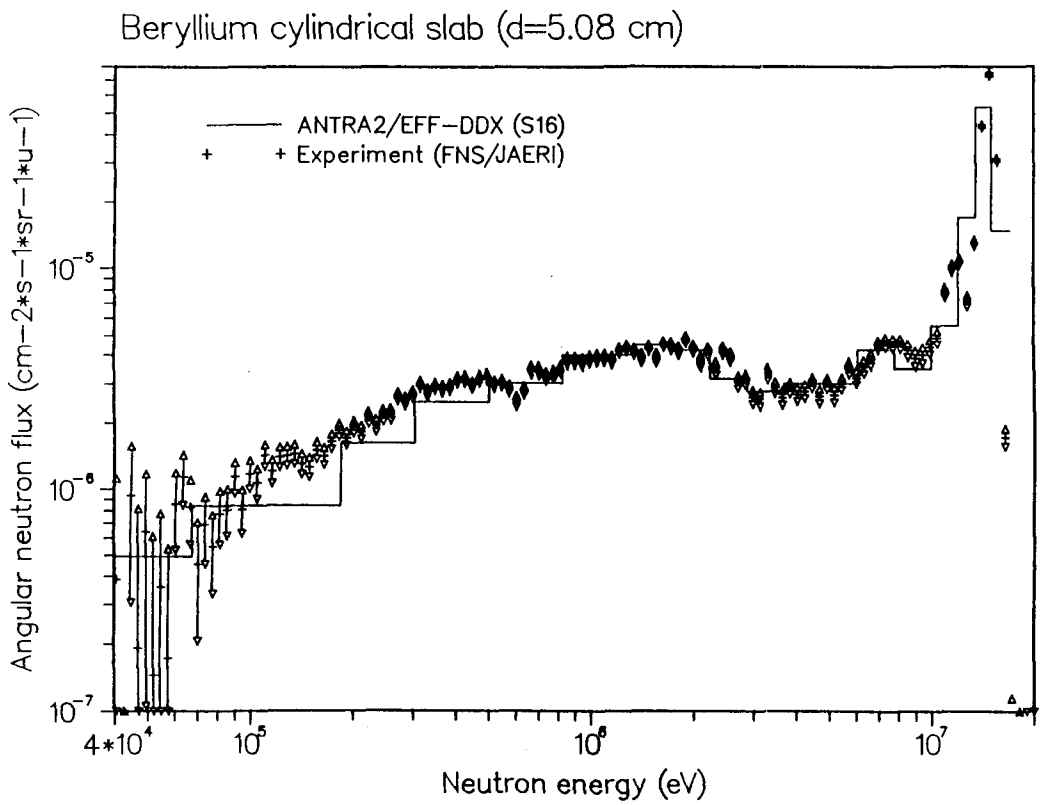

Fig. 6 : Neutron leakage spectra of a 5.08 cm thick beryllium cylindrical slab : Comparison between calculation and experiment at an angle of 41.8 °.

Table I: Neutron multiplication factors for spherical beryllium shells with various inner (r_i) and outer (r_o) radii

r_i [cm]	r_o [cm]	Experiment /8, 10/	Calculations	
			ANTRA1 EFF-1	BLANK /8/ ENDF/B-IV
3.0	4.5	1.14 ± .036	1.10	-
6.0	11.0	1.365 ± .04	1.359	1.39
3.0	11.0	1.525 ± .043	1.547	1.60

There is good agreement within the experimental uncertainty both using EFF-1 and ENDF/B-IV-data in the transport calculation. Actually the 14 MeV neutron multiplication in thin beryllium spherical shells is determined by the magnitude of the (n, 2n) cross-section, which is identical in ENDF/B-IV, -V and EFF-1, but it is rather insensitive to the angle-energy distribution of the secondary neutrons which differs completely in these evaluations.

In case of the 5 cm thick beryllium spherical shell the neutron leakage spectrum had been measured from 0.35 MeV up to 15 MeV by the time-of-flight method at Kurchatov Institute. Fig. 3 shows the experimental and the calculated spectra obtained by ANTRA1-, ONETRAN- and MCNP-calculations using the same basic beryllium data from the EFF-1-file. These is perfect agreement in the calculated spectra for the various calculational approaches and an overall good agreement with the experimental data. There is an underestimation of the experimental spectrum below 0.7 MeV which also reflects into the partial multiplication factors (table II). The rather insufficient reproduction of the elastic peak, on the other hand, may be due to the fact that the experimental neutron source spectrum could not be used in the calculations and, furthermore, the experimental data points have been extracted from a graphical representation. It can be taken from table II, however, that it is possible to reproduce the partial neutron multiplication factors rather well with the EFF-1 data.

At FNS angular leakage spectra of neutrons emitted from cylindrical beryllium slabs have been measured at various angles. We chose the leakage spectrum at an angle of 41.8^0 for comparison with TWOTRAN- and ANTRA2-calculations, as this angle corresponds to an angular direction of the used quadrature set. An overall good agreement can be observed between the ANTRA2-calculation and the experimental data points; especially this holds above 0.5 MeV neutron energy (fig. 6). Below 0.5 MeV the experimental spectrum is underestimated by the calculation; this is also observed in case of MCNP-calculations using EFF-1-data /9/ and hence can be addressed to the beryllium cross-section data. Within the limits of the used energy

Table II: Partial neutron multiplication factors for the beryllium spherical shell of 5 cm thickness

Energy interval [MeV]	Experiment /8/	Calculations	
		ANTRA1 EFF-1	BLANK /8/ ENDF/B-IV
0.35 - 0.7	0.096 ± .005	0.075	0.075
0.7 - 3	0.20 ± .01	0.216	0.16
3 - 10	0.19 ± .01	0.179	0.20
10 - 15	0.69 ± .03	0.729	0.69

group structure the elastic peak is reproduced rather well although it does not allow to draw a conclusion on the quality of the elastic scattering cross-section at 14 MeV.

5. Conclusions and future work

The rigorous S_N-transport procedure, realized in the ANTRA1- and ANTRA2-code, respectively, has been validated by means of benchmark calculations for the 14 MeV neutron transport in one- and two-dimensional beryllium assemblies. The beryllium DDX-data in the pseudo-level representation on the European Fusion File EFF-1 have been used in these calculations. The beryllium DDX-data on the recently released ENDF/B-VI and the forthcoming EFF-2 data file are more appropriate for the rigorous S_N-transport procedure: both evaluations use a pointwise energy-angle representation of the DDX-data in the laboratory system. Work is in progress to enable the NJOY89 processing code for generating angle-discretized scattering matrices from DDX-data representations in the ENDF/B-VI format without making any use of Legendre approximations.

Comparisons to existing experimental beryllium benchmarks show good agreement for the neutron multiplication factors and, with some restrictions, for the neutron leakage spectra. The experimental data base, however, is to poor in order to draw reliable conclusions on the quality of the beryllium data: there is still a need for 14-MeV neutron multiplication experiments (preferably in spherical geometry) with larger beryllium shell thicknesses, including measurements of the neutron multiplication factors and the neutron leakage spectra at various shell thicknesses. Actually such experiments are underway at SWINPC (common US, PRC and Japan project; beryllium shell thicknesses from 3.2 to 14.85 cm) and at KfK (national project; beryllium shell thicknesses from 5 to 17 cm).

References

/1/ P.G. Young, L. Stewart: Evaluated Data for n + ^{9}Be Reactions, Los Alamos National Laboratory, LA-7932-MS (July 1979)

/2/ R.E. McFarlane, D.W. Muir and R.M. Boicourt: The NJOY nuclear data processing system, Vols. I, II, III, Los Alamos National Laboratory, Report LA-9303-M (May 1982)

/3/ U. Fischer, E. Wiegner: DOUBLE, a processing system for the generation of multigroup transfer matrices from single- and double-differential neutron cross-sections in angular representation, Kernforschungszentrum Karlsruhe 1986, unpublished

/4/ A. Takahashi et al.: Method for calculating anisotropic neutron transport using scattering kernel without polynomial expansion, J. Nucl. Sci. Techn. 16 (1979), 1 - 15

/5/ A. Schwenk-Ferrero: GANTRAS - a system of codes for the solution of the multigroup transport equation with a rigorous treatment of anisotropic neutron scattering - plane and spherical geometry, Kernforschungszentrum Karlsruhe, KfK-4163 (November 1986)

/6/ U. Fischer, A. Schwenk-Ferrero, E. Wiegner: Neutron Multplication in Lead: A Comparative Study Based on a New Calculational Procedure and New Nuclear Data, Proc. First Int. Symp. on Fusion Nuclear Technology, Tokyo, Japan, April 10 - 19 (1988), Part C, 139 - 144

/7/ A. Schwenk-Ferrero: Verfahren zur numerischen Lösung der Neutronentransportgleichung mit strenger Behandlung der anisotropen Streuung, Kernforschungszentrum Karlsruhe, KfK-4788 (September 1990)

/8/ V.A. Zagryadskij et al.: Calculated Neutron Transport Verifications by Integral 14-MeV Neutron Source Experiments with Multiplying Assemblies, Proc. First Int. Symp. on Fusion Nuclear Technolgy, Tokyo, Japan, April 10 - 19 (1988), Part B, 353 - 358

/9/ Y. Oyama, H. Maekawa: Measurement and Analysis of an Angular Neutron Flux on a Beryllium Slab Irradiated with Deuterium-Tritium Neutrons, Nucl. Sc. Eng. 97, 220 - 234 (1987)

/10/ V.A. Zagryadskij et al.: Measurement of Neutron Leakage from ^{238}U, ^{232}Th and Be Spherical Assemblies with a Central 14-MeV Source, International Atomic Energy Agency, INDC (CCP)-277/G (April 1987)

/11/ A.A. Andrasenko et al.: Measurement and Comparison with Calculations of Neutron Leakage Spectra from U, Pb, Be Spheres with Central 14 MeV Neutron Source, Proc. Specialists CMEA Meeting on Neutronics and Thermohydraulics of OTR Project, Varna, Bulgaria, May 5 - 7, 1987

Outline of IAEA Benchmark Problem Based on the Time-of-Flight Experiment on Beryllium Slabs at FNS/JAERI

Hiroshi MAEKAWA and Yukio OYAMA
Departement of Reactor Engineering
Japa Atomic Energy Research Institute
Tokai-mura, Naka-gun, Ibaraki-ken, 319-11 Japan

Background

1986 Dec. IAEA AGM on Nuclear Data for Fusion Reactor Technology, Gaussig, GDR
AGM proposed a calculational benchmark based on Pb sphere experiment at TUD.

1988 Aug. JAERI prepared the benchmark problem based on Pb sphere experiment at TUD. IAEA distributed it to the participants.

1989 May IAEA Specialists' Meeting on FENDL, Vienna
*1-D calculations agree well among the participants each other.
*There are some deviations between the calculations and the experiment.
*AGM requested a benchmark problem based on FNS experiments.

1989 Dec. JAERI prepared the IAEA benchmark problem based on the Time-of-Flight Experiment on Beryllium Slabs at FNS/JAERI and sent it IAEA.

Purpose of This Presentation

*To explain the Be TOF experiment in detail.

*To ex plain the outline of the benchmark problem.

TOF Experiment on Be Slabs

Experimental method is shown in following references:

(1) Y. Oyama & H. Maekawa, Nucl. Instr. Methods, A245, 173 (1986).
(2) Y. Oyama & H. Maekawa, Nucl. Sci. Eng., 97, 220 (1987).

Experimental Arrangement

* FNS First Target Room
15 m x 15 m x (8.5 + 3) m^H, grating floor
* 80-degree beam line
* Target is located at 5.5 m from south and west walls and 1.8 m high from the grating floor.

Collimator System

Inner diameter : 50 mm
Material : Iron & Paraffin with B_2O_3 (30 wt%)
Plag : SS304 & Lucite

*Measured area on the back surface of assembly was confirmed experimentally.

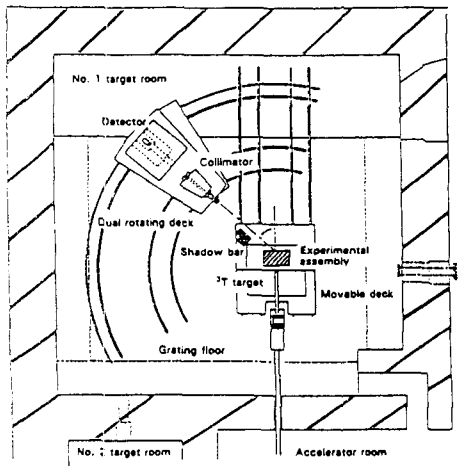

Experimental Arrangement and Target Room

Slab Assembly

* Experimental assembly was made up in a pseudo-cylindrical slab shape by stacking rectangular Be blocks.

Size of assembly

Radius : 315 mm (area equivalent)
Thickness : 50.8 mm (0.9 mfp), 152.4 mm (2.7 mfp)

Be block

Size : 50.8 mm x 50.8 mm x 50.8 mm
50.8 mm x 50.8 mm x 101.6 mm
Density : 1.837 g/cm^3
Purity : 98.92 wt %
Main impurity : BeO

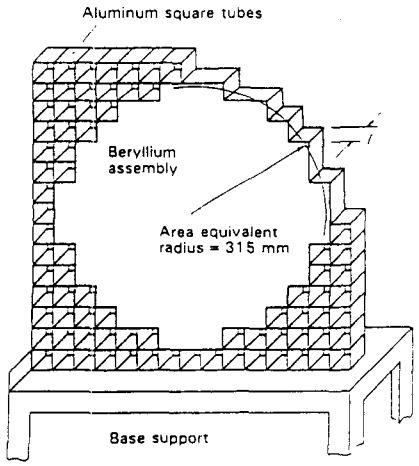

Concept of the experimental assembly
The aluminum square tubes are fastened by the outer frame (not shown), which was made of long aluminum square tubes.

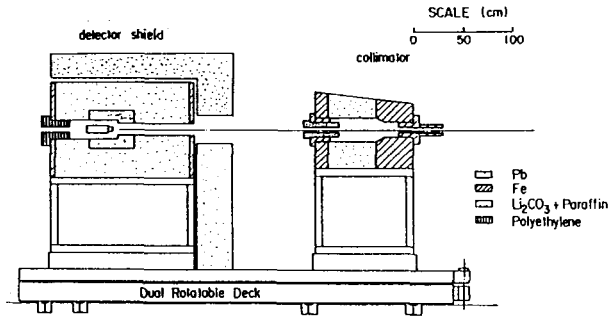

Collimater and Detector Shield

Estimation of effective measured area

$$A_S = \int_0^\infty 2\pi r \cdot f(r) dr$$

A_S : effective measured area

f(r): collimator-detector response function

$$f(r) = N \frac{C(r)}{S(r)}$$

r : distance from the central axis

N : normalization factor

C(r): neutron counts from position r

S(r): source intensity at position r

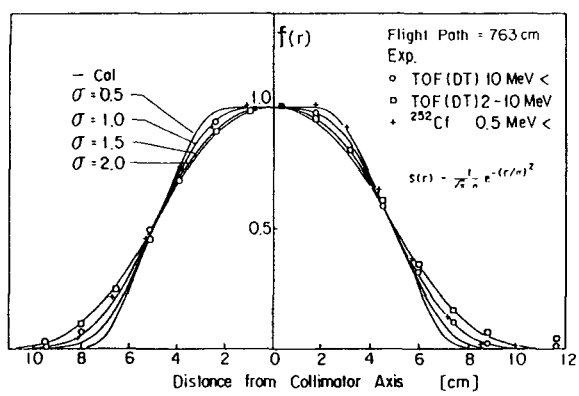

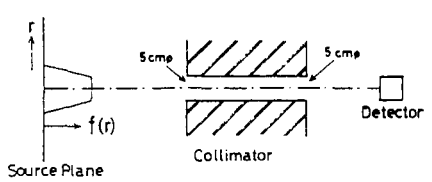

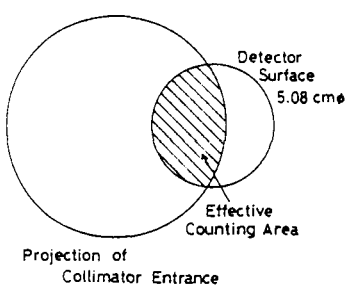

Detector System

Detector : 50.8mm dia. x 50.8mm NE213

Shielding material : Paraffin with Li_2CO_3 (20 wt%) & Pb

Electronics

* Output signal from the detector is splited two.
  normal & attenuated by 1/10
* Two sets of pules shape discriminator for neutron-gamma separation and time-analyzer.
* Two bias levels.
  ===> To eliminate the contribution of carbon interaction.
  To extend the lower energy limit (about 50 keV).

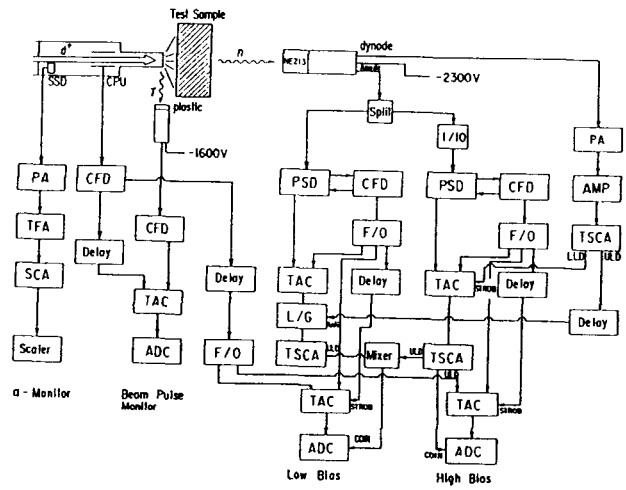

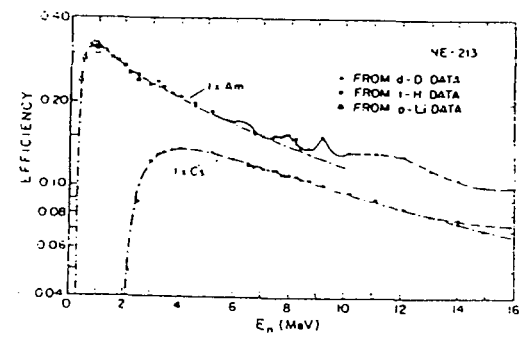

Fig. Contributions to the americium efficiency curve by nonelastic neutron interactions with carbon.

(M. Drosg, et al., Nucl. Inst. Meth. 176 477-480 (1980))

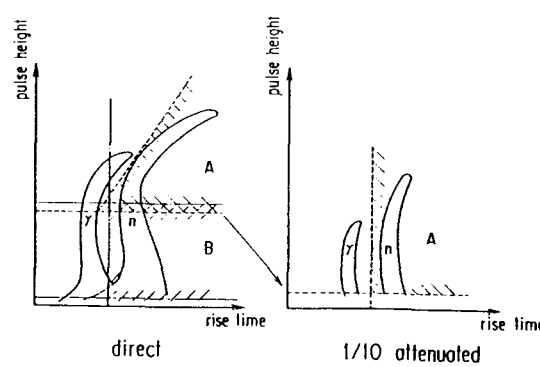

Estimation of Detector Efficiency

1) Monte Carlo calculation
   Cross section data of H, C : ENDF/B-IV
   Light output efficiency : Verbinski's data

2) Spectrum measurement of ^{252}Cf by TOF
   ===> To determine the relative efficiency near the bias level.
   Nuclear temperature : 1.42 MeV

3) Absolite check by D-T neutrons

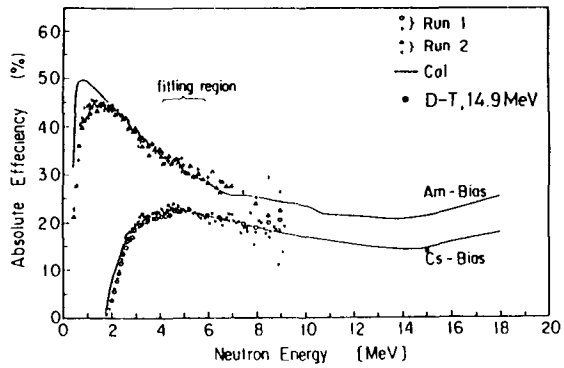

Absolute detector efficiency curve

Data Reduction

$$\phi(\Omega,En) = \frac{C(En)}{\varepsilon(En)\,\Delta\Omega\,As\,Sn\,T(E)}$$

[n/sr/cm2/unit lethargy/source neutron]

C(En) : counts per unit lethargy for neutrons of energy En
ε(En) : detector efficiency for neutrons of energy En
ΔΩ : solid angle subtended by the detector to the point on the surface center of assembly (= Ad/L^2) where Ad : area of detector and L : flight path
As : effective measured area defined by the detector-collimator system on the plane perpendicular to the axis at the surface of assembly
Sn : neutron yield, T(E) : attenuation by air

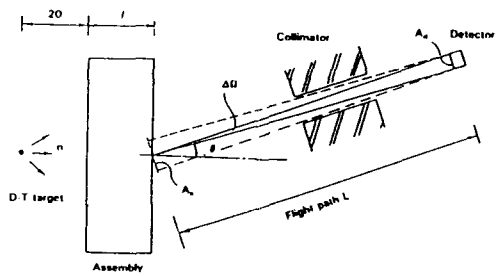

Illustration of the parameters in the measured flux

Condition of Neutron Generator

Reaction	:	d - T
Pulse width	:	2 ns
Repitition rate	:	4 μs
Peak current	:	30 mA
Beam energy	:	330 keV

Neutron yield monitor : associated α-particle method

Measured angle : 0, 12.2, 24.9, 41.8, 66.8 deg. corresponding to the angles of the S_{16} quadrature set for S_N calculation.

Error Analysis

Energy

Item	Random	Systematic
Time resolution	± 2 %	
Time zero		+ 2 % for 15 cm

Flux

Item	Random	Systematic
ε(En) Sn ΔΩ	± 3~5 %	< + 2 %
As	± 0.5 %	< ± 2 %
C(En)	± 1~20 %	< + 1 %
T(En)		negligible

Content of Benchmark Problem in Diskette

README.DOC	Description of IAEA Benchmark Problem
BETOFTG.DAT	Source neutron sprctrum measured
BETOF5.DAT	50.8mm-thick angular neutron flux
BETOF15.DAT	152.4mm-thick angular neutron flux
ENERGY.DAT	Boundary energy

* Two types of comparison are requested in the problem.

1) To compare the measured and calculated angular fluxes directly in graph.

2) To compare the integrated flux over four energy regions in C/E values (ratio of calculated to experimental values).

Samples of Calculational Model

1) 2-D S_N code DOT3.5

*It is important to averaged over μ and R (< 5 cm).

2) MonteCarlo code MCNP

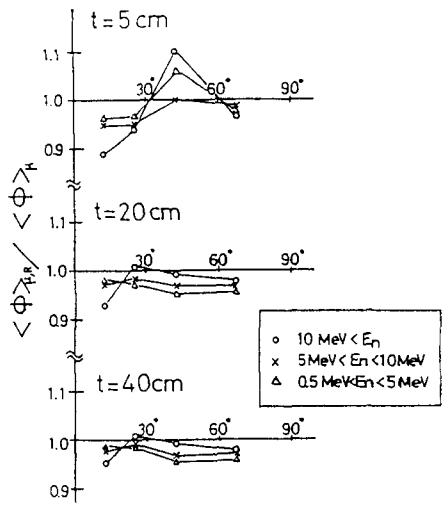

A sample of difference between
the average over μ at R=0
and the average over μ and R (< 5cm).

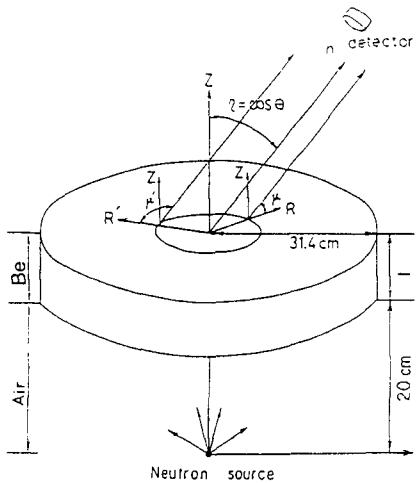

$$\langle\phi\rangle_{\mu} = \frac{\sum \phi(\gamma,\mu)\,\omega_{\mu}}{\sum \omega_{\mu}}$$

$$\langle\phi\rangle_{\mu,R} = \frac{\sum \langle\phi\rangle_{\mu}\, 2\pi r \Delta r}{\sum 2\pi r \Delta r}$$

Calculational Model for 2-D S_N Code

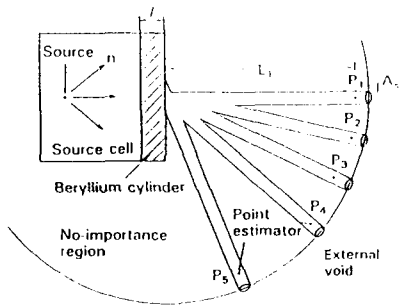

Model for MCNP calculation

The five detectors are located at the same time, and the no-importance region plays a role in the collimator system.

Appendix

IAEA Benchmark Problem Based on the Time-of-Flight Experiment on Beryllium Slabs at FNS/JAERI

Hiroshi MAEKAWA and Yukio OYAMA

Fusion Reactor Physics Laboratory
Department of Reactor Engineering
Japan Atomic Energy Research Institute
Tokai-mura, Naka-gun, Ibaraki-ken, 319-11 Japan

(Phone) 81-292-82-6074 (for H.M.) or -6075 (for Y.O.)
(Telefax) 81-292-82-5709
(BITNET) J2773@JPNJAERI (for H.M.) or J3240@JPNJAERI (for Y.O.)

1. Numerical Data and Their Format

a) Type of format : IBM-PC, MS-DOS file
1.2MB or 320kB for 5" diskette
720kB for 3.5" diskette
The data file written in the diskette for NEC-PC and MAC-PC is available.

b) There are the following four files except this "README.DOC" text:
BETOFTG.DAT ····· Source neutron spectrum
BETOF5.DAT ····· 50.8 mm-thick angular neutron flux
BETOF15.DAT ····· 152.4 mm-thick angular neutron flux
ENERGY.DAT ····· Boundary energy

c) Units of the data
Source spectrum [n/sr/lethargy/source]
Angular flux [n/sr/cm²/lethargy/source]

d) Data format for experimental data

·Comment		1 line	20A4
·Energy (mid-point)	[MeV]	I = 1, 150	6E12.4
·Angular flux	[See above]	I = 1, 150	6E12.4
·Error (fraction)	[%]	I = 1, 150	6E12.4

e) Number of data set

BETOFTG.DAT	1	0 degree
BETOF5.DAT	4	0, 24.9, 42.8, 66.8 degrees
BETOF15.DAT	5	0, 12.2, 24.9, 42.8, 66.8 degrees

*In the case of 50.8 mm-thick and 12.2 degree, it was revealed that the measured flux was contaminated by some of direct neutrons from the target and too difficult to analysis. Therefore the data of 50.8 mm-thick and 12.2 degree is not included in the file.

f) Data format for boundary energy (ENERGY.DAT)

·Comment	1 line	20A4
·Boundary energy [MeV]	I = 1, 151	8F9.5

2. Flight Path and Effective Measured Area

The flight path and effective measured area are summarized as follows. The meaning of them is described in the references. These data are useful for Monte Carlo calculations.

Table Flight path and measured area

50.8 mm-thick Assembly

Angle	Flight Path [cm]	Measured Area [cm²]
0	738	85.87
24.9	740	86.34
41.8	744	87.26
66.8	753	89.33

152.4 mm-thick Assembly

Angle	Flight Path [cm]	Measured Area [cm²]
0	728	83.53
12.2	729	83.69
24.9	731	84.22
41.8	736	85.46
66.8	748	88.16

3. Calculational Model

The calculational model is of course depend on the code used. Basic data are as follows:

Radius of assembly	: 31.5 cm
Thickness of assembly	: 5.08 and 15.24 cm
Distance between target and assembly	: 20 cm
Be atom density	: 1.215×10^{23} atoms/cm³
Area of detector	: $\pi \cdot 2.54^2$ [cm²]

4. How to Calculate the Angular Flux

(1) Neutron source

You can use the data of "BETOFTG.DAT" as the source. Before you start the calculation you should interpolate the spectrum to adjust it to the group structure used. It is notable that the integrated source spectrum multiplied by 4π is not unity (1.0) but 1.086.

The source neutrons are generated isotropically at the target position.

(2) Two-demensional discrete ordinate code such as DOT3.5

You can easily understand from the reference 4) how to do. It is important to average over the measured area when the calculated angular flux is compared with the measured one.

(3) Monte Carlo calculation

You can see a sample of method in the reference 1).

5. Comparison

Two types of comparison will be done for this benchmark problem.

(1) To compare the measured and calculated angular fluxes directly in graph.

(2) To compare the integrated flux over following four energy regions in C/E values (Ratio of calculated to experimental values);

Table Integrated Angular Flux

50.8 mm-thick Assembly

Energy* / Angle	10.183 (14)	1.9557 (47)	0.5070 (74)	0.0974 (107)
0.0	3.922-4#(0.18%)	1.302-5 (0.90%)	8.831-6 (0.85%)	3.847-6 (1.53%)
24.9	2.566-5 (0.55%)	6.180-6 (1.08%)	5.093-6 (0.88%)	3.765-6 (1.00%)
41.8	1.016-5 (0.92%)	5.746-6 (1.20%)	5.022-6 (0.94%)	3.484-6 (1.15%)
66.8	4.567-6 (1.10%)	5.423-6 (0.91%)	4.706-6 (0.71%)	3.140-6 (0.88%)

152.4 mm-thick Assembly

Energy* / Angle	10.183 (14)	1.9557 (47)	0.5070 (74)	0.0974 (107)
0.0	7.727-5 (0.21%)	5.759-6 (0.74%)	5.091-6 (0.62%)	4.171-6 (0.74%)
12.2	2.330-5 (0.33%)	4.941-6 (0.67%)	4.591-6 (0.54%)	3.642-6 (0.64%)
24.9	1.041-5 (0.51%)	4.581-6 (0.70%)	4.362-6 (0.55%)	3.524-6 (0.62%)
41.8	4.748-6 (0.72%)	3.961-6 (0.74%)	4.002-6 (0.56%)	3.153-6 (0.66%)
66.8	1.336-6 (2.08%)	2.657-6 (1.20%)	2.940-6 (0.76%)	2.399-6 (0.66%)

*Lower energy boundary for each region in MeV and the group number of lower boundary from the higher energy group.

#Read as 3.922×10^{-4}. Data in parenthese is experimental error.

6. References

When you publish the results using this numerical data, you should refer at least following references 1) and 2).

1) Oyama Y., Maekawa H.: "Measurement and Analysis of an Angular Neutron Flux on a Beryllium Slab Irradiated with Deuteron-Tritium Neutrons," Nucl. Sci. Eng., 97, 220-234 (1987).

2) Oyama Y., Maekawa H.: "Measurements of Angular Neutron Flux Spectra for Fusion Candidate Material Slabs by Time-of-Flight Method --- Compilation of Experimental Data --- ," JAERI-M 90-092 (1990).

3) Oyama Y., Maekawa H.: "Measurements of Angle-Dependent Neutron Spectra from Lithium-Oxide Slab Assemblies by Time-of-Flight Method," JAERI-M 83-195 (Nov. 1983).

4) Oyama Y., Yamaguchi S., Maekawa H.: "Analysis of Time-of-Flight Experiment on Lithium-Oxide Assemblies by a Two-Dimensional Transport Code DOT3.5," JAERI-M 85-031 (March 1985).

5) Oyama Y., Maekawa H.: "Spectral Measurement of Angular Neutron Flux on the Restricted Surface of Slab Assemblies by the Time-of-Flight Method," Nucl. Instr. Methods, A245 173-181 (1986).

6) Oyama Y., Yamaguchi S., Maekawa H.: "Measurements and Analyses of Angular Neutron Flux Spectra on Graphite and Lithium-Oxide Slabs Irradiated with 14.8 MeV Neutrons," J. Nucl. Sci. Technol., 25, 419-428 (1988).

7) Oyama Y.: "Experimental Study of Angular Neutron Flux Spectra on a Slab Surface to Assess Nuclear Data and Calculational Methods for a Fusion Reactor Design," JAERI-M 88-101 (June 1988).

JAERI's Analyses of IAEA Benchmark Problem, Integral Experiment on Be Assembly and TOF Experiment on Pb Slabs Using JENDL-3

H. MAEKAWA, Y. OYAMA and K. KOSAKO
Departement of Reactor Engineering
Japa Atomic Energy Research Institute
Tokai-mura, Naka-gun, Ibaraki-ken, 319-11 Japan

Following three benchmark experiments are used in present integral test of JENDL-3.

1) Time-of-Flight Experiment on Be Slabs
   ===> IAEA Benchmark Problem

2) Integral Experiment on Be Cylindrical Slab
   ===> 9th ANS Topical Meeting on Fusion Nuclear Technolgy, Oct. 7-11, 1990, Oak Brook

3) Time-of-Flight Experiment on Pb Slabs
   ===> ISFNT-2, June 2-7, 1991, Karlsruhe

Integral Experiment on Be Cylindrical Slab

Material	:	Be block (impurity : 1.08 wt%, mainly BeO)
Radius	:	315 mm
Thickness	:	457 mm

In-System Neutron Spectrum

> 2 MeV	14mm-dia. spherical NE213 spectrometer
< 1 MeV	two proton-recoil proportional counters H_2-counter, H_2/Kr-counter

Reaction Rates

* $^{6}Li(n,t)^{4}He$ (tritium production rate)
  ^{6}Li-glass scintillator (10mm dia. x 0.1mmt)
*Fission rate ^{235}U micro-fission chamber
*Foil Activation Method

$^{58}Ni(n,2n)^{57}Ni$	> 13 MeV	$^{90}Zr(n,2n)^{89}Zr$	> 12 MeV
$^{93}Nb(n,2n)^{92m}Nb$	> 10 MeV	$^{27}Al(n,\alpha)^{24}Na$	> 6 MeV
Ti $(n,x)^{48}Sc$	> 5 MeV	$^{56}Fe(n,p)^{56}Mn$	> 4 MeV
$Ti(n,x)^{47}Sc$	> 1 MeV	$^{58}Ni(n,p)^{58}Co$	> 1 MeV
$^{115}In(n,n')^{115m}In$	> 0.5 MeV	$^{197}Au(n,\gamma)^{198}Au$	thermal

Gamma-ray Heating Rate

*interporation method using TLDs
*G-function using NE213 spectrometer

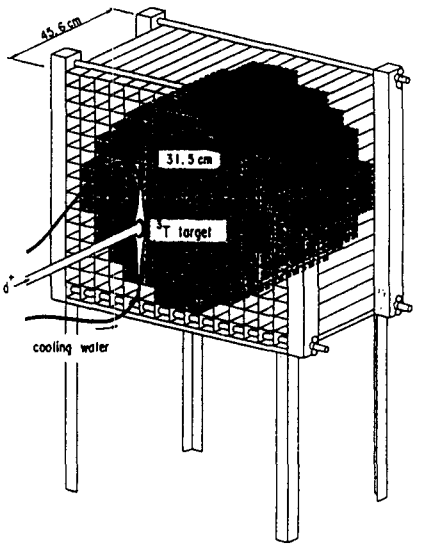

Time-of-Flight Experiment on Pb Slabs

Assembly	:	Pb cylindrical slab
Material	:	Pb block (purity : 99.998 %)
Radius	:	315 mm
Thickness	:	50.6, 203, 405 mm
Angle	:	0, 12.2, 24.9, 41.8, 66.8 degrees

Measuring Techniques : Same as previous ones
(Such as TOF expriment on Be slabs)

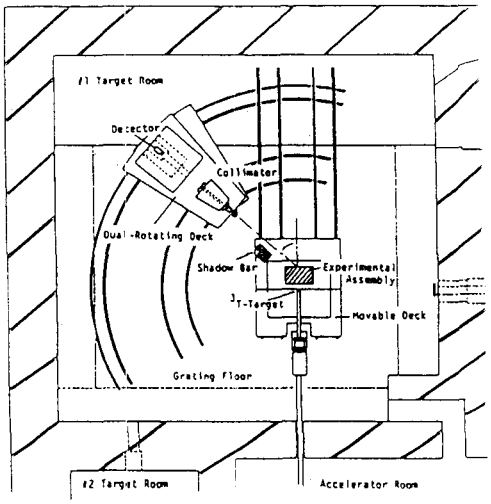

ANALYSIS

Code	Library	Nuclear data file
MCNP-3A	FSXLIB	JENDL-3
		JENDL-3PR1
		ENDF/B-IV
	BMCCS2	LANL
DOT3.5	FSXJ3T2/FUSION-J3 (125 neutron - 40 gamma-ray)	JENDL-3
	GICX-40 (42 neutron - 21gamma-ray)	ENDF/B

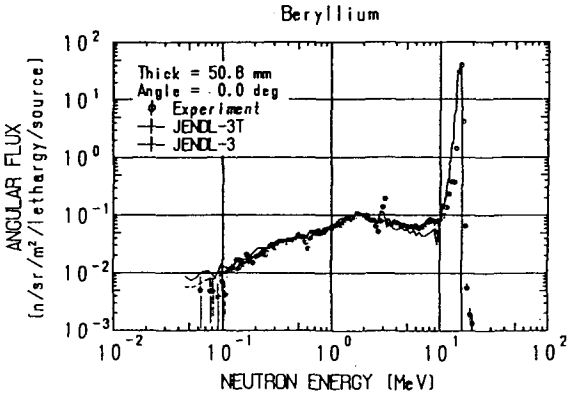
Beryllium
Thick = 50.8 mm
Angle = 0.0 deg
Experiment
JENDL-3T
JENDL-3
ANGULAR FLUX
[n/sr/m²/lethargy/source]
NEUTRON ENERGY [MeV]

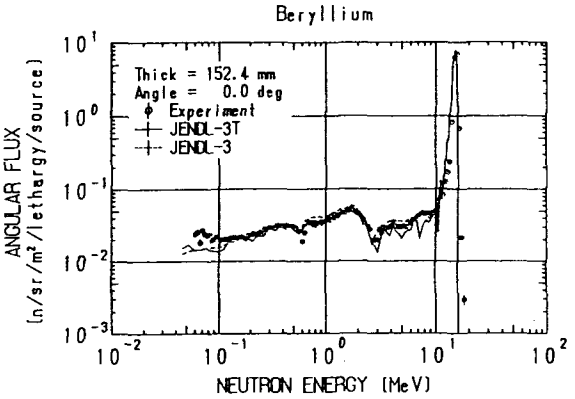
Beryllium
Thick = 152.4 mm
Angle = 0.0 deg
Experiment
JENDL-3T
JENDL-3
ANGULAR FLUX
[n/sr/m²/lethargy/source]
NEUTRON ENERGY [MeV]

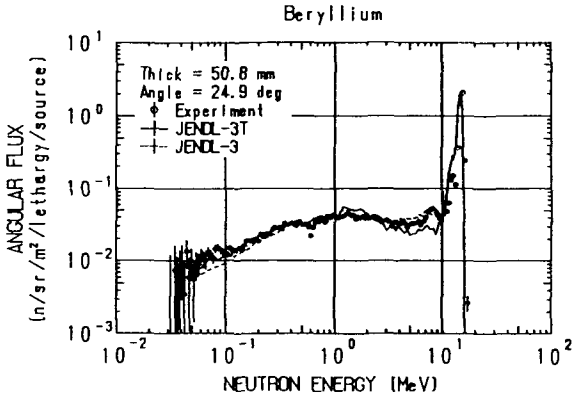
Beryllium
Thick = 50.8 mm
Angle = 24.9 deg
Experiment
JENDL-3T
JENDL-3
ANGULAR FLUX
[n/sr/m²/lethargy/source]
NEUTRON ENERGY [MeV]

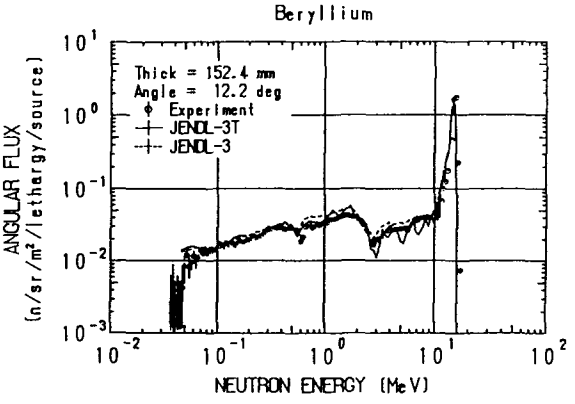
Beryllium
Thick = 152.4 mm
Angle = 12.2 deg
Experiment
JENDL-3T
JENDL-3
ANGULAR FLUX
[n/sr/m²/lethargy/source]
NEUTRON ENERGY [MeV]

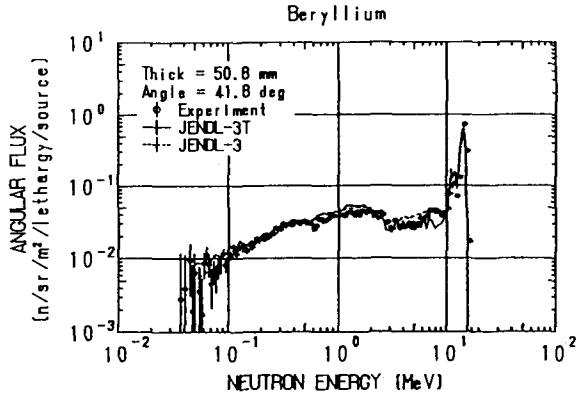
Beryllium
Thick = 50.8 mm
Angle = 41.8 deg
Experiment
JENDL-3T
JENDL-3
ANGULAR FLUX
[n/sr/m²/lethargy/source]
NEUTRON ENERGY [MeV]

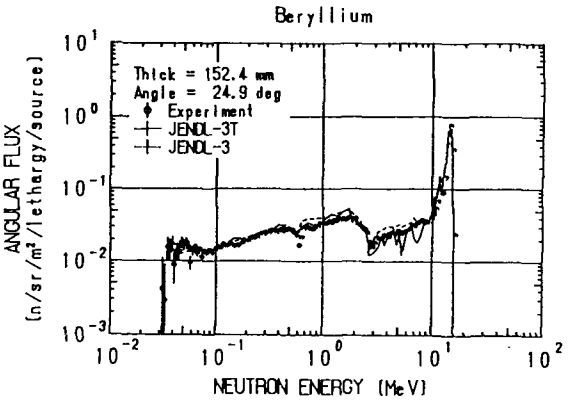
Beryllium
Thick = 152.4 mm
Angle = 24.9 deg
Experiment
JENDL-3T
JENDL-3
ANGULAR FLUX
[n/sr/m²/lethargy/source]
NEUTRON ENERGY [MeV]

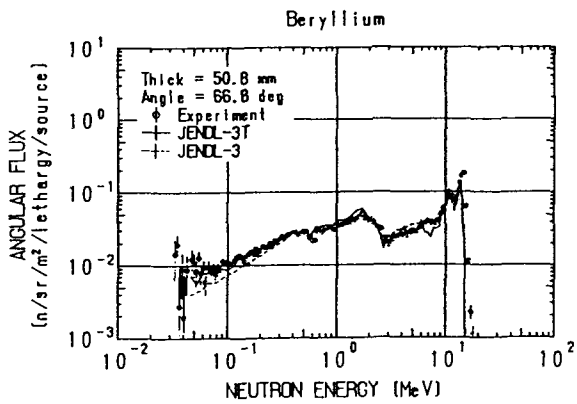
Beryllium
Thick = 50.8 mm
Angle = 66.8 deg
Experiment
JENDL-3T
JENDL-3
ANGULAR FLUX
[n/sr/m²/lethargy/source]
NEUTRON ENERGY [MeV]

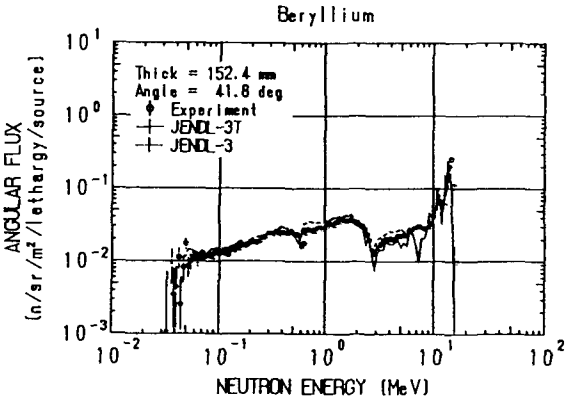
Beryllium
Thick = 152.4 mm
Angle = 41.8 deg
Experiment
JENDL-3T
JENDL-3
ANGULAR FLUX
[n/sr/m²/lethargy/source]
NEUTRON ENERGY [MeV]

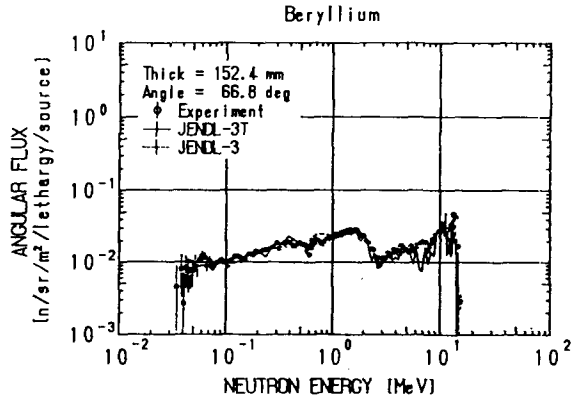
Beryllium
Thick = 152.4 mm
Angle = 66.8 deg
Experiment
JENDL-3T
JENDL-3
ANGULAR FLUX
[n/sr/m²/lethargy/source]
NEUTRON ENERGY [MeV]

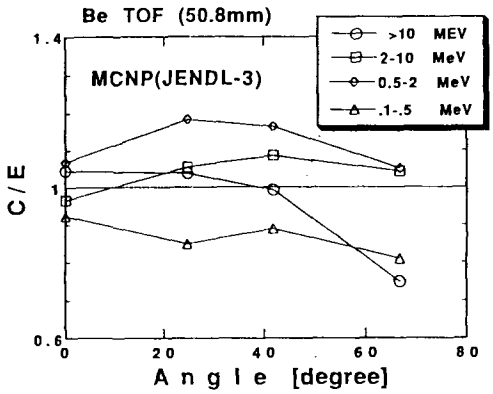
Be TOF (50.8mm)
MCNP(JENDL-3)
>10 MEV
2-10 MeV
0.5-2 MeV
.1-.5 MeV
C/E
Angle [degree]

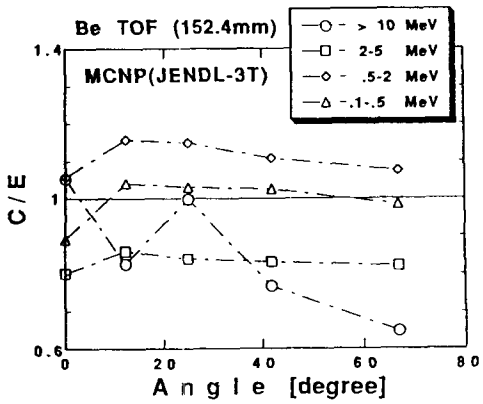
Be TOF (152.4mm)
MCNP(JENDL-3T)
> 10 MeV
2-5 MeV
.5-2 MeV
.1-.5 MeV
C/E
Angle [degree]

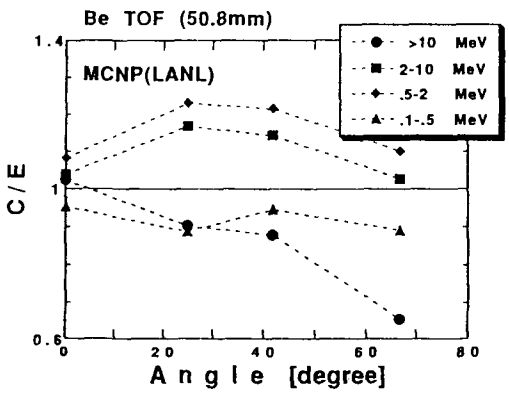
Be TOF (50.8mm)
MCNP(LANL)
>10 MeV
2-10 MeV
.5-2 MeV
.1-.5 MeV
C/E
Angle [degree]

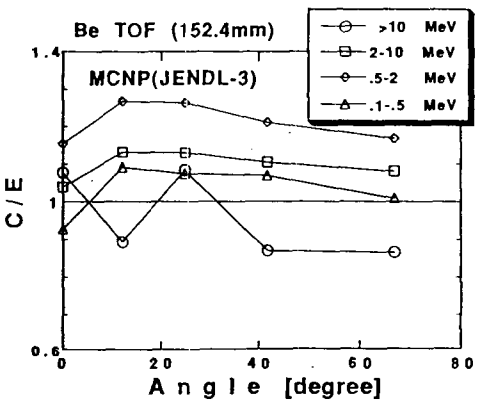
Be TOF (152.4mm)
MCNP(JENDL-3)
>10 MeV
2-10 MeV
.5-2 MeV
.1-.5 MeV
C/E
Angle [degree]

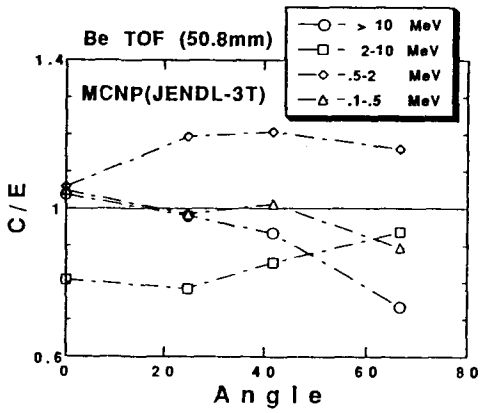
Be TOF (50.8mm)
MCNP(JENDL-3T)
> 10 MeV
2-10 MeV
.5-2 MeV
.1-.5 MeV
C/E
Angle

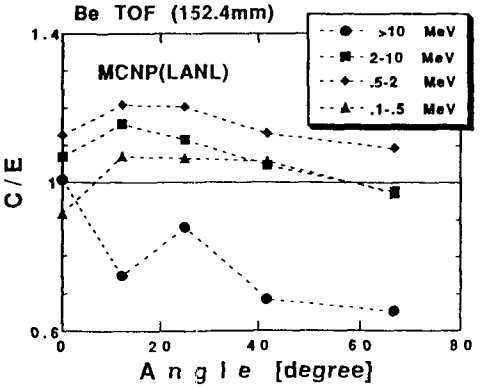
Be TOF (152.4mm)
MCNP(LANL)
>10 MeV
2-10 MeV
.5-2 MeV
.1-.5 MeV
C/E
Angle [degree]

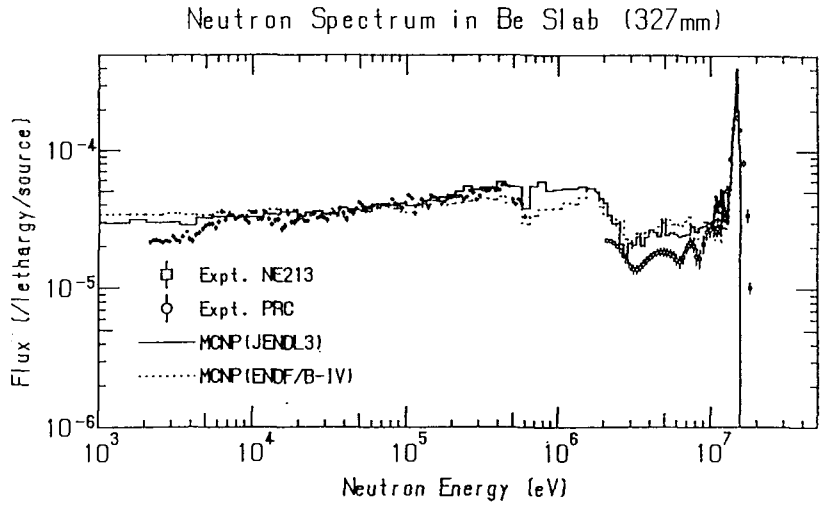
Neutron Spectrum in Be Slab (327mm)
Flux (/lethargy/source)
Expt. NE213
Expt. PRC
MCNP(JENDL3)
MCNP(ENDF/B-IV)
Neutron Energy (eV)

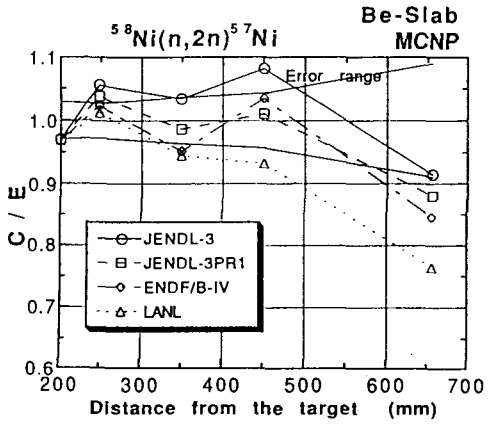
Be-Slab
MCNP
58Ni(n,2n)57Ni
Error range
C / E
JENDL-3
JENDL-3PR1
ENDF/B-IV
LANL
Distance from the target (mm)

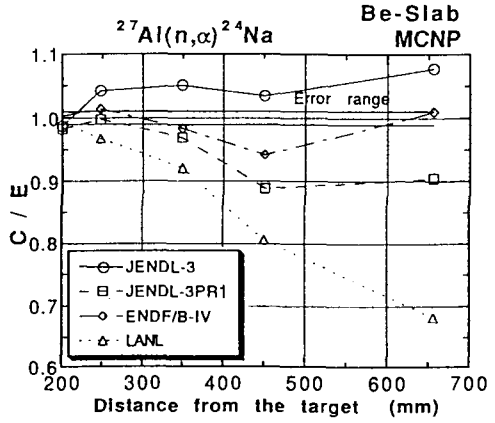
Be-Slab
MCNP
27Al(n,α)24Na
Error range
C / E
JENDL-3
JENDL-3PR1
ENDF/B-IV
LANL
Distance from the target (mm)

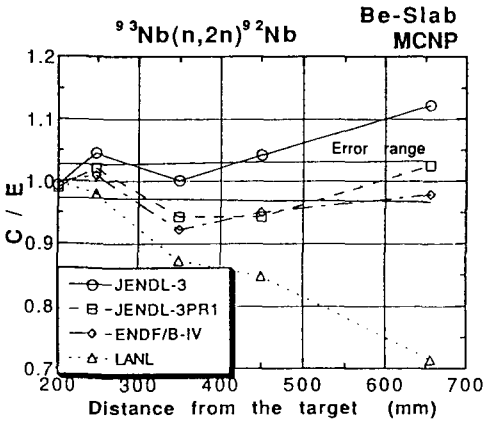
Be-Slab
MCNP
93Nb(n,2n)92Nb
Error range
C / E
JENDL-3
JENDL-3PR1
ENDF/B-IV
LANL
Distance from the target (mm)

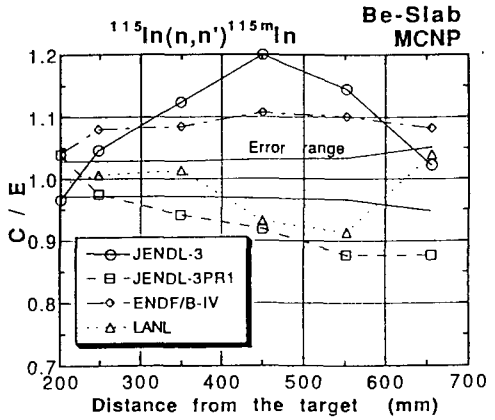
Be-Slab
MCNP
115In(n,n')115mIn
Error range
C / E
JENDL-3
JENDL-3PR1
ENDF/B-IV
LANL
Distance from the target (mm)

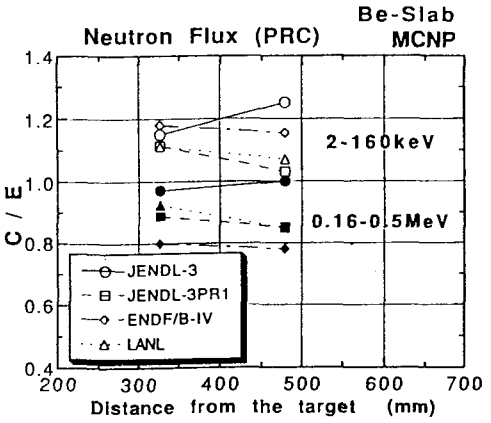
Be-Slab
MCNP
Neutron Flux (PRC)
2-160keV
0.16-0.5MeV
C / E
JENDL-3
JENDL-3PR1
ENDF/B-IV
LANL
Distance from the target (mm)

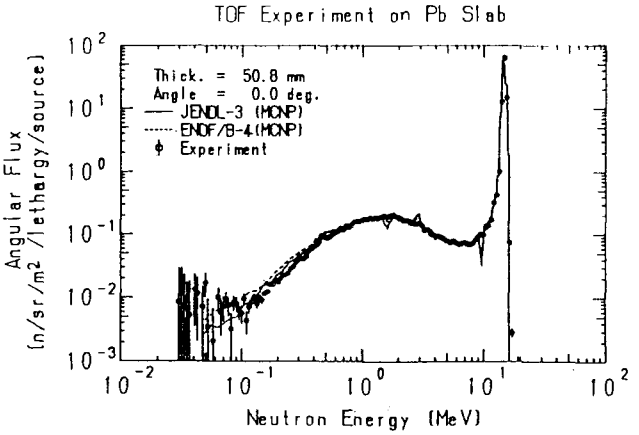
TOF Experiment on Pb Slab
Thick. = 50.8 mm
Angle = 0.0 deg.
JENDL-3 (MCNP)
ENDF/B-4(MCNP)
Experiment
Angular Flux
(n/sr/m2 /lethargy/source)
Neutron Energy (MeV)

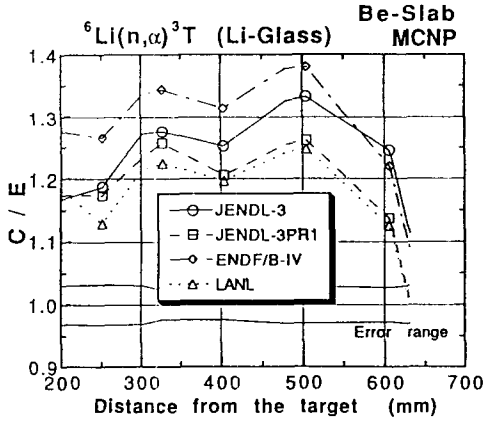
Be-Slab
^{6}Li(n,α)^{3}T (Li-Glass) MCNP
C / E
JENDL-3
JENDL-3PR1
ENDF/B-IV
LANL
Error range
Distance from the target (mm)

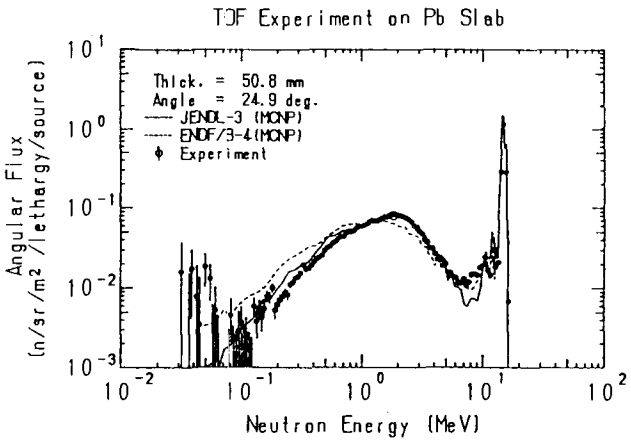
TOF Experiment on Pb Slab
Thick. = 50.8 mm
Angle = 24.9 deg.
JENDL-3 (MCNP)
ENDF/B-4(MCNP)
Experiment
Angular Flux
(n/sr/m² /lethargy/source)
Neutron Energy (MeV)

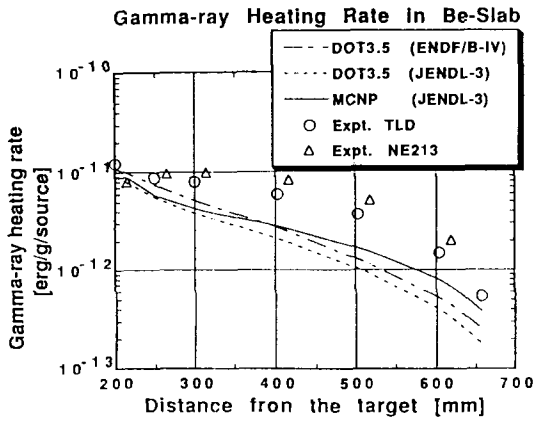
Gamma-ray Heating Rate in Be-Slab
DOT3.5 (ENDF/B-IV)
DOT3.5 (JENDL-3)
MCNP (JENDL-3)
Expt. TLD
Expt. NE213
Gamma-ray heating rate
[erg/g/source]
Distance fron the target [mm]

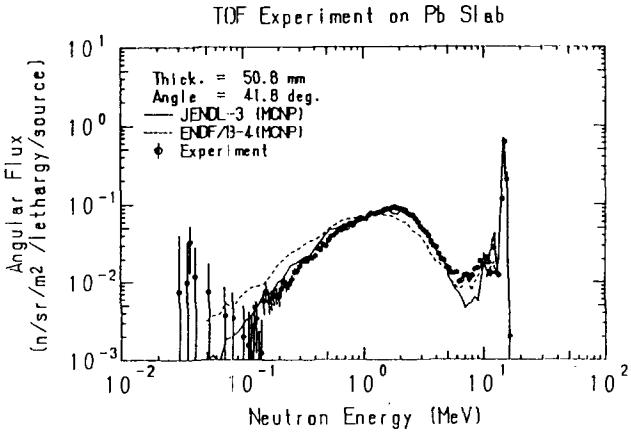
TOF Experiment on Pb Slab
Thick. = 50.8 mm
Angle = 41.8 deg.
JENDL-3 (MCNP)
ENDF/B-4(MCNP)
Experiment
Angular Flux
(n/sr/m² /lethargy/source)
Neutron Energy (MeV)

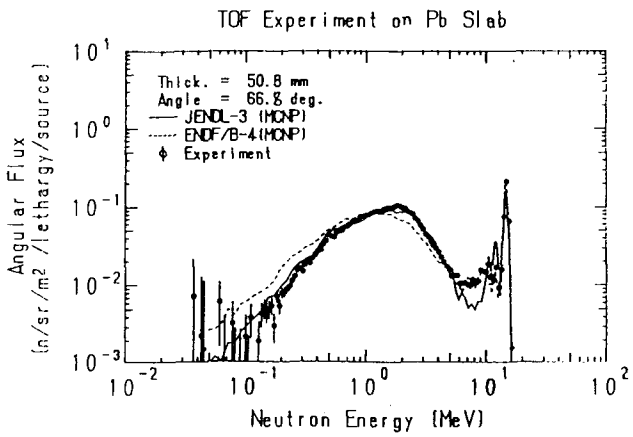
TOF Experiment on Pb Slab
Thick. = 50.8 mm
Angle = 66.8 deg.
JENDL-3 (MCNP)
ENDF/B-4(MCNP)
Experiment
Angular Flux
(n/sr/m² /lethargy/source)
Neutron Energy (MeV)

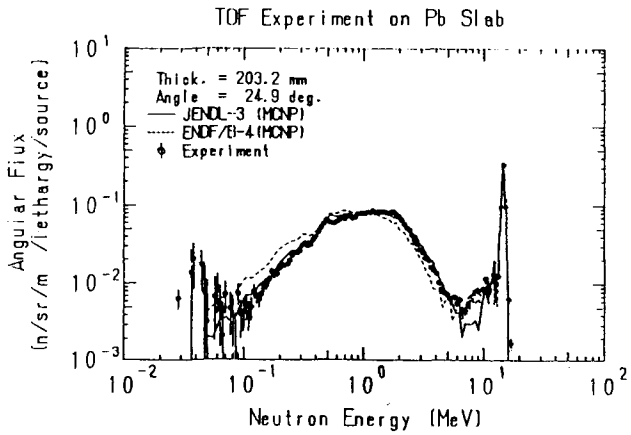
TOF Experiment on Pb Slab
Thick. = 203.2 mm
Angle = 24.9 deg.
JENDL-3 (MCNP)
ENDF/B-4(MCNP)
Experiment
Angular Flux
(n/sr/m /lethargy/source)
Neutron Energy (MeV)

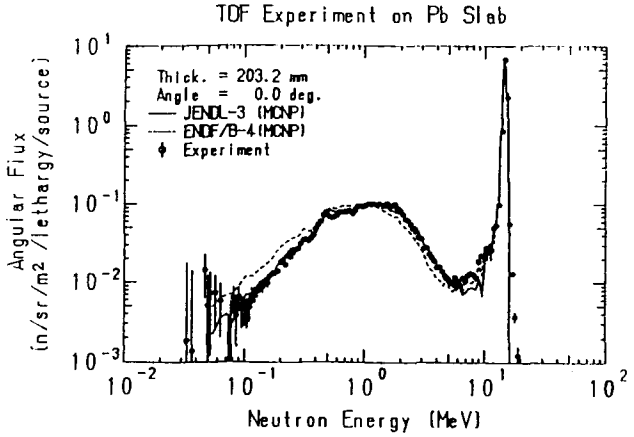
TOF Experiment on Pb Slab
Thick. = 203.2 mm
Angle = 0.0 deg.
JENDL-3 (MCNP)
ENDF/B-4(MCNP)
Experiment
Angular Flux
(n/sr/m² /lethargy/source)
Neutron Energy (MeV)

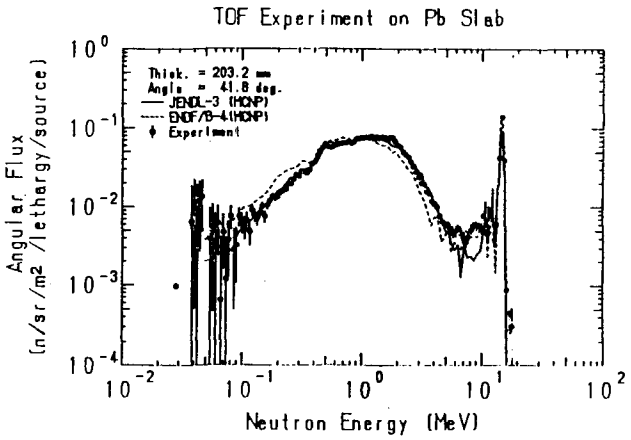
TOF Experiment on Pb Slab
Thick. = 203.2 mm
Angle = 41.8 deg.
JENDL-3 (MCNP)
ENDF/B-4(MCNP)
Experiment
Angular Flux
(n/sr/m² /lethargy/source)
Neutron Energy (MeV)

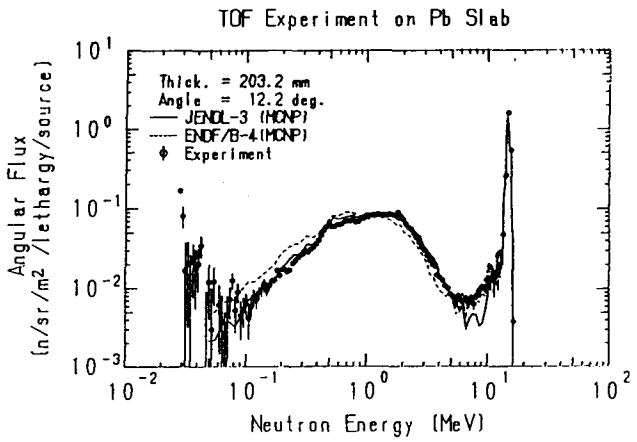
TOF Experiment on Pb Slab
Thick. = 203.2 mm
Angle = 12.2 deg.
JENDL-3 (MCNP)
ENDF/B-4(MCNP)
Experiment
Angular Flux
(n/sr/m2 /lethargy/source)
Neutron Energy (MeV)

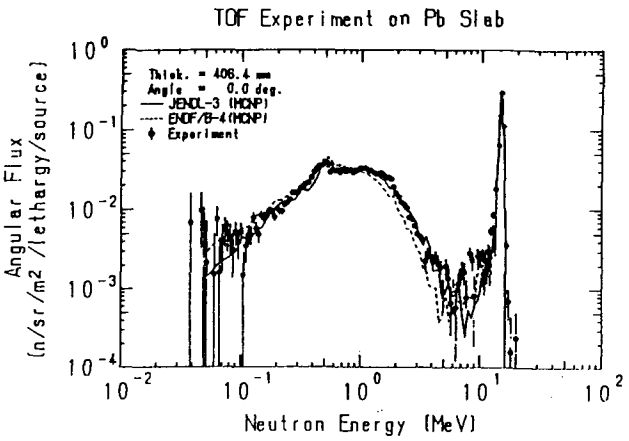
TOF Experiment on Pb Slab
Thick. = 406.4 mm
Angle = 0.0 deg.
JENDL-3 (MCNP)
ENDF/B-4(MCNP)
Experiment
Angular Flux
(n/sr/m2 /lethargy/source)
Neutron Energy (MeV)

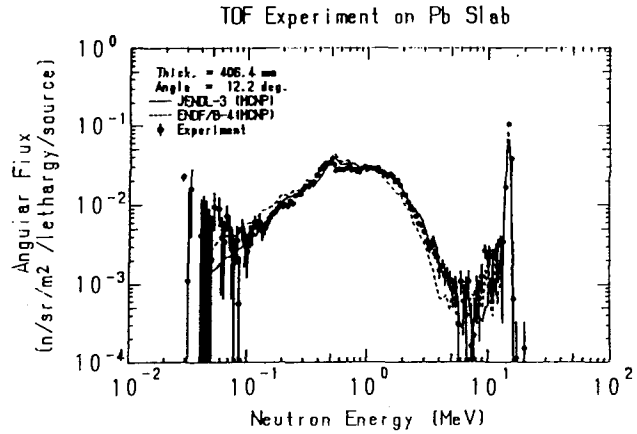
TOF Experiment on Pb Slab
Thick. = 406.4 mm
Angle = 12.2 deg.
JENDL-3 (MCNP)
ENDF/B-4(MCNP)
Experiment
Anguiar Flux
(n/sr/m2 /lethargy/source)
Neutron Energy (MeV)

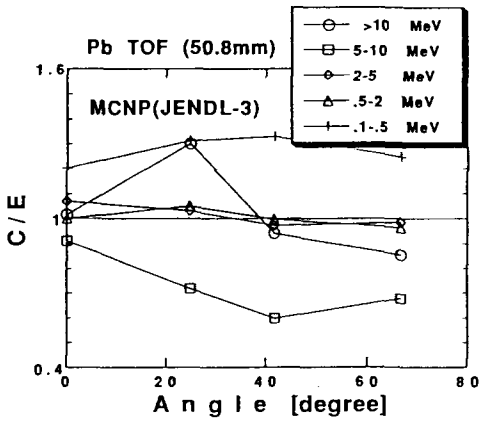
Pb TOF (50.8mm)
MCNP(JENDL-3)
>10 MeV
5-10 MeV
2-5 MeV
.5-2 MeV
.1-.5 MeV
C/E
Angle [degree]

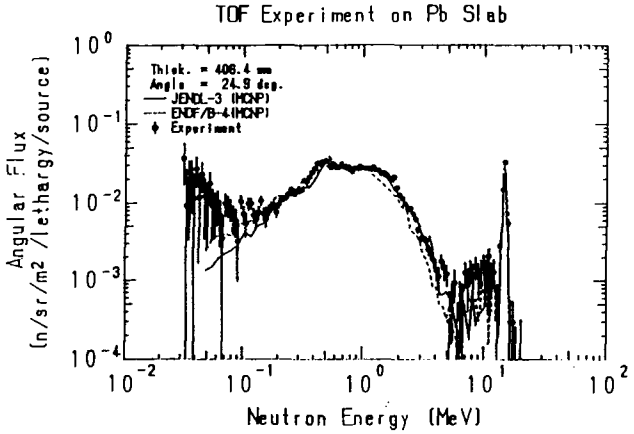
TOF Experiment on Pb Slab
Thick. = 406.4 mm
Angle = 24.8 deg.
JENDL-3 (MCNP)
ENDF/B-4(MCNP)
Experiment
Angular Flux
(n/sr/m2 /lethargy/source)
Neutron Energy (MeV)

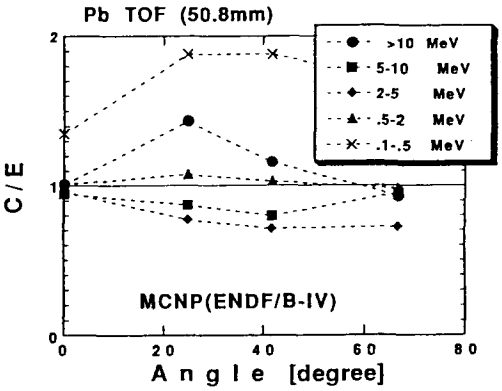
Pb TOF (50.8mm)
MCNP(ENDF/B-IV)
>10 MeV
5-10 MeV
2-5 MeV
.5-2 MeV
.1-.5 MeV
C/E
Angle [degree]

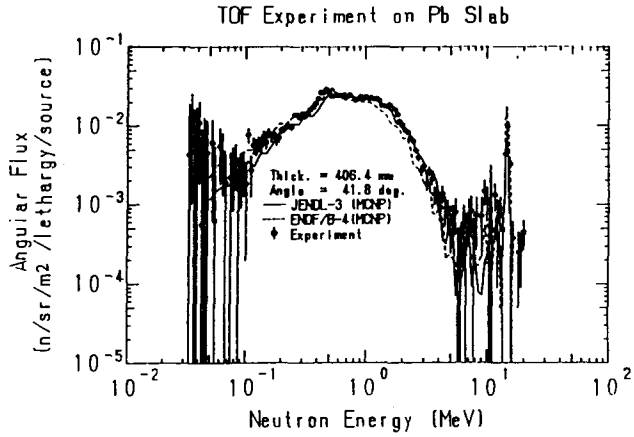
TOF Experiment on Pb Slab
Thick. = 406.4 mm
Angle = 41.8 deg.
JENDL-3 (MCNP)
ENDF/B-4(MCNP)
Experiment
Anguiar Flux
(n/sr/m2 /lethargy/source)
Neutron Energy (MeV)

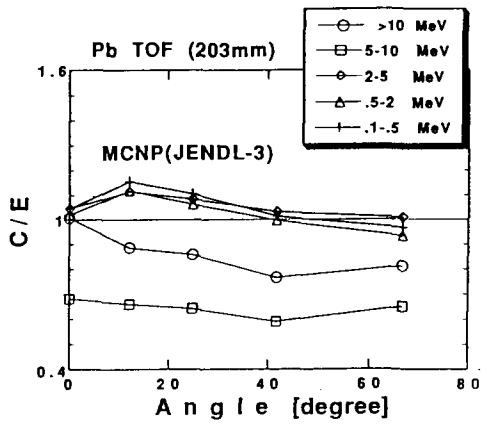
Pb TOF (203mm)
MCNP(JENDL-3)
>10 MeV
5-10 MeV
2-5 MeV
.5-2 MeV
.1-.5 MeV
C/E
Angle [degree]

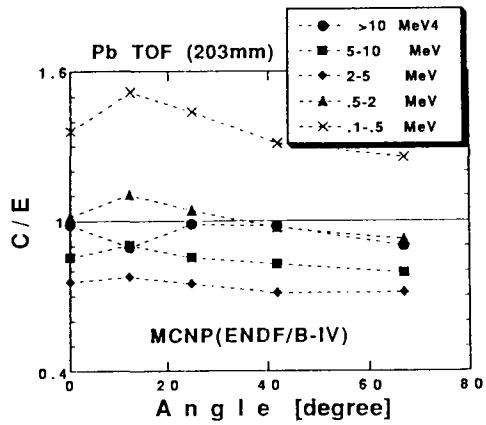

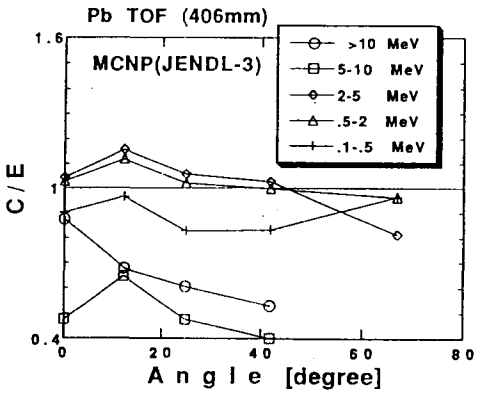

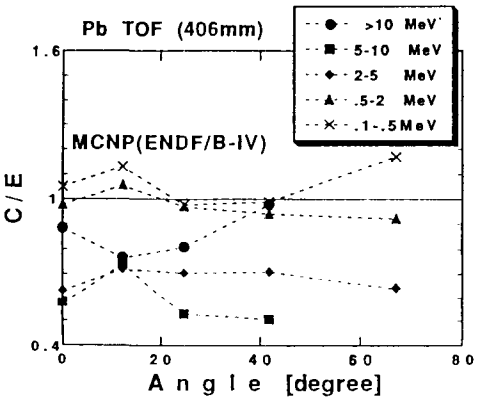

Cross Section Data of Be at 14.1 MeV [barn]

	Total	Elastic	(n,2n)
JENDL-3	1.489	0.955	0.483
	(1.000)	(1.000)	(1.000)
JENDL-3T	1.489	0.896	0.542
	(1.000)	(0.938)	(1.122)
JENDL-3PR1	1.489	0.925	0.513
	(1.000)	(0.969)	(1.062)
ENDF/B-VI	1.522	1.009	0.485
	(1.022)	(1.057)	(1.004)
ENDF/B-IV	1.486	0.934	0.521
	(0.998)	(0.978)	(1.079)

*The value in parentheses is the ratio to the value of JENDL-3.

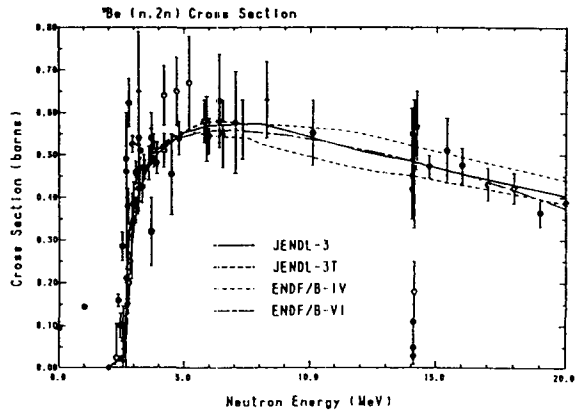

Fig. (n,2n) cross section curves.

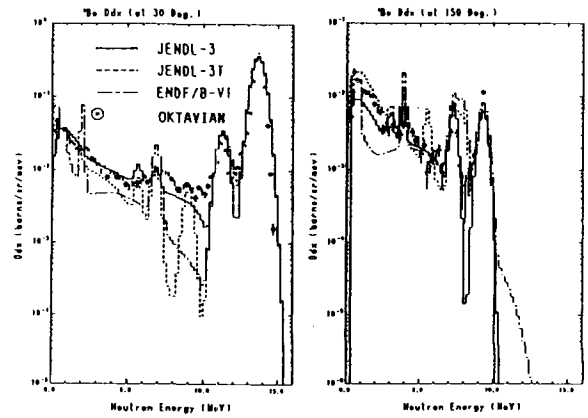

Fig. Typical double differential cross section (DDX).

Summary for Status of Be Nuclear Data in JENDL-3

1) The status of Be neutron data in JENDL-3 is fairly good for the fusion neutronics application comparing the preliminary versions of JENDL-3, ENDF/B-IV and LANL.
2) Some minor changes are required for the ^{9}Be(n,2n) cross section in JENDL-3 including secondary neutron energy and angular distributions.
3) There are some room of improvement by a few % for the cross sections of total, elastic scattering, (n,2n) and so on around 14 MeV.
4) Further examinations are required for the nuclear data relevant to the gamma-ray heating.

Summary for Status of Pb Nuclear Data in JENDL-3

1) The neutron data of Pb in JENDL-3 improves very much from those in JENDL-3T.
2) Good agreements are observed between calculated and measured spectra except the region between 5 and 11 MeV.
3) Some minor changes are required for the Pb(n,2n) cross section in JENDL-3 including secondary neutron energy and angular distributions.
4) There are some room of improvement by a few % for the cross section of total, elastic scattering, (n,2n) and so on around 14 MeV.

Cross Section Data of Pb at 14.1 MeV [barn]

	Total	Elastic	Inelastic	(n,2n)
JENDL-3	5.4334	2.7404	0.4990	2.1914
	(1.000)	(1.000)	(1.000)	(1.000)
JENDL-3T				2.037
				(0.930)
JENDL-2	5.419	2.915	0.5801	1.921
	(0.997)	(1.064)	(1.163)	(0.877)
ENDF/B-VI	5.2920	2.8553	0.3397	2.0921
	(0.974)	(1.042)	(0.681)	(0.955)
ENDF/B-IV	5.2963	2.8087	0.3428	2.1446
	(0.975)	(1.025)	(0.687)	(0.979)
EFF	5.2963	2.8087	0.3997	2.1015
	(0.975)	(1.025)	(0.801)	(0.959)

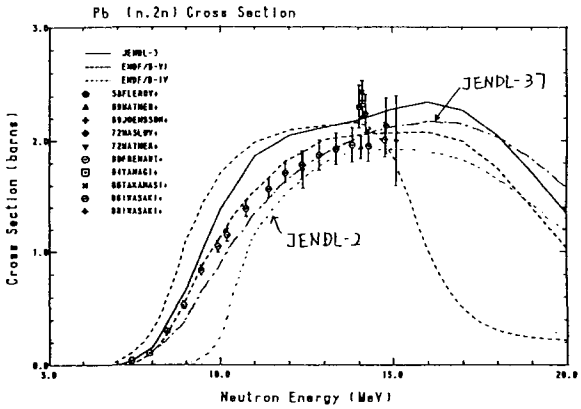

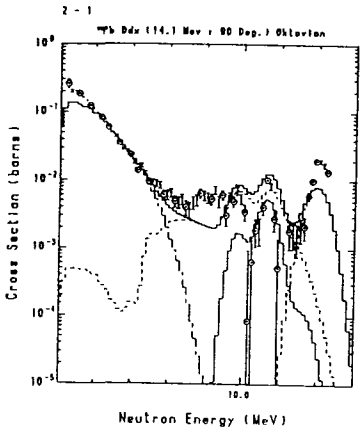

MEASUREMENT AND CALCULATION OF NEUTRON LEAKAGE FROM Be SHELLS WITH THE Cf-252 CENTRAL SOURCE

S.I BESSONOV, A.A.BORISOV, D.Yu.CHUVILIN, S.A.KONAKOV
I.V.Kurchatov Institute of Atomic Energy, Moscow, USSR

This experiment, carried out at I.V.Kurchatov Institute of Atomic Energy recently, is devoted to the testing of $^{9}Be(n,2n)$ cross section in the energy range close to the energies of secondary neutrons from this reaction.

The measurements were performed by the manganese bath method in a sphere with inner diameter d=60 cm and outer diameter D=132 cm. The thicknesses of spherical shells were 3, 5 and 8 cm. The neutron yield of the source was 10^{7}n/s.

The manganese activation rate was measured by scintillation γ-spectrometer. The relative error was less then 1 % (0.6-0.8 %) due to use of multiple measurements.

The measurements of neutron leakages from Be relative to the measurements without the experimental sample were compared with calculations by the BLANK code with ENDF/B-IV and ENDF/B-VI data of Be.

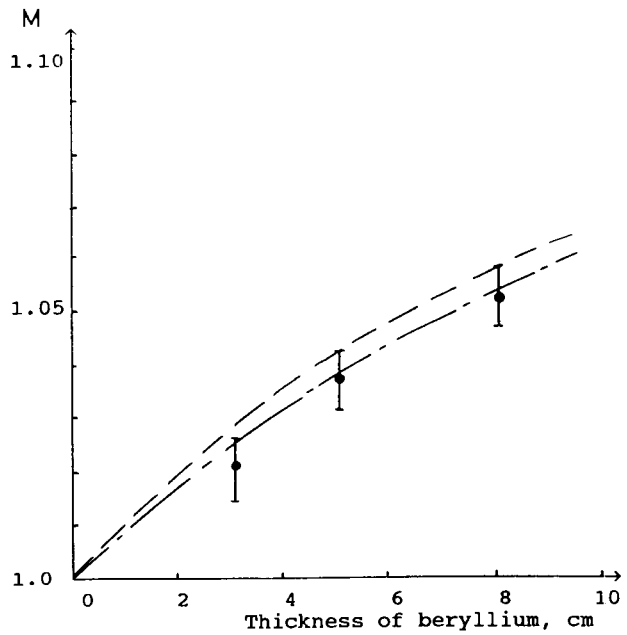

Fig 1. Neutron leakage multiplication as a function of Be layer thickness.
Calculation — — — ENDF/B-IV,
—— - —— ENDF/B-VI
Experiment

A comparison of results is shown in Fig. 1. It is seen that experiment and calculation agree wthin the errors. This confirms that (n,2n) cross section of Be in ENDF/B-IV and ENDF/B-VI data averaged on the Cf spectrum satisfactorily describes the experimental results.